DAMPING ESTIMATION OF PLATES JOINED AT A POINT USING STATISTICAL ENERGY ANALYSIS

by

AKHILESH CHANDRA REDDY KATIPALLY

Submitted to the Graduate degree program in Aerospace Engineering and the Graduate faculty of the University of Kansas in partial fulfillment of the requirements for the degree of master of science

_____

Chairperson Dr. Mark S. Ewing

_____

Dr. Rick Hale

_____

Dr. Adolfo Matamoros

DATE DEFENDED: 6th June 2011

The Thesis Committee for Akhilesh Chandra Reddy Katipally

certifies that this is the approved version of the following thesis:

DAMPING ESTIMATION OF PLATES JOINED AT A POINT USING STATISTICAL ENERGY ANALYSIS

_____

Chairperson Dr. Mark S. Ewing

DATE APPROVED: 10th June 2011

ABSTRACT

The loss factors and coupling loss factors of a 2-plate, coupled system were estimated using the Statistical Energy Analysis methodology. In particular the Power Input Method (P.I.M.) and the Transient Statistical Energy Analysis Method (T.S.E.A.) were applied to both steady state and transient excitation cases. The effects of various process parameters such as frequency resolution, frequency bandwidths, type of hammer tip and measurement points on the estimated loss factors were also investigated for 3 different levels of damping. Possible reasons for the occurrence of negative coupling loss factor estimations using the T.S.E.A. method have been discovered to be the flexibility of the joint between the plates and the frequency resolution of the measured data.

The effect of frequency resolution and damping on the estimated loss factors was examined both numerically and experimentally. First, a two degree of freedom (2-DOF) system was numerically simulated with varying model loss factors of 0.1%, 7.5% and 75% and frequency resolutions of 0.05 Hz, 0.2Hz and 1 Hz. The estimated loss factors were found to be highly dependent on the frequency resolution only in the lightly damped case. Experiments were then performed on 2 Aluminum plates coupled at a point, varying both the damping (by adding constrained layer damping) and the frequency resolution. It was seen that the coupling loss factors were not dependent on the damping levels, whereas the loss factors increased as the damping increased as expected. As the frequency resolution was decreased the loss factors in some frequency bands, especially the lower frequency bands, tended to negative values. The loss factors estimated, using the power input method, were in good agreement with both shaker and hammer excitations.

Modal density and modes in band were also calculated and compared with the theoretical results. Significant variation between the theoretical values and the experimental values was seen only in the ‘No damping’ case and only in the lower frequency bands.

The main aims of using the T.S.E.A. method were to interpret the results from the dissertation by M. L. Lai, to find out the practical limitations of the method and to establish the degree of agreement of the asymptotic loss factor estimations with respect to the P.I.M. A numerical simulation was run on a 2-DOF system to show how the loss factor varies with time for a transient hit. It also showed that the theoretical coupling coefficients were off by more than 150% when a double hit occurs. Experiments were conducted to check for the effects of frequency resolution and frequency bandwidth on the estimated coupling loss factors. An increase in the damping levels of the plates caused the number of negativities in the “apparent time varying coupling loss factor” estimates to decrease while simultaneously decreasing the time taken to reach an asymptotic value. Possible reasons for the occurrence of negative coupling loss factors were discussed.

ACKNOWLEDGEMENTS

I would like to thank, first and foremost, my advisor Dr. Mark S Ewing for providing me the opportunity, the resources and the facilities to work under him. He has helped me out in more than one way to finish my work in a timely fashion.

Additional thanks also go to my committee members Dr. Rick Hale and Dr. Adolfo Matamoros for being a part of my committee and offering their advice and support at all times.

I would also like to thank the Aerospace Engineering department in general and Amy Borton in particular for keeping me in the loop with regards to deadlines and other important notifications.

I would particularly like to thank Wes Ellison, lab director, for providing the technical support as and when needed.

Final thanks go to my family and friends for giving the moral and financial support during my stay in Lawrence.

TABLE OF CONTENTS

LIST OF FIGURES

LIST OF TABLES

1.0 INTRODUCTION

Any structural deformation that repeats itself after an interval is called vibration or oscillation [2]. Engineered structures contain components which possess finite levels of stiffness, mass and dissipative energy transfer characteristics due to inherent damping. Imposition of alternating external loads on such structures can result in very high amplitude vibrations at numerous distinct resonant frequencies [3]. Any structure undergoing vibration stores both kinetic energy (on account of its mass) and potential energy (due to stiffness) and a means to dissipate energy (damping) [2]. Any structure vibrating at a resonant frequency with insufficient damping tends to vibrate at high amplitudes which tend to radiate sound and which might ultimately lead to structural failure. Hence it is of utmost importance to predict these resonant frequencies and prevent high amplitude vibrations via adequate structural damping [3].

Damping in a structure is defined as any effect which tends to reduce the amplitude of oscillation. Several types of damping are inherently present in any structure[4]. They can be classified into two types. They are internal damping of the structure and structural damping at the various joints. If any structure has low inherent damping, additional damping can be added to a structure which can be classified into active damping and passive damping.

Active damping is achieved by actuators which control the motion of the structure whereas passive damping is achieved by adding a layer of visco-elastic material which, in constrained layer damping, is covered by a layer of constraining material to the structure. Constrained layer damping dissipates the energy of the structure as heat because of the shearing deformation of the visco-elastic material. Under the influence of dynamic loads, the visco-elastic material dissipates energy by disrupting the bonds of its long-chain molecules to convert the kinetic energy to dissipative thermal energy (heat).[5]

There are several notations which describe the damping level of a structure, namely the equivalent modal damping ratio, ξ , loss factor, η, and quality factor Q. For loss factors ranging from 0 to 0.3 the relationship between them is given by the following equation[5].

$$\eta = 2\xi = \frac{C}{m\omega} = \frac{1}{Q} \tag{1.1}$$

The actual relationship between η and ξ is given by $\eta = 2\xi\sqrt{1-\xi^2}$ which is within 5% of equation (1.1) when $\eta < 0.3$. [5]

1.1 LOSS FACTOR

The loss factor (η) is defined as the ratio of the dissipated power (π_D) per radian to the total energy of the plate (E_{Total}) [6].

$$\eta = \frac{\pi_D}{\omega E_{Total}} \tag{1.2}$$

Under steady state conditions, since the stored energy in a structure remains constant, the power input to a structure is dissipated by the structure itself. Thus the dissipated power can be replaced with power input (π_{in}) to give the following equation.

$$\eta = \frac{\pi_{in}}{\omega E_{Total}} = \frac{E_{in}}{\omega \varepsilon_{Total}} \tag{1.3}$$

Here, E_{in} is the energy input to the structure and ε_{Total} is the integrated total energy.

The integrated total energy is the sum of the integrated potential energy and the integrated kinetic energy of the system.

$$\varepsilon_{Total} = \varepsilon_k + \varepsilon_P = 2\varepsilon_k \tag{1.4}$$

We assume that the integrated total energy is twice the integrated kinetic energy, which for an idealized single degree of freedom system causes no more than a 0.5 % error for $\eta > 0.1$ and a 3 % for $\eta > 0.2$ [7]. This assumption is used throughout this thesis.

1.2 EXPERIMENTAL METHODS TO ESTIMATE LOSS FACTORS

The experimental methods to estimate loss factors can be broadly classified into

1. Time domain decay-rate methods.
2. Frequency domain modal analysis curve fitting methods.
3. Methods based on the flow of energy and power.[8]

1.2.1 TIME DOMAIN DECAY RATE METHODS

Decay rate methods, as the name suggests, compute the loss factors from the decay response of the free decay of structures. This decaying response of the structure can be generated by either an impulse, used in Random Decrement Technique [9], or by an interrupted steady–state excitation, used in Reverberation Decay Method [10] or by clever processing of input output measurements, used in Impulse Response Decay Method [11] .

For the above three techniques, the procedure to evaluate loss factors is the same. That is, the loss factor is proportional to the logarithm of the assumed exponential decay of response, irrespective of whether the response is acceleration, velocity or displacement.

1.2.2 HALF POWER BANDWIDTH METHOD

The ‘half power bandwidth method’ is an example of frequency domain based method. The ‘half power bandwidth method’ or the ‘peak picking method’ is the simplest method for the estimation of modal parameters. The method treats each distinct peak in the frequency response function (FRF) as an individual system and finds out the apparent equivalent modal viscous damping level. [12].

The procedure of using the peak-picking method is:

(1) Picking the natural frequency

(2) Estimating the equivalent viscous modal damping

For estimating the damping, the half power points have to be first identified. The half power points are the frequencies which have amplitude of half the squared amplitude of the deflection (or velocity or acceleration) FRF “peak” and are given by $\frac{V_{\max}}{\sqrt{2}}$, as shown in Figure 1.

The loss factor can then be estimated using the equation (1.5)

$$\eta = \frac{\omega_b - \omega_a}{\omega_i} \tag{1.5}$$

The half power bandwidth method can only be used on a structure in the lower frequency ranges where the natural frequencies are widely spaced and it cannot be used in higher frequency ranges where the structure is modally dense and the “peaks” of the FRF might be so “close” that the response does not decrease to “half power” levels in the vicinity of a peak. The use of the half power bandwidth method also requires a high frequency resolution so that the peak point and half power points can be measured accurately. This method is also dependent on a high quality FRF which typically requires the time domain input and output signals to be averaged

multiple times. Hence, the half power bandwidth method can be used for lightly damped structures with well separated modes as long as an appropriate frequency resolution is used.

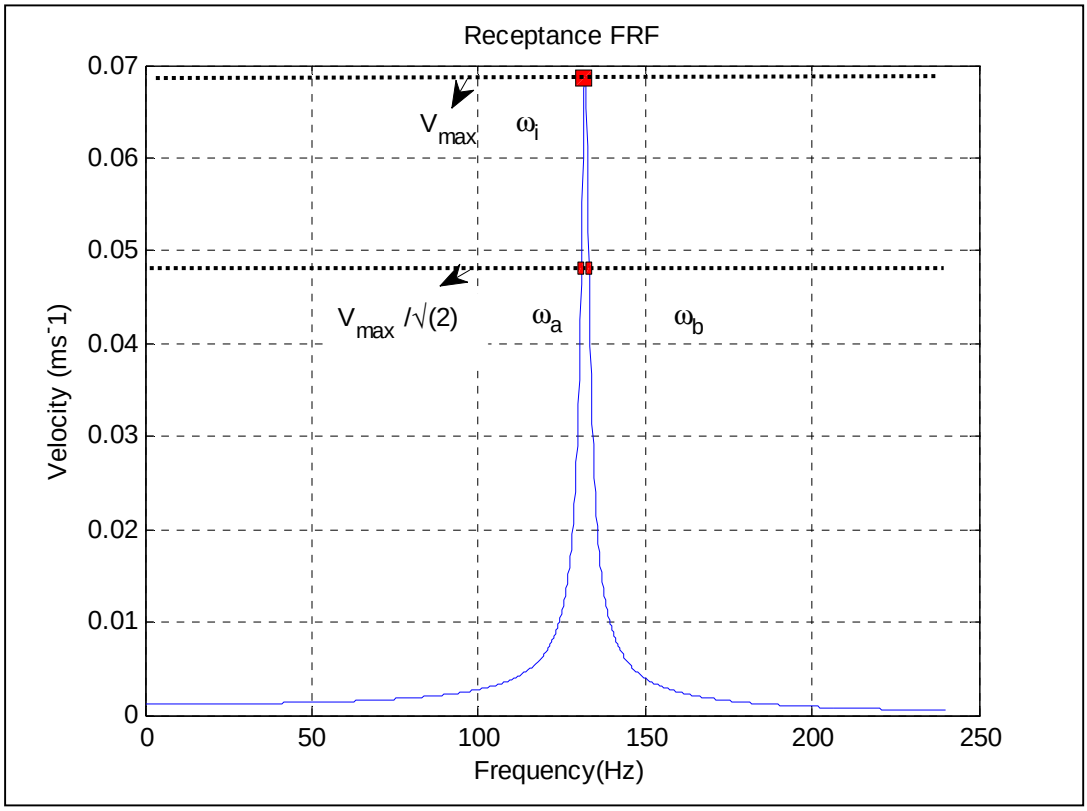

Figure 1: Mobility FRF of a single degree of freedom system as used to measure damping using half power bandwidth method

1.2.3 POWER INPUT METHOD

The Power Input Method (P.I.M) is based on a comparison of the dissipated energy of a system to the total energy of the system under steady state vibration. Since P.I.M. is based on the definition of the loss factor, theoretically it is unbiased and it is applicable at all frequencies. At higher frequencies, where the modes overlap, the P.I.M is used to calculate loss factors over broad frequency ranges. These band averaged loss factors are used in models based on Finite Element Method (FEM) and Statistical Energy Analysis (SEA) [13].

Since the power input into a system is dissipated by the system under steady state conditions, we can replace the dissipated power with the power input.

$$\eta = \frac{\pi_{in}}{\omega E_{Total}} = \frac{E_{in}}{\omega \varepsilon_{Total}} \tag{1.6}$$

Here, η is the loss factor, ω is the frequency, π_{in} is the input power, E_{in} is the input energy, E_{Total} is the total energy of the structure and ε_{Total} is the integrated total energy. The formulae to calculate the values of the total power input into the structure and the energy of the structure are given by equations (2.35).

1.2.4 TRANSIENT STATISTICAL ENERGY ANALYSIS METHOD

This method was proposed by M. L. Lai and A. Soom in their paper 'Prediction of Transient Vibrations Envelopes using Statistical Energy Analysis Techniques' [14]. This method was proposed as an alternative to the Power Input Method under transient excitations using the basic S.E.A relationship of the energy transferred between the subsystems to calculate the coupling loss factors between them. The power input method for transient excitations uses the steady state loss factors for estimating the power flow between subsystems of the structure whereas the T.S.E.A. method on the other hand uses a new 'apparent time varying coupling coefficient' to characterize the power flow between subsystems.

The basic T.S.E.A. relationship between 2 subsystems is given by

$$E_{12}^{tr}(t) = 2C_{12}(t)(\varepsilon_1^k(t) - \varepsilon_2^k(t)) \tag{1.7}$$

Here,

C_{12} (t) is the apparent time varying coupling coefficient between subsystems 1 and 2.

$E_{12}^{tr}(t)$ is the time varying energy transferred from subsystem 1 to subsystem 2.

$\varepsilon_i^k(t)$ is the integrated kinetic energy of subsystem i.

Equation (1.7) is the basis for the T.S.E.A method. Making an assumption that the energy stored in the coupling is very small when compared to the energy transferred between the subsystems leads us to the relationship between the coupling coefficients which then leads to the formulation of the T.S.E.A Method as stated by the equation (2.49)

$$C_{12}(t) = C_{21}(t) \tag{1.8}$$

Both C_{12} (t) and C_{21} (t) will asymptotically approach a constant value C which is the steady state coupling coefficient.

1.3 TYPES OF EXCITATION

1.3.1 SINUSOIDAL EXCITATION

Sinusoidal excitation is one of the oldest methods for exciting a structure for modal testing and is still widely used [12]. As shown in Figure 2 below, the force input consists of a sinusoidal wave of a particular frequency, here 159 Hz, thus exciting the structure only at that frequency.

Since the response characteristics of a structure are dependent on the frequency at which it is excited, this type of excitation can be used for direct parameter identification, because of the satisfactory signal to noise ratio, with the half power bandwidth method. The downside to this type of excitation is that it is very time-consuming to excite the structure at multiple natural frequencies.

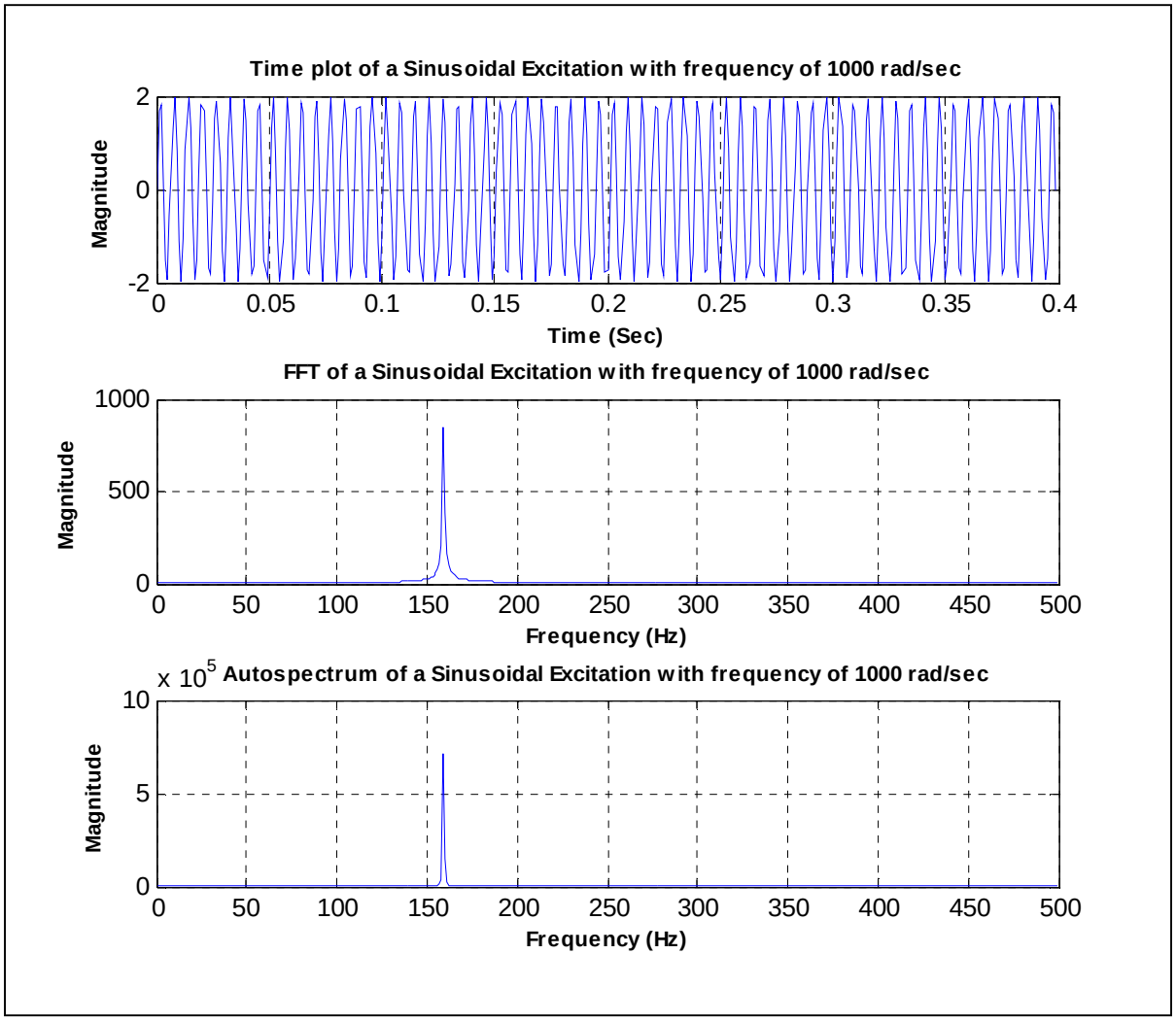

Figure 2 : Time plot, FFT and auto spectrum of a sinusoidal excitation with frequency 1000 radians/sec

1.3.2 RANDOM FORCE EXCITATION

The force signal for random excitation is a stationary random signal with Gaussian distribution having a constant spectral density. It is generated by using a random number generator and is a non-repeating sequence of numbers. As seen in Figure 3, the random force has "frequency content" over a broad frequency range and thus it excites all the natural frequencies of a structure in any large frequency band. For a structure that behaves nonlinearly, random

excitation has the tendency to linearize the behavior from the measurement data. It correctly models the amount of energy dissipation of the structure during vibration [12]. Hence random force excitation is preferred while using the power input method.

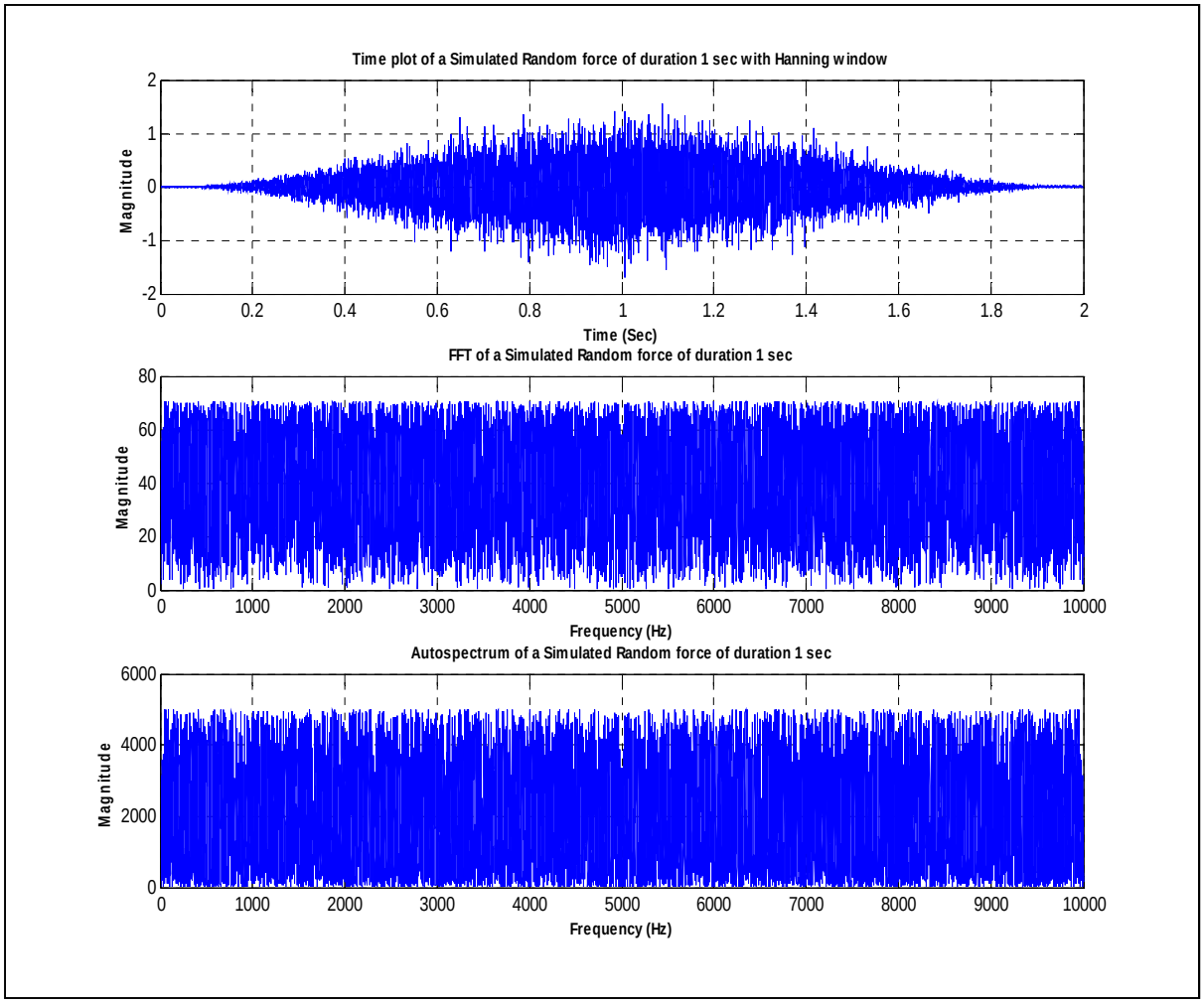

Figure 3 : Time plot, FFT and auto spectrum of a simulated random force excitation with no noise

For a structure excited with a random force, since neither the force input nor the response is periodic, leakage errors might occur. For the signal to be transformed into frequency domain using the Fourier transform, the signal should satisfy the Dirichlet condition, which states that the value of the signal and its time derivative at the start and end of a time record must have the same

value, preferably equal to zero. This leakage can be minimized by using a Hanning window. A Hanning window is a raised cosine function which zeros out the signal and its first derivative, at the beginning and at the end of the time record of a time domain signal.

1.3.3 TRANSIENT EXCITATION

The time domain signal of an impact excitation is a pulse of limited duration. The frequency band that an impact force excites is directly related to the impact duration as

$$F = \frac{1}{\Delta t} \tag{1.9}$$

Here, F is the highest frequency excited by the impact and Δt is the duration of the impact. As seen in Figure 4 the maximum frequency excited by the impact force of duration 0.001 second is about 1000 Hz.

Transient excitation is a relatively simple, cheap, convenient and portable excitation technique which requires minimum hardware. Since there is no physical connection between the excitation source and the structure there are no errors involved because of the loading of the test structure due to the mass of the shaker. Examples of transient forces include shock loading, impacts, for example is using an impact hammer with a calibrated force gauge, earthquakes and wind gusts.

To minimize leakage errors the measured input force from the impact must always include a nascent (pre impact) time interval at the beginning of the time record thus satisfying the Dirchlet condition. The main disadvantage of impact excitation is that it is difficult to control either the force level or the frequency range of the impact which could affect the signal to noise

ratio, resulting in poor quality data. Repetitiveness is another issue with transient excitation. In addition, some structures are too delicate to be hammered upon.[12]

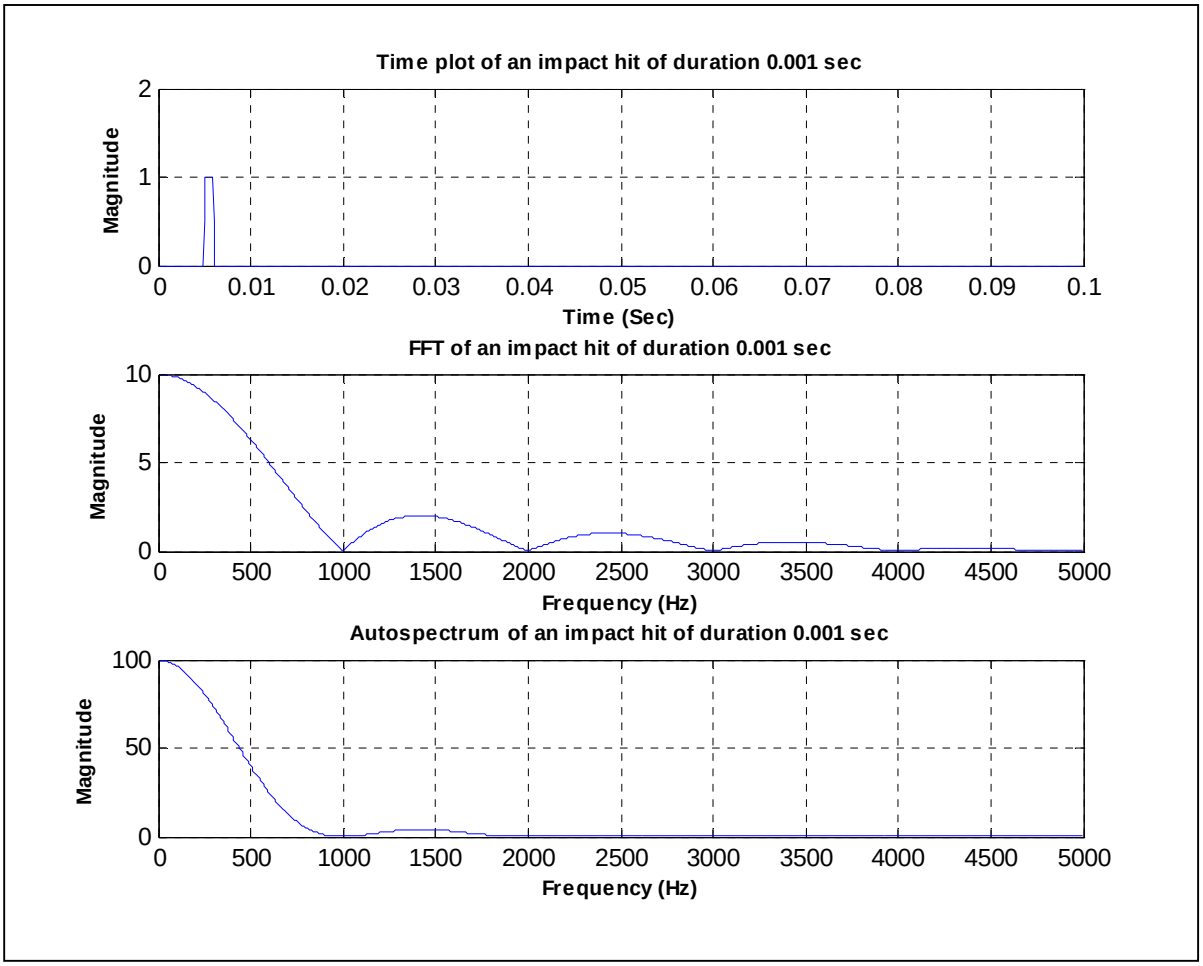

Figure 4 : Time plot, FFT and auto spectrum of an impact hit of duration 0.001 seconds

2.0 THEORY OF STATISTICAL ENERGY ANALYSIS

2.1 LITERATURE REVIEW

Statistical Energy Analysis was developed at a time when estimation of damping and other modal parameters were limited by the lack of computational resources and limitations of existing techniques. Estimation of damping and other modal parameters by classical methods, used widely then, were limited to well-defined and widely-spaced modes particularly at low frequencies. Even the computational models used then only predicted the modal parameters of the lower order modes of rather idealized (simplified) models of structures [15].

The aerospace and automotive industries have been the primary contributors to the development of new methods based on statistical averaging, both temporally and spatially, of response functions. Increasing complexity of structures, better damping predictions and the demand to predict parameters over a wide frequency range while simultaneously reducing the computational effort required lead to the development of Statistical Energy Analysis. The fundamental principle involved in S.E.A is the conservation of energy. Complex structures like aircraft wings and automobiles are described in S.E.A by a set of simple structures like plates and beams and by S.E.A parameters like loss factors and coupling loss factors.

The first paper on Statistical Energy Analysis was written by Lyon and Maidanik [16] who considered two linearly coupled oscillators. They reported that the power flow is directly proportional to the difference in the modal energy in the two oscillators and the direction of the power flow is dependent on the sign of the difference. Further developing it, they applied the idea to 2 multimodal systems which were randomly excited. They divided the structure into groups of modes in narrow frequency bands and enforced an energy balance in each frequency band independently.

The basic power flow equation given in reference [16] is

$$j_{12} = -j_{21} = g_{12}(\theta_1 - \theta_2) \tag{2.1}$$

Here,

j_{12}, j_{21} are the power flows between oscillators 1 and 2.

θ_1, θ_2 are the modal energies (defined as temperatures in the paper).

g_{12} is the coupling constant of proportionality which is dependent on the system parameters.

Modal energy is defined as the ratio between the total energy (E_i) in a frequency band to the number of modes (n_i) in that band.

$$\theta_i = \frac{E_i}{n_i} \tag{2.2}$$

Assumptions made in the formulation of Statistical Energy Analysis are as follows:

1. The structure of interest is divided into simple subsystems and an energy balance enforced in multiple frequency bands such that the modes in a particular band have the same energy.[16]
2. Since the energies are concentrated near natural frequencies, to get a better statistical estimate each frequency band should have a large number of modes.
3. The frequency band should not be so huge such that the modal energies vary significantly in a frequency band of interest.
4. The structure is assumed to be under a reverberant field, which is defined as a sound field which is dominated by reflected sound waves in which the flow of energy in all directions is equally probable.[17]

Initial work in S.E.A assumed a weak coupling between sub-systems. Ungar [18] applied S.E.A to a strongly coupled case. Gresch in 1968 [19] applied S.E.A to a system of 3 oscillators with non- conservative coupling between them.

The S.E.A method assumes the presence of steady state conditions, but Manning and Lee in [20] applied Statistical Energy Analysis to a transient case by adding an additional energy term to the basic SEA equation describing the power input into the system. Because of the time-varying nature of the transient problem, the energy of the system also changes with time. The time rate of change of energy term addresses this particular aspect of the transient case.

$$\pi_{in} = \frac{dE}{dt} + \omega\eta E \tag{2.3}$$

Here, π_{in} is the input power and is given by equation (2.8) and $\omega\eta E$ is the dissipated energy described by equation (2.12). Equation (2.3) is called the quasi-transient equation because of the addition of an additional energy term while simultaneously retaining steady state coefficients. Equation (2.1), which is applicable under steady-state conditions, is also assumed to be applicable in the transient case [21].

For a system with 2 oscillators, described by Figure 6, combining equations (2.3) and (2.1) we get,

$$\pi_{in} = \frac{dE}{dt} + \omega E_1(\eta_1 + \eta_{12}) - \omega E_2(\eta_{21}) \tag{2.4}$$

The above equation (2.4) describes the power flow in a structure having 2 sub-systems under a transient force.

Mercer [22] in 1971 developed an expression using perturbation analysis describing the energy flow between 2 oscillators connected by a weak coupling and under a transient load. He

concluded that the energy flow between the 2 oscillators is directly proportional to the energy difference and also the magnitude of the transient impact force.

Pinnington and Lednik [23] studied and compared the exact transient energy response of a 2 oscillator system with the results from quasi transient statistical energy analysis of a 2 oscillator system. They compared and reported that the peak levels, integral of the transmitted energy and the decay rates are similar for both the methods but the time taken to reach the peak level is less in the case of the quasi- transient statistical energy analysis (T.S.E.A) method.

Another approach to solve transient problems using the statistical energy analysis method was proposed by Lai and Soom [14]. They further improved equation (2.1) by using new "apparent time varying coupling loss factors" instead of steady state loss factors to describe the energy flow between any 2 oscillators so that all the parameters involved vary with time.

$$E_{21}^{tr}(t,\omega_c) = 2\omega_c(\eta_{21}(t,\omega_c)\varepsilon_2^k(t,\omega_c) - \eta_{12}(t,\omega_c)\varepsilon_1^k(t,\omega_c)) \tag{2.5}$$

Here,

$E_{21}^{tr}(t,\omega_c)$ is the energy transferred from oscillator 2 to oscillator 1 and is a function of the time and frequency band.

ω_c is the center frequency of the frequency band.

ε^k is the integrated kinetic energy.

$\eta_{ij}(t,\omega_c)$ is the apparent time varying coupling loss factor.

2.2 BASIC CONCEPTS

Statistical Energy Analysis deals with the flow on energy in a structure. It is based on the principle of conservation of energy which is "Energy can neither be created nor destroyed it can only be transformed from one state to another". Hence the energy imparted into a structure can

either be stored in it or has to be dissipated as heat. For example under transient conditions energy stored in the system varies but once steady state conditions are reached the energy stored in a system remains constant and all the energy imparted into the structure is dissipated.

2.2.1 STRUCTURE CONTAINING A SINGLE OSCILLATOR

Consider a single oscillator structure having a mass M, stiffness K and damping coefficient C. Under an applied random force $f(t)$, the equation of motion for a 1-DOF system is given by

$$M\ddot{x} + C\dot{x} + Kx = f(t) \tag{2.6}$$

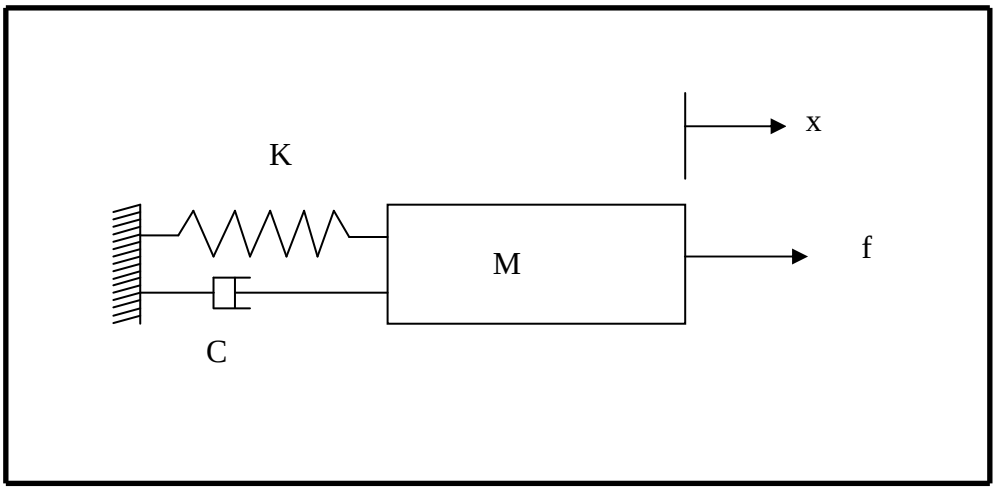

Figure 5 : Single degree of freedom oscillator

For a random force f (t), the time averaged power input is given by [24] as:

$$\pi_{in} = \lim_{T\to\infty} \frac{1}{2T} \int_{-T}^{T} f(t)v(t)dt \tag{2.7}$$

Here, $v(t)$ is the velocity of the oscillator. Applying Parseval's theorem and transforming to the frequency domain, we get

$$\pi_{in} = \frac{1}{2\pi} \int_{-\infty}^{\infty} F^{*}(\omega)V(\omega)d\omega \tag{2.8}$$

Here * denotes the complex conjugate of the force. Since power is a real quantity, equation (2.8) can be further reduced to:

$$\pi_{in} = \frac{1}{2\pi} \int_{-\infty}^{\infty} S_{FF} \, \mathrm{Re}(Y) d\omega \tag{2.9}$$

Here, Y is the mobility frequency response function (FRF). S_{FF} is the auto-spectrum of the force and is given by:

$$S_{FF} = F^{*}(\omega) F(\omega) \tag{2.10}$$

On further simplification, we get

$$\pi_{in} = \frac{C}{\pi} \int_{0}^{\infty} |Y|^2 \, S_{FF} d\omega \tag{2.11}$$

Equation (2.8) is used to calculate the experimental power input into the system from the measured data. The time-averaged power dissipated is given by the definition of loss factor given by (1.2) as

$$\pi_{diss} = \eta \omega E_{Total} \tag{2.12}$$

Assuming the kinetic energy is twice the total energy, we get the total energy as

$$E_{Total} = 2E_k = \lim_{T \to \infty} \frac{M}{2T} \int_{-T}^{T} v^2(t) dt \tag{2.13}$$

The relationship between the loss factor and damping coefficient given by

$$\eta = \frac{C}{M\omega} \tag{2.14}$$

Substituting equations (2.13) and (2.14) in equation (2.12), we get

$$\pi_{diss} = \lim_{T \to \infty} \frac{C}{2T} \int_{-T}^{T} v(t)^2 dt \tag{2.15}$$

Applying Parseval's theorem on equation (2.15) and transforming into frequency domain we get

$$\pi_{diss} = \frac{C}{2\pi} \int_{-\infty}^{\infty} V^*(\omega) V(\omega) d\omega \tag{2.16}$$

Equation (2.16) can be further simplified by using the following definition of Frequency Response Function (FRF), Y

$$|Y|^2 = \frac{S_{vv}}{S_{FF}} = \frac{V^*(\omega) V(\omega)}{F^*(\omega) F(\omega)} \tag{2.17}$$

$$\pi_{diss} = \frac{C}{\pi} \int_{0}^{\infty} |Y|^2 S_{FF} d\omega \tag{2.18}$$

Equations (2.11) and (2.18) prove the relationship between the power input and power dissipated to be

$$\pi_{in} = \pi_{diss} = \eta \omega E \tag{2.19}$$

2.2.2 STRUCTURE CONTAINING TWO OSCILLATORS

For a structure with two distinct sub-systems or oscillators, the energy balance equation consists of an additional term of the dissipated power at the junction of the two subsystems.

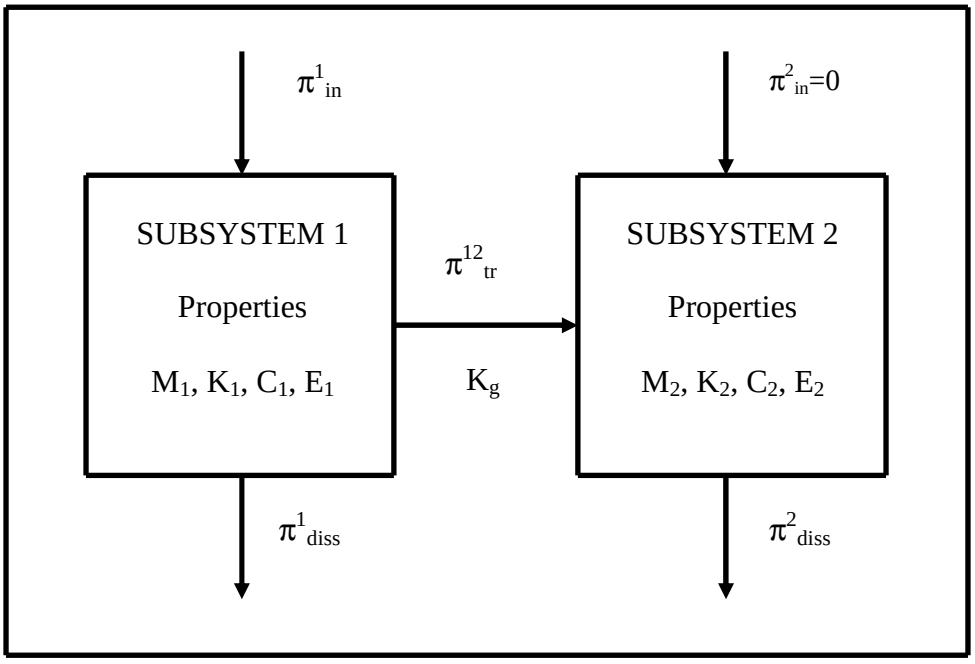

Figure 6 : Structure with 2 oscillators

Consider the structure in Figure 6. Oscillator 1 is excited by a force which imparts power π^1_{in} into the structure. Oscillator 2 is not excited by any external force and hence the power input into it is 0. At the intersection of the 2 oscillators there is a net energy flow from subsystem 1 to 2.

The formula for the transferred power is given by Powell [21] as

$$\pi_{tr}^{12} = \omega\eta_{12}(E_1 - E_2) \tag{2.20}$$

For a simple case of spring coupling between the oscillators, the equation of motion for a 2-degree of freedom system is given by

$$\begin{pmatrix} M_1 & 0 \\ 0 & M_2 \end{pmatrix}\begin{Bmatrix} \ddot{x}_1 \\ \ddot{x}_2 \end{Bmatrix}+\begin{pmatrix} C_1 & 0 \\ 0 & C_2 \end{pmatrix}\begin{Bmatrix} \dot{x}_1 \\ \dot{x}_2 \end{Bmatrix}+\begin{pmatrix} K_1+K_g & -K_g \\ -K_g & K_2+K_g \end{pmatrix}\begin{Bmatrix} x_1 \\ x_2 \end{Bmatrix}=\begin{Bmatrix} F \\ 0 \end{Bmatrix} \tag{2.21}$$

From the above equation, the force transferred can be represented by

$$F_{tr}^{12} = K_g x_1 \tag{2.22}$$

The power transferred can be calculated from the equation (2.22) as

$$\pi_{tr}^{12} = \frac{1}{2}K_g \dot{x}_2 x_1 = \frac{1}{2}C_2 S_{vv} = \pi_{diss}^2 \tag{2.23}$$

Thus, the power balance equations of the above structure can be represented as

$$\begin{aligned} \pi_{in}^1 &= \pi_{diss}^1 + \pi_{tr}^{12} \\ \pi_{diss}^2 &= \pi_{tr}^{12} \end{aligned} \tag{2.24}$$

2.2.3 SYSTEM OF 2 MULTIMODAL OSCILLATORS

For a system of multimodal oscillators, modal energy, which is defined as the total energy in a band divided by the number of modes in a band, instead of total energy, is the primary parameter of the energy balance equations. The power transferred depends on the difference between the modal energy and not the difference in the total energy. The formula to

calculate the modal energy from the total energy is given by equation (2.2) stated in the previous section.

Experimentally, measuring the total energy of the oscillator is difficult so the difference between the total energies can be substituted by twice the difference in the kinetic energies of the oscillators. This assumption is used in all works related to Statistical Energy Analysis.

Re-writing the equation (2.1) for multimodal structures, we get the total transferred energy as

$$\pi_{tr}^{12} = \sum_{n=1}^{N_1} \sum_{m=1}^{N_2} C_{mn}(\theta_{1,n} - \theta_{2,m}) \tag{2.25}$$

Upon simplifying the equation (2.25), we get the equation for the total power transferred as

$$\pi_{tr}^{12} = 2C_{12}N_1N_2(\frac{E_1^{\ k}}{N_1} - \frac{E_2^{\ k}}{N_2}) \tag{2.26}$$

In multimodal oscillators, loss factors and coupling loss factors are generally calculated in specific frequency bands having a finite number of modes. The bandwidth of a frequency band is selected such that all the modes in a band have almost equal modal energies. The coupling coefficients of all the modal interactions in a frequency band are of similar magnitude.

Since S.E.A is based on the assumption of the presence of a large number of modes, frequency bands having high modal densities give better results than bands at lower frequencies where the modes are sparsely populated. Hence S.E.A is better suited at higher frequency ranges.

Defining the coupling loss factors as $\eta_{12} = \frac{CN_2(\omega_c)}{\omega_c}$ and $\eta_{12} = \frac{CN_2(\omega_c)}{\omega_c}$, we get the relationship between the transferred power, the kinetic energies of the oscillators and the coupling loss factors η_{12} and η_{21} in a frequency band of bandwidth $\Delta\omega$ and center frequency ω_c as

$$\pi_{tr}^{12}(\omega_c) = 2\omega_c(\eta_{12}(\omega_c)E_1^k(\omega_c) - \eta_{21}(\omega_c)E_2^k(\omega_c)) \tag{2.27}$$

Here, $E^k(\omega_c)$ is the kinetic energy in a frequency band centered at ω_c .

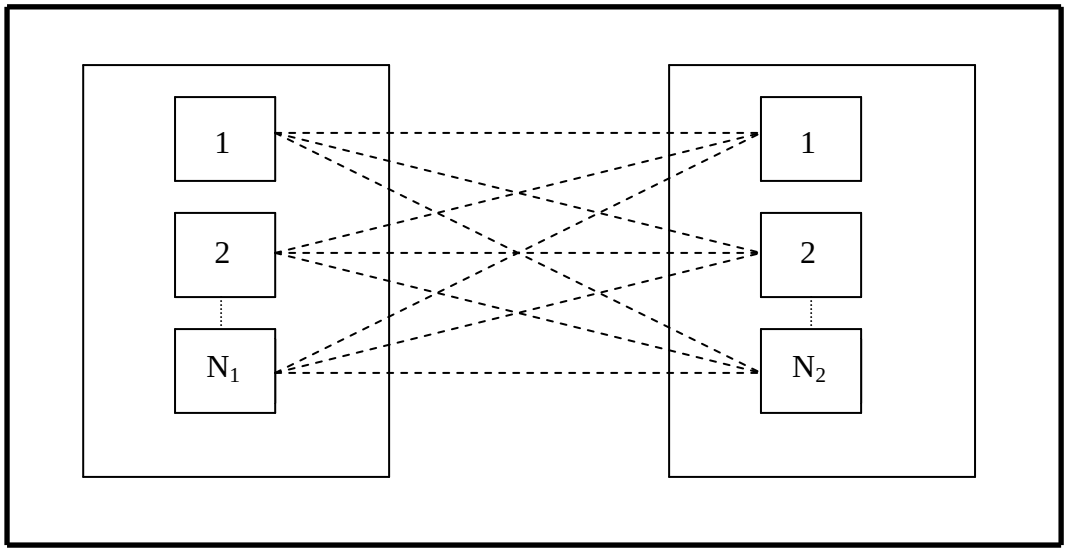

Figure 7 : Interaction of modes in multi-modal sub-systems from reference[1]

The coupling loss factors η_{12} and η_{21} are related to each other by the consistency relation given in [25]. For $i \neq j$, we have

$$n_i \eta_{ij} = \eta_{ji} n_j \tag{2.28}$$

Where, n_i and n_j are the modal densities of subsystems i and j respectively.

2.3 DEVELOPMENT OF THE POWER INPUT METHOD (TRADITIONAL SEA)

As defined in Chapter 1, the Power Input Method is based on the very definition of loss factor. For a structure with a single oscillator, the equation for the P.I.M can be derived from equation (2.19) as

$$\eta = \frac{\pi_{in}}{\omega E_{Total}} = \frac{E_{in}}{\omega \varepsilon_{Total}} = \frac{\pi_{in}}{2\omega E^k} = \frac{E_{in}}{2\omega \varepsilon^k} \tag{2.29}$$

The power input to a structure can be calculated from experimental data using equation (2.8). The kinetic energy of the system can be from the velocity data calculated as

$$E^k = \frac{M}{2\pi}\int_{-\infty}^{\infty} S_{vv}\, d\omega \tag{2.30}$$

Combining equations (2.29), (2.30), (2.9) we get

$$\eta = \frac{\int_{-\infty}^{\infty} S_{FF}\,\mathrm{Re}(Y)\, dw}{M\omega\int_{-\infty}^{\infty} S_{vv}\, d\omega} \tag{2.31}$$

Similarly, for a system with two oscillators the formula to estimate the loss factors and coupling loss factors can be derived from equation (2.24) stated in the previous section.

Combining equations (2.12), (2.24), (2.20) and (2.28) we get the formula for the power input method for a 2 oscillator system as

$$\begin{aligned} \pi_{in}^1 &= 2\left[\eta_1\omega E_1^k + \omega\eta_{12}E_1^k - \omega\eta_{21}E_2^k\right] \\ \pi_{in}^2 &= 2\left[\eta_2\omega E_2^k + \omega\eta_{21}E_2^k - \omega\eta_{12}E_1^k\right] \end{aligned} \tag{2.32}$$

Equation (2.32) can be represented in matrix form by

$$\begin{Bmatrix} \pi_{in}^1 \\ \pi_{in}^2 \end{Bmatrix} = 2\omega \begin{bmatrix} \eta_1 + \eta_{12} & -\eta_{21} \\ -\eta_{12} & \eta_2 + \eta_{21} \end{bmatrix} \begin{Bmatrix} E_1^k \\ E_2^k \end{Bmatrix} \tag{2.33}$$

For multimodal systems, where the frequency range of interest is divided into bands, and for the ease in calculation of the loss factors, i.e. directly using matrix inversion techniques, the equation (2.33) can be modified to include power input to both systems as

$$\begin{bmatrix} \pi_{in}^{1,I} & 0 \\ 0 & \pi_{in}^{2,II} \end{bmatrix} = 2\omega_c \begin{bmatrix} \eta_1 + \eta_{12} & -\eta_{21} \\ -\eta_{12} & \eta_2 + \eta_{21} \end{bmatrix} \begin{bmatrix} E_{1,I}^k & E_{1,II}^k \\ E_{2,I}^k & E_{2,II}^k \end{bmatrix} \tag{2.34}$$

The Roman numeral I denotes that the power input is supplied to the subsystem 1and no power is imparted into subsystem 2.Similarly, II denotes the power input is supplied only to the subsystem 2. ω_c is the center frequency of the frequency band of width $\Delta\omega$.

Equations (2.30), (2.8) calculate the kinetic energy and the power input for the whole frequency range. The power input and kinetic energy for in a frequency band of width $\Delta\omega$ and center frequency ω_c are given by

$$\begin{aligned} \pi_{in} &= \frac{1}{\pi}\int_{\omega_c-\Delta\omega/2}^{\omega_c+\Delta\omega/2} F^*(\omega)V(\omega)d\omega \\ E^k &= \frac{M}{2\pi}\int_{\omega_c-\Delta\omega/2}^{\omega_c+\Delta\omega/2} S_{vv}d\omega \end{aligned} \tag{2.35}$$

Generalizing the power input method to include N Multimodal Systems, the power balance equations [26] become

$$\begin{bmatrix} \pi_{in}^{1,I} & 0 & \dots & 0 \\ 0 & \pi_{in}^{2,II} & \dots & 0 \\ \vdots & \vdots & \ddots & \vdots \\ 0 & 0 & \cdots & \pi_{in}^{N,N} \end{bmatrix} = 2\omega_c \begin{bmatrix} \eta_1 + \sum_{i\neq 1 i=1}^{N}\eta_{1i} & -\eta_{21} & \cdots & -\eta_{N1} \\ -\eta_{12} & \eta_2 + \sum_{i\neq 2 i=1}^{N}\eta_{2i} & \cdots & -\eta_{N2} \\ \vdots & \vdots & \ddots & \vdots \\ -\eta_{1N} & -\eta_{2N} & \cdots & \eta_N + \sum_{i\neq N i=1}^{N}\eta_{Ni} \end{bmatrix} \begin{bmatrix} E_{1,I}^k & E_{1,II}^k & \cdots & E_{1,N}^k \\ E_{2,I}^k & E_{2,II}^k & \cdots & E_{2,N}^k \\ \vdots & \vdots & \ddots & \vdots \\ E_{N,I}^k & E_{N,II}^k & \cdots & E_{N,N}^k \end{bmatrix} \tag{2.36}$$

The above equation can be written in a compact form as

$$[\pi_{in}] = 2\omega_c [\eta]\left[E^k\right] \tag{2.37}$$

Or, in terms of the loss factor matrix, equation (2.37) can be written as

$$[\eta] = \frac{1}{2\omega_c}[\pi_{in}]\left[E^k\right]^{-1} \tag{2.38}$$

Here, η is the Loss Factor Matrix, ω_c is the center frequency, π_{in} is the input power matrix and E^k is the Kinetic energy matrix.

The power input method has been successfully used to predict the loss factors and the coupling loss factors of several systems throughout the years. Bies and Hamid [27] in 1980 applied the power input method to calculate the in situ coupling loss factors and loss factors between two rectangular plates with non parallel edges. They concluded that good agreement was obtained between measured values and predicted values.

Carfagni and Pierini [28] applied the power input method to various plates of different sizes with constrained layer damping. The plate was excited with an impact hammer. They noted that to achieve good results using the power input method the following guidelines have to be followed.

1. The input point mobility should be measured with utmost precision because errors in its measurement lead to incorrect loss factors, which was also noted by [29].
2. Multiple taps must be avoided. Taps must be made perpendicularly and always at the same point on the plate.
3. The excitation point should not be along a node line or along the edges of the plate to avoid local edge effects.

Carfagni et al. [30] also conducted the same experiments using a shaker to simulate steady state conditions and to reduce the errors due to hammer excitation. References [30] and [28] concluded that loss factors are dependent more on the damping added than on the size of the plates. They also noted that the quality of loss factor measured can be improved by increasing the number of measurement points.

Liu and Ewing [8] recommended that errors due to specimen /excitation source interaction can be decreased by using long stingers, light weight and small shakers, and high spatial discretization.

Panuszka et al. in their paper [31] presented the effect of joints on the coupling loss factor measured. They showed that the measured coupling loss factors depend on both the position and the number of point joints. The measured coupling loss factors increase with an increase in the number of point joints. They also showed that the measured coupling loss factors depend on the thicknesses of the plates.

2.3.1 PRACTICAL LIMITATIONS

Even though the Power Input Method (P.I.M) has no theoretical limitations it is practically limited to the range of $0.1<\eta<0.001$ [32].

The reasons given were

a) For high damping levels, a large number of measurement points are required to correctly capture the reverberant field in the structure.
b) For low damping levels, minute phase errors in the measured data lead to negative loss factors.

It has been shown in [5] that Power input method can be used for increasingly heavily damped structures by considering the response of increasingly more points on the structure.

Minute phase errors lead to an incorrect input cross spectrum, which is given in terms of the Fourier transform of the force and velocity by

$$S_{FV} = F^{*}(\omega)V(\omega) \tag{2.39}$$

As shown in Figure 8, phase errors result in negative power input in certain frequency bands which result in negative (or incorrect) loss factors. Phase changes occur rapidly as a structure undergoes resonance and the phase changes occur over a very small frequency range in lightly damped structures which are difficult to resolve well [1]. Phase errors can be eliminated by minimizing measurement noise and by improving the frequency resolution. It is shown in this thesis that selecting the correct frequency resolution is directly related to the quality of the loss factor estimated.

The power input method is also not suitable for systems having many subsystems because of the complexity in inverting the large kinetic energy matrix given by equation (2.36)[29].

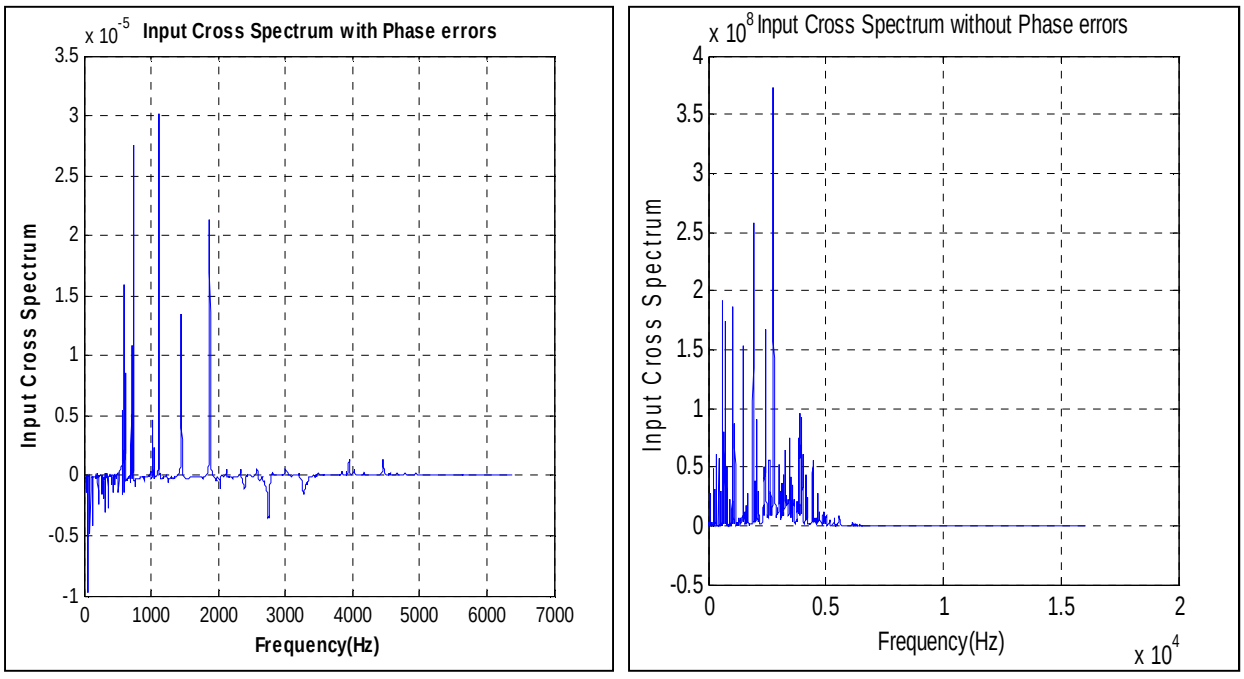

Figure 8 : Changes in input cross spectrum because of phase errors

2.4 DEVELOPMENT OF THE TRANSIENT STATISTICAL ENERGY ANALYSIS (LAI AND SOOM) METHOD

Statistical Energy Analysis was first applied to the transient case by Manning and Lee. They investigated a transient problem by adding a time varying energy term to the power balance equations. Even though the power input and the energy of the sub-systems change with time they used steady state coupling loss factors to relate the two terms. Manning and Lee's formulation to solve for the S.E.A parameters for a single oscillator case is given by equation (2.3) and is restated here.

$$\pi_{in} = \frac{dE}{dt} + \omega\eta E \tag{2.40}$$

The term $\frac{dE}{dt}$ is the instantaneous change in total energy of the oscillator.

For the 2-oscillator case, as described by Figure 6, the power balance equations for the transient case can be given as

$$\begin{aligned} \frac{dE_1}{dt} &= \pi_{in}^1 - \pi_{diss}^1 + \pi_{tr}^{12} \\ \frac{dE_2}{dt} &= \pi_{in}^2 - \pi_{diss}^2 + \pi_{tr}^{12} \end{aligned} \tag{2.41}$$

Here, E_1 is the total energy of oscillator 1, π_{in}^1 is the power input into oscillator 1, π_{diss}^1 is the power dissipated by oscillator 1 and π_{tr}^{12} is the power transferred from oscillator 1 to oscillator 2. Integrating the equations (2.41) with respect to time gives us the energy balance relationship between the oscillators.

$$\begin{aligned} \frac{d\varepsilon_1(t)}{dt} &= E_{in}^1(t) - E_{diss}^1(t) + E_{tr}^{12}(t) \\ \frac{d\varepsilon_2(t)}{dt} &= E_{in}^2(t) - E_{diss}^2(t) + E_{tr}^{12}(t) \end{aligned} \tag{2.42}$$

Here, $\varepsilon_1(t)$ is the integrated total energy of oscillator 1, $E_{in}^1(t)$ is the energy input into oscillator 1, $E_{diss}^1(t)$ is the energy dissipated by oscillator 1 and $E_{tr}^{12}(t)$ is the energy transferred from oscillator 1 to oscillator 2.

The energy transferred between the oscillators is related to the difference between the integrated kinetic energy of 2 oscillators by a coupling coefficient. Manning and Lee used the steady state coupling coefficient to describe the energy transferred. In the T.S.E.A method, proposed by Lai and Soom, because of the time varying nature of the energy terms, a new coupling coefficient termed as the-"apparent time varying coupling coefficient" is used[26]:

$$E_{tr}^{12}(t) = 2C_{12}(t)\left(\varepsilon_1^k(t) - \varepsilon_2^k(t)\right) \tag{2.43}$$

Here, $C_{12}(t)$ is the "apparent time varying coupling coefficient" and $\varepsilon_1^k(t)$ is the integrated kinetic energy of oscillator 1. $C_{12}(t)$ will asymptotically approach a constant value denoted by C which is the coupling coefficient used by Manning and Lee.

2.4.1 MULTIMODAL SYSTEMS

For multimodal systems as described by Figure 7, the energy balance equations in a frequency band of width $\Delta\omega$ and center frequency ω_c are given by

$$\begin{aligned}\frac{d\varepsilon_1(t,\omega_c)}{dt} &= E_{in}^1(t,\omega_c) - E_{diss}^1(t,\omega_c) + E_{tr}^{12}(t,\omega_c)\\ \frac{d\varepsilon_2(t,\omega_c)}{dt} &= E_{in}^2(t,\omega_c) - E_{diss}^2(t,\omega_c) + E_{tr}^{12}(t,\omega_c)\end{aligned} \tag{2.44}$$

For multimodal systems, every mode interacts with every other mode. Hence to calculate the energy transferred in a frequency band the energy transferred between the individual modes can be directly summed. This leads to an expression which is similar to the power transferred given by equation (2.25).

$$E_{tr}^{12}(t,\omega_c)=\sum_{n=1}^{N_1}\sum_{m=1}^{N_2}C_{mn}(t)(\varepsilon_{1,n}(t)-\varepsilon_{2,m}(t)) \tag{2.45}$$

Here, $\varepsilon_{1,n}(t)$ is the integrated modal energy of the mode n of the oscillator1.

A couple of assumptions are made to further simplify equation (2.45). They are

1. Integrated modal energies up to time t in a band with bandwidth $\Delta\omega$ and center frequency ω_c are assumed to be equal.[26]
2. The energy stored in the physical coupling, for example a series of rivets or a bolted joint, is small when compared to the total energy transferred from one oscillator to the other. This assumption leads us to the relationship between the coupling coefficients as

$$C_{mn}(t)=C_{nm}(t) \tag{2.46}$$

By using the above 2 assumptions and using the value for the kinetic energy in the band instead of the total energy we have

$$E_{tr}^{12}(t,\omega_c)=2<C(t,\omega_c)>N_1N_2(\frac{\varepsilon_1^k(t,\omega_c)}{N_1}-\frac{\varepsilon_2^k(t,\omega_c)}{N_2}) \tag{2.47}$$

Here, $<C(t,\omega_c)>$ is the statistical mean of the "apparent time varying coupling coefficient". N_1 and N_2 are the number of modes in a given band.

Defining the "apparent time varying coupling loss factors" $\eta_{12}(t,\omega_c)$ and $\eta_{21}(t,\omega_c)$ as

$$\begin{aligned}\eta_{12}(t,\omega_c)&=\frac{<C(t,\omega_c)>N_2}{\omega_c}\\ \eta_{21}(t,\omega_c)&=\frac{<C(t,\omega_c)>N_1}{\omega_c}\end{aligned} \tag{2.48}$$

Equation (2.47) reduces to the form

$$E_{tr}^{12}(t,\omega_c)=2\omega_c(\eta_{12}(t,\omega_c)\varepsilon_1^k(t,\omega_c)-\eta_{21}(t,\omega_c)\varepsilon_1^k(t,\omega_c)) \tag{2.49}$$

The "apparent time varying coupling loss factors" are related by the compatibility relationship, which is similar to the compatibility relationship between steady state loss factors given by (2.28), as

$$n_1\eta_{12}(t,\omega_c) = n_2\eta_{21}(t,\omega_c) \tag{2.50}$$

Here, $n_1 = \frac{N_1}{\Delta\omega}$ is the modal density of oscillator 1 in a frequency band of width $\Delta\omega$.

The energy dissipated is also similar to equation (2.12) and can be given as

$$E_{diss} = 2\eta\omega\varepsilon^k(t,\omega_c) \tag{2.51}$$

Combining equations (2.44), (2.49), (2.51) we get the instantaneous response, or rate of change of the kinetic energy, as

$$\frac{d\varepsilon_1(t,\omega_c)}{dt} = E_{in}^1(t,\omega_c) - 2\eta_1\omega_c\varepsilon_1^k(t,\omega_c) + 2\omega_c(\eta_{12}(t,\omega_c)\varepsilon_1^k(t,\omega_c) - \eta_{21}(t,\omega_c)\varepsilon_1^k(t,\omega_c)) \tag{2.52}$$

The "apparent time varying coupling loss factor" can calculated from equation (2.49). In a 2-oscillator system, a transient force is first applied only to oscillator 1 and the energy stored in both of the oscillators and the transferred energies are measured. Then the transient force is applied to oscillator 2 and the energies are measured in a similar fashion. The transferred energies thus measured in both the above cases, coupled with the relationship given in (2.45) can be used to calculate the coupling loss factors as

$$2\omega_c\begin{bmatrix}\varepsilon_{1,I}^k(t,\omega_c) & -\varepsilon_{2,I}^k(t,\omega_c)\\ \varepsilon_{1,II}^k(t,\omega_c) & -\varepsilon_{2,II}^k(t,\omega_c)\end{bmatrix}\begin{Bmatrix}\eta_{12}(t,\omega_c)\\ \eta_{21}(t,\omega_c)\end{Bmatrix} = \begin{Bmatrix}E_{tr}^{12,I}\\ E_{tr}^{12,II}\end{Bmatrix} \tag{2.53}$$

Or, in compact form equation (2.53) can be represented as

$$2\omega_c \left[\varepsilon^k\right]\{\eta\} = \{E_{tr}\} \tag{2.54}$$

Here,

$\{\eta\}$ is the apparent time varying coupling loss factor matrix.

$\{E_{tr}\}$ is the transferred energy matrix.

$\left[\varepsilon^k\right]$ is the integrated kinetic energy matrix.

Lai and Soom[14] have shown that the time varying loss factors asymptotically approach the values computed in a steady state SEA.

2.4.2 CALCULATION OF ENERGY TERMS FROM EXPERIMENTAL DATA

The energy terms used in the T.S.E.A. method are functions of both time and frequency. To calculate the energy of an oscillator up to a time t, only the experimental data up to time t has to be involved in the calculations and the remaining data has to be converted into zeros. (This is called zero padding the data)

The formula to calculate the integrated kinetic energy in the time domain is

$$\varepsilon^k(t) = \frac{M}{2}\int_{-\infty}^{\infty} v(\tau)v_t(\tau)d\tau \tag{2.55}$$

Where, $v_t(\tau) = v(\tau)$ when $\tau \le t$ and $v_t(\tau) = 0$ when $\tau \ge t$

Applying Parsevals theorem and transforming into the frequency domain, and calculating the kinetic energy in a frequency band $\Delta\omega$ centered at ω_c we have the kinetic energy as

$$\varepsilon^k(t,\omega_c) = \frac{M}{2\pi}\int_{\omega_c - \Delta\omega/2}^{\omega_c + \Delta\omega/2} \mathrm{Re}\left\{v(\omega)v_t^*(\omega)\right\}d\omega \tag{2.56}$$

When the experimental data is in acceleration terms then equation (2.56) has to be changed into acceleration terms as

$$\varepsilon^k(t,\omega_c) = \frac{M}{2\pi}\int_{\omega_c-\Delta\omega/2}^{\omega_c+\Delta\omega/2} \frac{\mathrm{Re}\left\{A(\omega)A_t^*(\omega)\right\}}{\omega^2}\,d\omega \tag{2.57}$$

Similarly the energy transferred can be calculated as

$$\begin{aligned}\varepsilon_{tr}(t,\omega_c) &= \frac{1}{\pi}\int_{\omega_c-\Delta\omega/2}^{\omega_c+\Delta\omega/2} \mathrm{Re}\left\{F_t(\omega)v^*(\omega)\right\}d\omega \\ \varepsilon_{tr}(t,\omega_c) &= \frac{1}{\pi}\int_{\omega_c-\Delta\omega/2}^{\omega_c+\Delta\omega/2} \mathrm{Im}\left\{F_t(\omega)\frac{A^*(\omega)}{\omega}\right\}d\omega\end{aligned} \tag{2.58}$$

2.4.3 PRACTICAL LIMITATIONS

The T.S.E.A. Method proposed by Lai and Soom [14] can theoretically be used in all frequency ranges and for a variety of fixtures, but the practical usage of this method is limited. Since the energy transferred between 2 subsystems is the core measurement used in the estimation of loss factors, the method is practically limited to only those junctions where the energy transferred can be explicitly measured. In particular it can be used at point junctions where a force transducer can be placed to measure the force transferred but cannot be used at line junctions.

Another limitation to this method is that the method is overly dependent on the junction properties. Any flexibility at the point junction might cause the assumption of zero coupling energy which can cause the energy transferred, given by the equation (1.7), to be negative leading to estimation of negative coupling loss factors at those frequencies.

3.0 EXPERIMENTAL SETUP

The Experimental setup is as shown in the figures below. The test setup consists of

1. Data acquisition unit – An 8 channel Data Physics Signalcalc Mobilyzer Model -70502.
2. Work station with Data Physics SignalCalc 730 Dynamic Signal Analyzer software.
3. Shaker – Ling Model number V203.
4. Power Amplifier – LDS Model number PA25E.
5. Modally Tuned Hammer – PCB Model number 086C03.
6. 7 Accelerometers – PCB Model number 352A71.
7. 2 Force Transducers – PCB Model number 208A02, PCB 708A50.
8. Signal conditioner – 16 channel PCB ICP Model number 584.

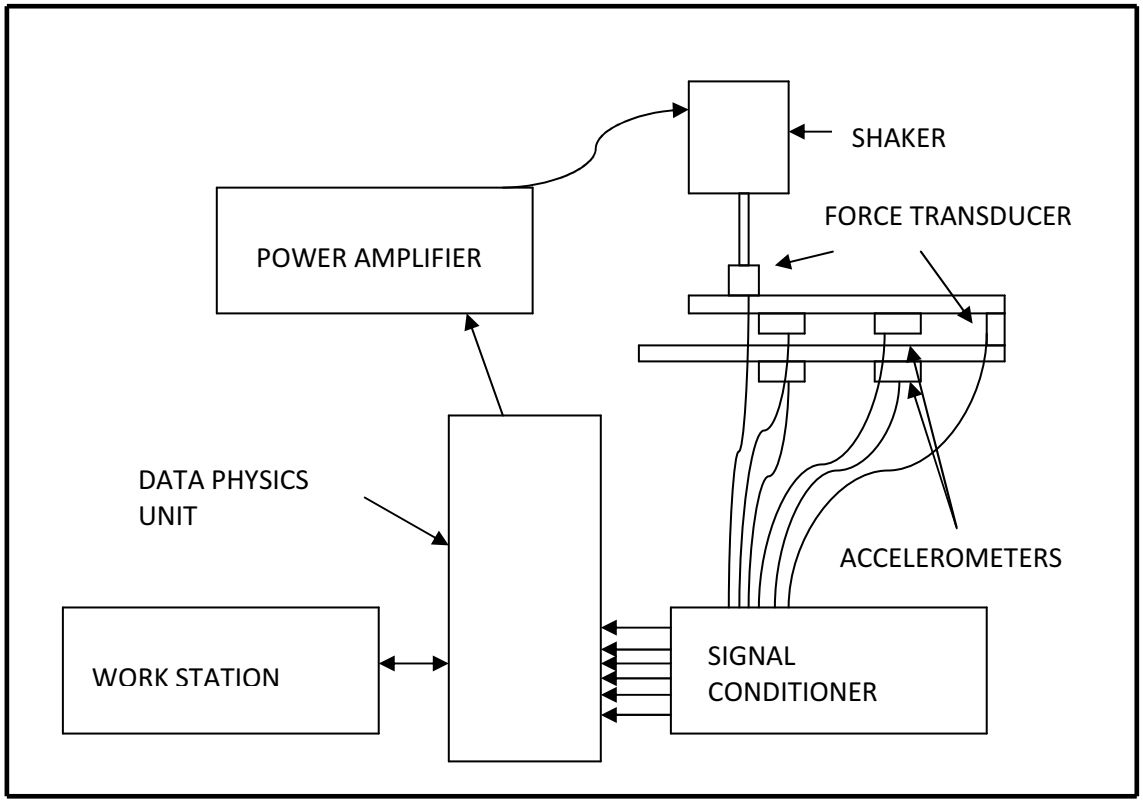

Figure 9 : Experimental setup – Persistent excitation

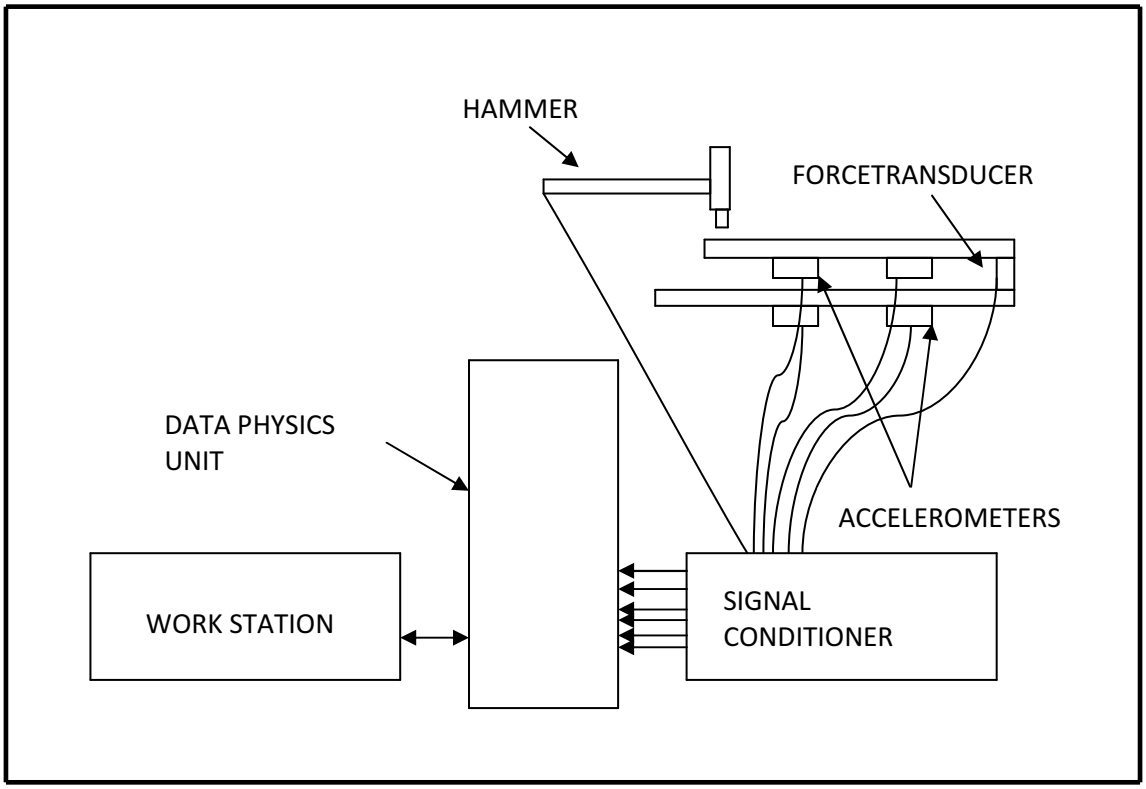

Figure 10 : Experimental setup – Transient excitation

The test article is excited either using a hammer to induce transient conditions or by a shaker with a pseudo random excitation to induce steady state conditions. The workstation is loaded with the Data Physics SignalCalc 730 Dynamic Signal Analyzer software which controls the Data Physics Signalcalc Mobilyzer unit. The Data Physics Signalcalc Mobilyzer has both input channels for data acquisition and output channels through which it can send a drive signal to the shaker. This signal is passed through a power amplifier so that the test article is sufficiently excited at all the frequencies. The shaker is connected to the test article using a thin stinger and a force transducer, which measures the force input into the system. Accelerometers are placed on the other side of the test article to measure the accelerations of the plate. A force transducer is used to connect the 2 plates and since it is in the load path it measures the force transferred

between the 2 subsystems. These measurements are filtered to ensure that no aliasing takes place. To maintain consistency in the units involved, the data measured is converted into and saved in SI units.

To simulate transient conditions the test article is excited with a hammer. The hammer is directly connected to the signal conditioner and does not require any input signals. The tip of the hammer can be changed depending on the frequencies that are to be excited. The plates are suspended from a stiff frame with two steel strings per plate, giving essentially “free” boundary conditions with regard to out of plane vibrations [33].

To test the effect of damping on the estimation of loss factors and coupling loss factors, visco-elastic damping (3M-F9469PC) is added to the test articles. A constraining layer, in this case a brass sheet with thickness between 0.005 inches and 0.010 inches, is rolled over the visco-elastic layer to create an efficient constrained layer damping treatment. The excitation point is then chosen away from the axes of symmetry and anti-symmetry of the plate to be sure that all the high energy (low frequency) modes are sufficiently excited. As a matter of practicality the excitation point is not located on a visco-elastic layer to provide loading directly to the plates.

3.1 EXPERIMENTAL PLATES

The test articles are two aluminum plates (see Table 2) joined at a point by a force transducer. The force transducer is bolted to both the plates thus forming a physical bond between the 2 plates. These plates are called as the “Lai and Soom Plates” in this thesis as these plates were constructed to be as similar as possible to the plates used by Lai and Soom. Constrained layer damping is added on the back side of the plates and measurements are taken on the front side. The placement of the damping layers is described in Appendix B.

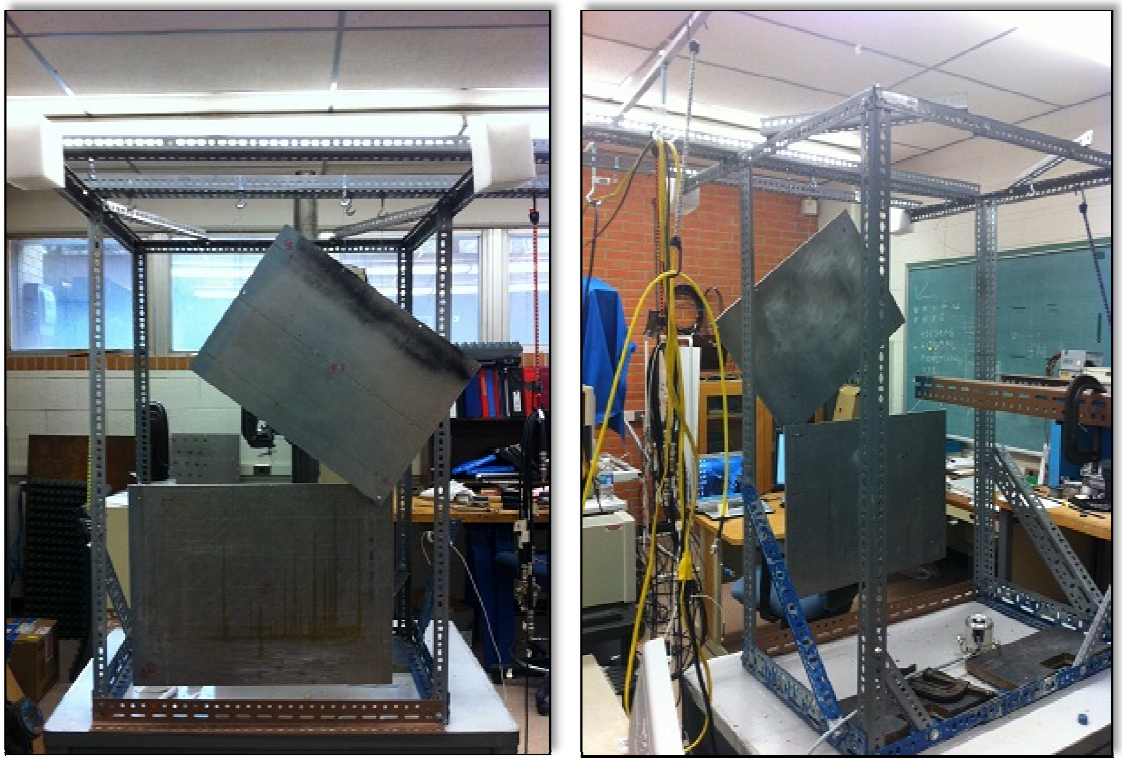

Figure 11 : Experimental plate setup – Plates joined at a point, No Damping added

TABLE 1 : PROPERTIES OF THE EXPERIMENTAL PLATES

CASES	DAMPING LAYER THICKNESS (cm)	CONSTRAINING LAYER VOLUME (cm^3)	MASS (g)
NO DAMPING ADDED	DAMPING NOT ADDED	CONSTRANING NOT ADDED	Plate1 : 4808 Plate2 : 3628
2 SHEETS OF DAMPING	3M F9469 PC 2 x 0.0127	BRASS SHEET 2 x 25.4 x 4.95 x 0.254	Plate1 : 4844 Plate2 : 3670
6 SHEETS OF DAMPING	3M F9469 PC 6 x 0.0127	BRASS SHEET 6 x 25.4 x4.95 x 0.254	Plate1 : 4925 Plate2 : 3752

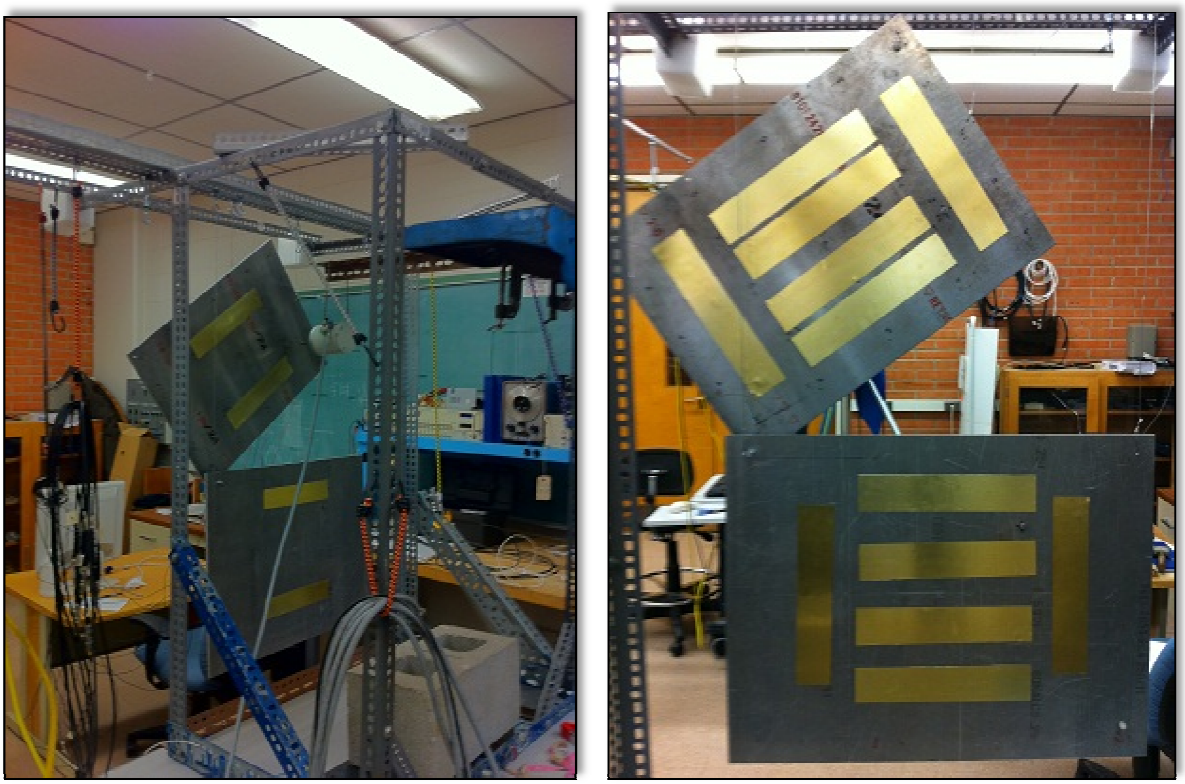

(a) 2 sheets of damping **(b) 6 sheets of damping**

Figure 12 : Aluminum plates with partial damping added

TABLE 2 : SPECIFICATIONS FOR THE EXPERIMENTAL PLATES

PLATE	MATERIAL	DIMENSIONS (m^3)
1	ALUMINUM AL CLAD 2024-T3 Thickness = 0.64 cm Elastic Modulus = 70 GPa Density = 2.7e3 Kg/m^3	0.61 x 0.47 x 0.00635
2		0.53 x 0.38 x 0.0065

4.0 ESTIMATION OF LOSS FACTORS USING THE POWER INPUT METHOD

4.1 NUMERICAL SIMULATION OF A SIMPLE 2-DOF SYSTEM

Consider a simple 2-DOF system as shown in Figure 13 below. The system consists of 2 oscillators joined together by a spring coupling K_c. This configuration is one of the simplest examples of a multiple degree of freedom system. Oscillator 1 consists of the mass M_1, spring with stiffness K_1 and a damper with coefficient C_1. Oscillator 2 consists of the mass M_2, spring with stiffness K_2 and a damper with coefficient C_2. The two masses M_1 and M_2 are free to move in only one direction, x, as shown in the figure. If a force is applied on any one of the oscillators, energy flows to the other through the spring coupling between them.

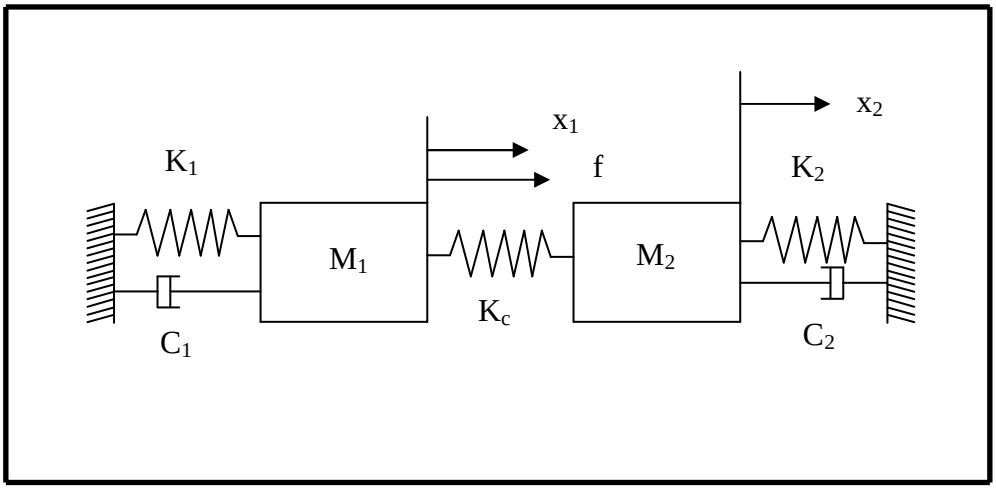

Figure 13 : Two degree of freedom oscillator

Summing the forces acting in the x direction, the equation of motion for the above system is given by equation (2.21) and restated here.

$$\begin{pmatrix} M_1 & 0 \\ 0 & M_2 \end{pmatrix}\begin{Bmatrix} \ddot{x}_1 \\ \ddot{x}_2 \end{Bmatrix}+\begin{pmatrix} C_1 & 0 \\ 0 & C_2 \end{pmatrix}\begin{Bmatrix} \dot{x}_1 \\ \dot{x}_2 \end{Bmatrix}+\begin{pmatrix} K_1+K_c & -K_c \\ -K_c & K_2+K_c \end{pmatrix}\begin{Bmatrix} x_1 \\ x_2 \end{Bmatrix}=\begin{Bmatrix} f \\ 0 \end{Bmatrix} \tag{4.1}$$

In matrix form the above equation (4.1) can be written as

$$[M]\{\ddot{x}\}+[C]\{\dot{x}\}+[K]\{x\}=\{F\} \tag{4.2}$$

This system of ordinary differential equations can be solved to give the velocities and displacements of the two oscillators. The system of ODE's can be solved either directly as a system of ODE's or by using the state matrix method described in [34].

A sample problem with given input loss factors is numerically solved with the power input method to estimate the loss factors and check for the differences between the estimated and the loss factors used to develop the model described by equation (4.2). The properties of the sample 2-DOF system are as follows. The masses M_1 and M_2 are 1 Kg each. The natural frequencies ω_{n1} and ω_{n2} are 149.8 radians/s and 200.1 radians/s respectively. The spring coupling K_c is 1000N/m. The spring stiffness K_1 and K_2 are 22500N/m and 40000N/m respectively. The blocked natural frequencies of the oscillators are ω_1=150 radians/s and ω_2=200 radians/s respectively. As there is no damping coupling involved at the junction of the two oscillators and since the spring coupling is an order of magnitude lower than the stiffness of the oscillators the junction is an example of a weak conservative coupling. The relationship between the K_{11} and the K_{22} terms of the stiffness matrix and the natural frequencies of the oscillators is given by

$$K_1 + K_c = \omega_{n1}^2 M_1 \tag{4.3}$$

The oscillator loss factors, η_1 and η_2, are the variables in this numerical simulation and are equal to 0.75, 0.075, 0.001 for three different cases. The oscillators are excited by rectangular pulse force of magnitude $\frac{(\delta(t)-\delta(t-\Delta t))}{\Delta t}$ with duration of 0.001 second to simulate transient conditions. Here, δ is the Dirac-delta function. To simulate steady state conditions the system is

excited by a random force (force with a constant spectral density and random phase) as shown in Figure 3.

The 2-DOF system is solved for the deflections x_1 and x_2 using the built-in ODE45 solver in Matlab. The formula to estimate the loss factors of the above simple system is given by equation (2.34). The force is first applied only on the oscillator 1 and the system response is calculated and saved. The force is then applied only on the second oscillator and the response of the whole system is calculated and saved. The procedure to solve for the system characteristics is as follows.

Consider the equation (2.8), which is the equation of motion of the any 2-DOF system. Pre-multiplying the equation (2.41) by $[M]^{-1}$ yields

$$\{\ddot{x}\}+[M]^{-1}[C]\{\dot{x}\}+[M]^{-1}[K]\{x\}=[M]^{-1}\{F\} \tag{4.4}$$

This system of second order differential equations can be converted into an equivalent system of four first-order ODE's by substituting the following equation (2.45) into equation (2.8).

$$\begin{aligned}\{\dot{y}_1\}&=\{\dot{x}\}\\ \{\dot{y}_2\}&=\{\ddot{x}\}\end{aligned} \tag{4.5}$$

Here, $\{y_1\},\{y_2\},\{x\}$ are all 2 x 1 matrices. The relationship between $\{y_1\},\{y_2\}$ is given by

$$\{\dot{y}_1\}=0\{y_1\}+I\{y_2\} \tag{4.6}$$

Rearranging the terms in the equation (4.4) and combining the equations (4.6) and (4.4) results in

$$\begin{Bmatrix} \dot{y}_1 \\ \dot{y}_2 \end{Bmatrix} = \begin{bmatrix} [0] & [I] \\ -[M]^{-1}[K] & -[M]^{-1}[C] \end{bmatrix} \begin{Bmatrix} y_1 \\ y_2 \end{Bmatrix} + \begin{Bmatrix} \{0\} \\ [M]^{-1}\{F\} \end{Bmatrix} \tag{4.7}$$

This approach is called the state- matrix approach [34]. Solving equation (4.7) results in the calculation of displacements and velocities of both the oscillators. Substituting the calculated velocity into the equations (2.34), (2.35) leads us to the estimated loss factors using the power input method. As the loss factor of an oscillator can be correctly estimated only near a natural frequency the power input method can be applied to above system only at 2 natural frequencies of the oscillators to estimate the correct value of the loss factor that is used to model the system.

The main aim of this numerical simulation is to check for the relationship between the frequency resolution Δf and the ability to correctly estimate the loss factor. This process of solving for the response characteristics of the 2-DOF system and the calculation of the loss factor is repeated for various input loss factors, different frequency resolutions Δf and different input forces - both a transient rectangular pulse force and a steady state excitation in the form of a random force.

4.1.1 PERSISTENT EXCITATION

The two oscillators of the sample 2-DOF system are excited by a random force and the system response characteristics are computed. The loss factors are then estimated using the power input method. The estimated loss factors and the input loss factors of the 2 oscillators are plotted in Figure 14 and Figure 15.

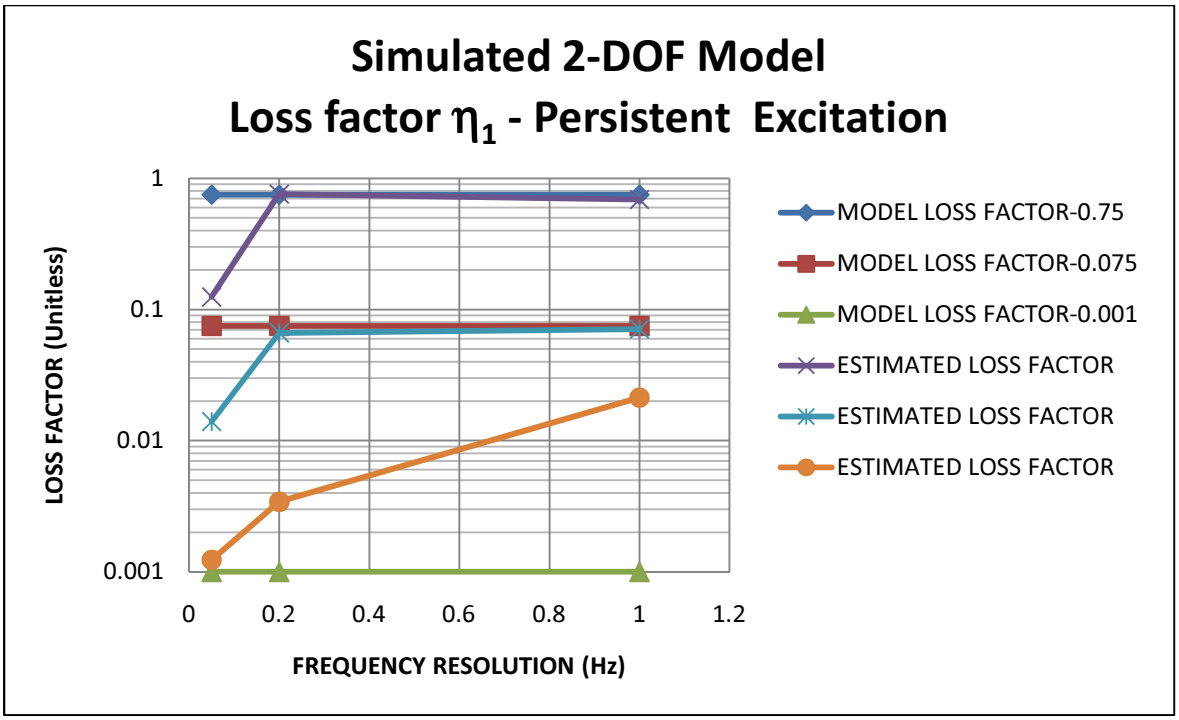

Figure 14 : Simulated η_1 with persistent excitation, varying model loss factors and Δf .

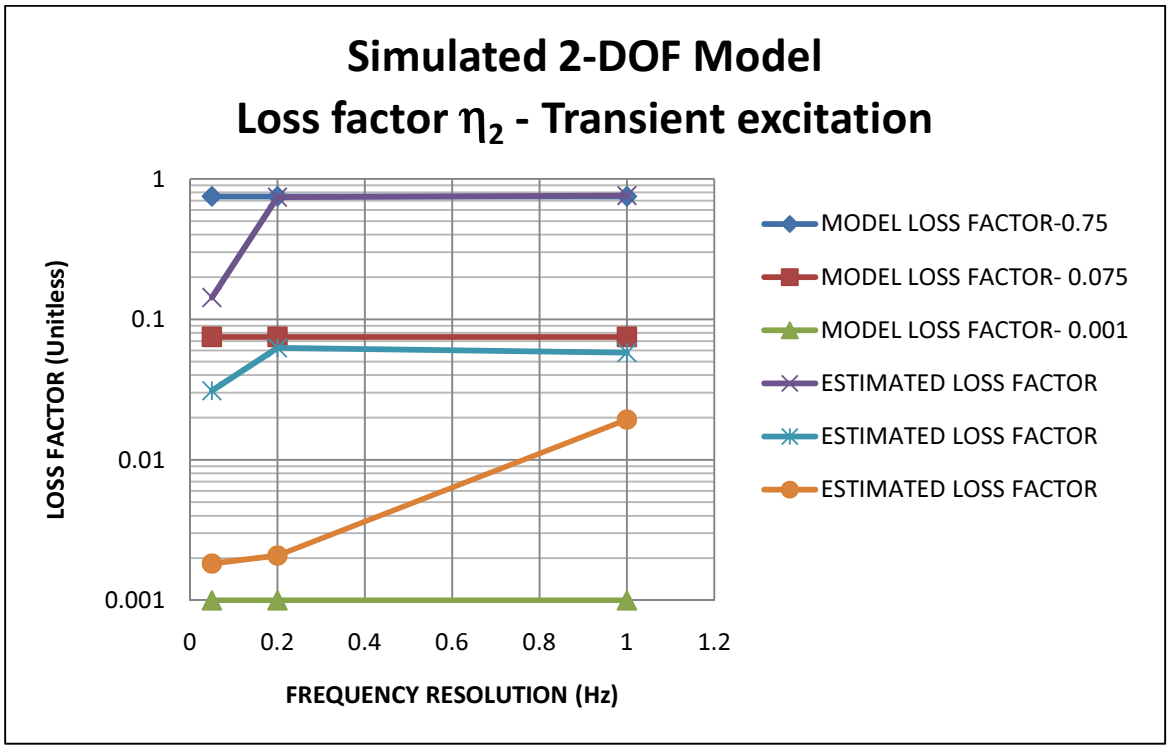

Figure 15 : Simulated η_2 with persistent excitation, varying model loss factors and Δf .

It is clear from the figures above that the loss factor range in which the power input method can be applied is very wide. It can successfully estimate an improbably high loss factor of 0.75 and also a very low damping loss factor value of 0.001. The above figures also convey that the quality of the estimated loss factor depends a lot on the frequency resolution Δf chosen.

Δf is inversely proportional to the sampling time (data capture duration), 'T'. So, a higher frequency resolution (lower numerical value of Δf) means a higher sampling time and more data points. Oscillators with low damping need a longer time for the vibrations to die down and hence need a higher frequency resolution (lower numerical value of Δf). This is also seen in the figures above. In particular insufficient frequency resolution (higher value of Δf) for lightly damped oscillators does not capture enough data points and as seen in the figures above the estimated loss factors are overestimated and are off by almost an order of magnitude.

On the other hand, oscillators with high input loss factors are less dependent on the value of Δf chosen. As seen, frequency resolutions of 0.2 Hz and 1 Hz result in estimated loss factors of 0.075 and 0.75. The loss factors estimated by a frequency resolution of 0.05 Hz are slightly off by a factor of about 2-3. However it has to be noted that the natural frequencies of the oscillators are 24, 32 Hz and hence we need such high sampling frequencies to estimate the loss factors.

4.1.2 TRANSIENT EXCITATION

The two oscillators of the sample 2-DOF system are excited by a rectangular pulse force generated by using 2 Heaviside step functions and the system response characteristics are computed. The loss factors are then estimated using the power input method. The estimated loss factors and the model loss factors of the 2 oscillators are plotted in Figure 16 and Figure 17.

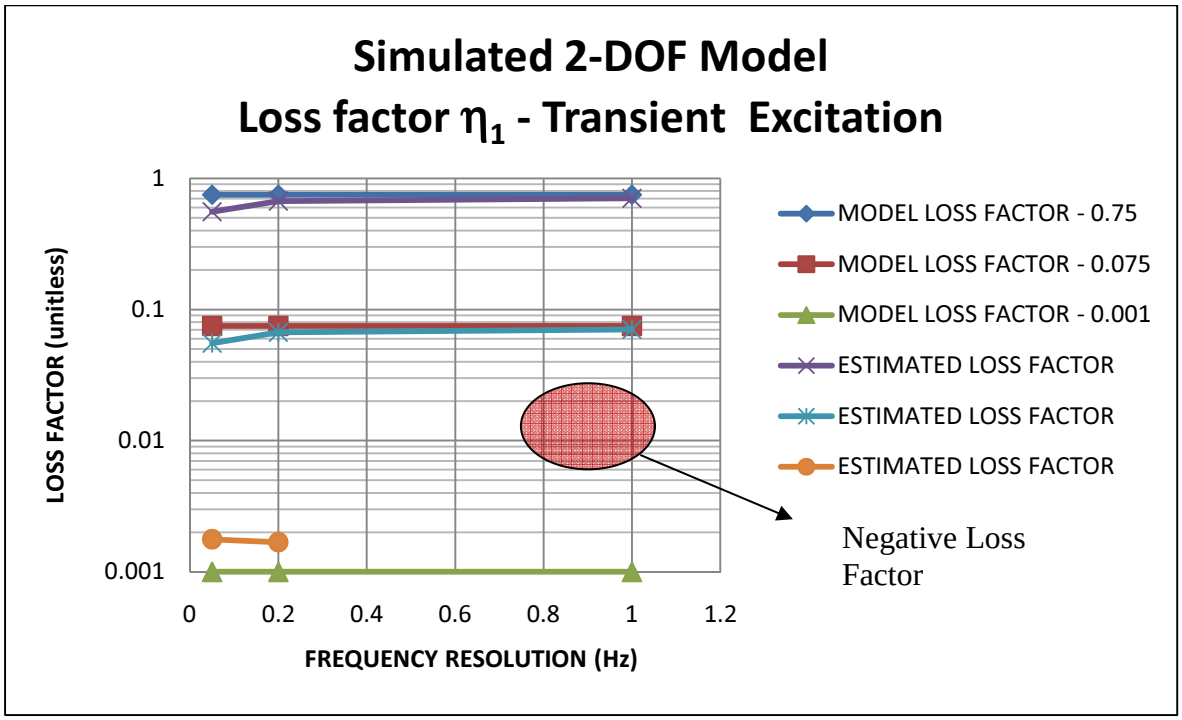

Figure 16 : Simulated η_1 with transient excitation, varying model loss factors and Δf .

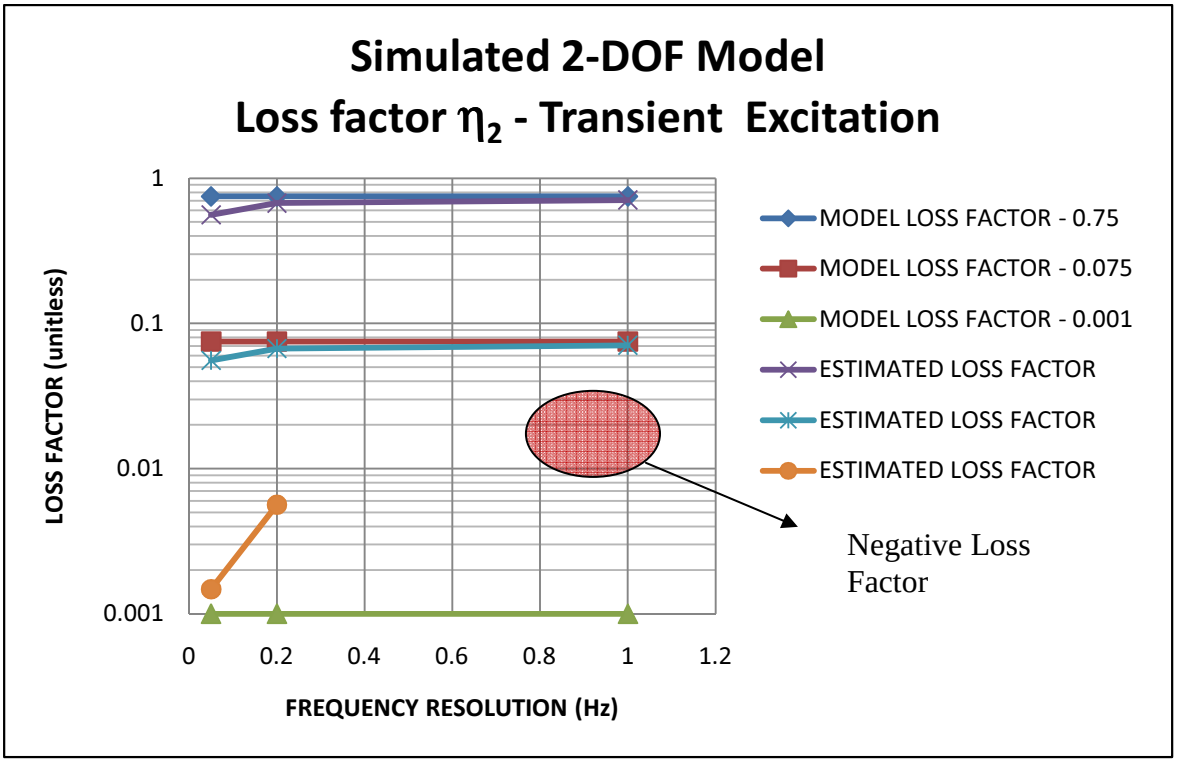

Figure 17 : Simulated η_2 with transient excitation, varying model loss factors and Δf .

The magnitude of the loss factor estimated by the power input method with the transient case is dependent on the frequency resolution, as it is with the persistent case, and this effect is seen much more clearly at lower damping levels. At high damping levels, the loss factor estimated is less dependent on the frequency resolution chosen and different levels of frequency resolution give loss factors which are close to the model loss factor. A frequency resolution Δf of 0.05 Hz at high damping levels estimates loss factors which are off by a factor of 1-2.

At lower damping levels, on the other hand, the effect of frequency resolution on the loss factor estimations is very clear. The estimated loss factor with a frequency resolution, Δf, of 1 Hz and a model loss factor of 0.001 is a negative value (-0.06 for oscillator 1). The exact mathematical relationship between estimated loss factor and frequency resolution is beyond the scope of this thesis and can be worked on in the future. However it is clear that, up to a point, increasing the frequency resolution solves the problem of negative loss factors.

4.2 EXPERIMENTAL RESULTS FOR THE LAI AND SOOM PLATES

The experiments were conducted on the Lai and Soom plates shown in Figure 11 and Figure 12 using the experimental setup described in Chapter 3. The experiments were conducted with both persistent and transient excitations.

For the persistent excitation case, the accelerometers were placed on the front side of the plates and a shaker was attached on the back side. To get a better statistical spatial average of the acceleration of the two plates, measurements were taken at 9 points on each plate and were distributed uniformly over the whole surface as shown in Figure 18. Plate 1 was first excited with a shaker and, since an 8 channel data acquisition unit was used, the experiment was repeated 3 times, changing the position of the accelerometers and keeping the excitation point

the same. Then, the same procedure was repeated with the shaker connected to plate 2. The excitation point was chosen away from known, low frequency node lines and away from the added damping sheets as shown in Figure 18. For the persistent excitation case, the experimental data was averaged 50 times to compute the required spectra.

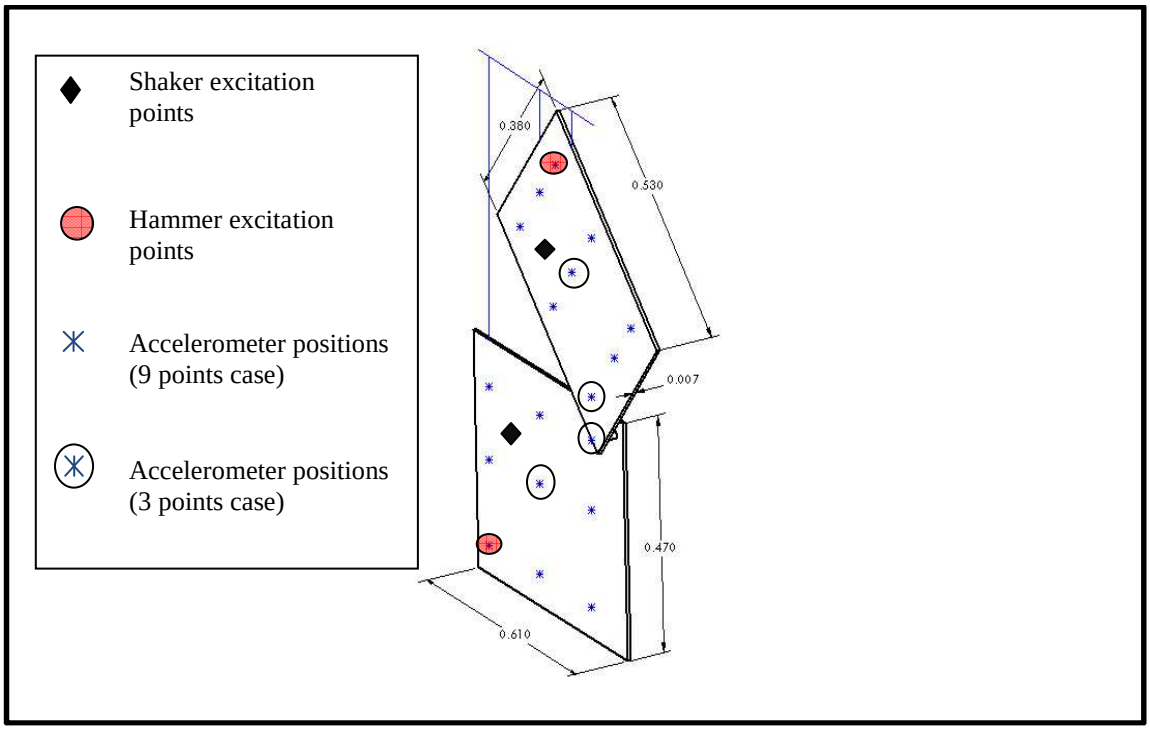

Figure 18 : Measurement and excitation points on the Lai and Soom plates

For the transient case, a modal hammer was used to excite the structure. Since the frequency range of interest was from 0-4000 Hz, a steel tip was used which could excite up to about 4500Hz. The hammer hit and the accelerometers were on the front end of the plate as shown in Figure 18. To compare results and to maintain consistency with the experiment setup in the dissertation[26] by M. L. Lai, the excitation points and the measurements points were replicated with those described in the dissertation. That is, three measurement points were chosen on each plate and were located along a diagonal of the plates. The plates were excited at the bottom-most and the top-most points as shown in Figure 18. The experimental data was averaged only 3 times

because of the difficulty in getting a good hit with the steel tip: an estimated 90% of the hits attempted were double hits for which the responses were not used in the calculations.

The experimental test settings were as follows

- Sampling frequency F = 32768 Hz.
- Frequency resolution Δf = 1 Hz.
- Number of samples N = 32768.
- Sampling time T = 1 s.
- Sampling resolution Δt = 30.52 μs.

Table 3 : Description of the Frequency bands used

BAND	STARTING FREQUENCY(Hz)	ENDING FREQUENCY(Hz)	CENTER FREQUENCY(Hz)
1	0	512	256
2	512	1024	768
3	1024	1536	1280
4	1536	2048	1792
5	2048	2560	2304
6	2560	3072	2816
7	3072	3584	3328
8	3584	4096	2840

Figure 19-Figure 22 show the results from the experimental tests from the 6 sheets of Constrained Layer Damping (CLD) added on the Lai and Soom plates. The figures show and compare the loss factors calculated using the power input method with both hammer and shaker excitations. They show a general agreement between the calculated loss factors with different

excitation sources. Figure 21 and Figure 22 show good agreement between the estimated loss factors in most bands, except for bands 2 and 3, centered at 768 Hz and 1280 Hz, in Figure 21 and bands 1 and 3, centered at 265 Hz and 1280 Hz, in Figure 22 . The coupling loss factors in Figure 19 and Figure 20 are also in good agreement with each other except for a few bands like band 6, centered at 3072 Hz, in Figure 20 and bands 2 and 3, centered at 768 Hz and 1280 Hz in Figure 19.

The possible reasons for the disagreement are

- Modes in those bands are not properly excited and hence calculated loss factors are different from the actual loss factors.
- Since the change in energy term, as in equation (2.3), is not included in the calculation of loss factor with the transient hit, the formula does not fully describe the physics of the problem.
- A bad hit some times can spoil the averaged data and the averaged estimated loss factor.

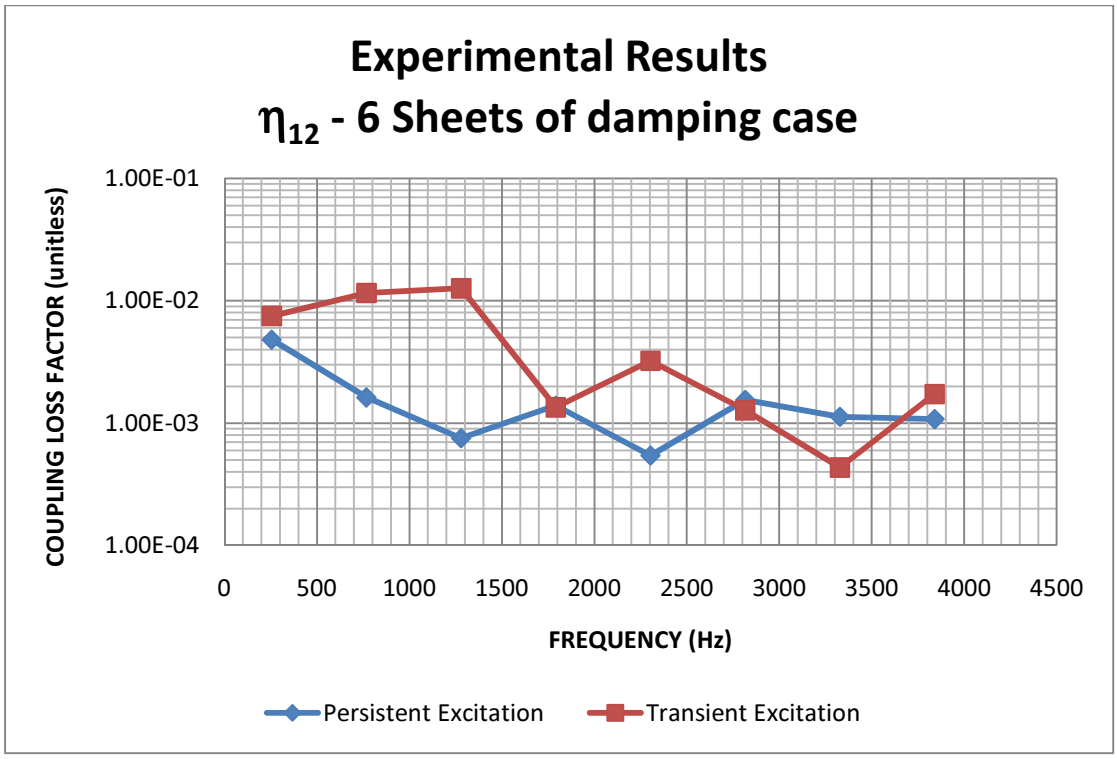

Figure 19 : Experimental Coupling Loss Factor η_{12} - Transient and persistent excitation

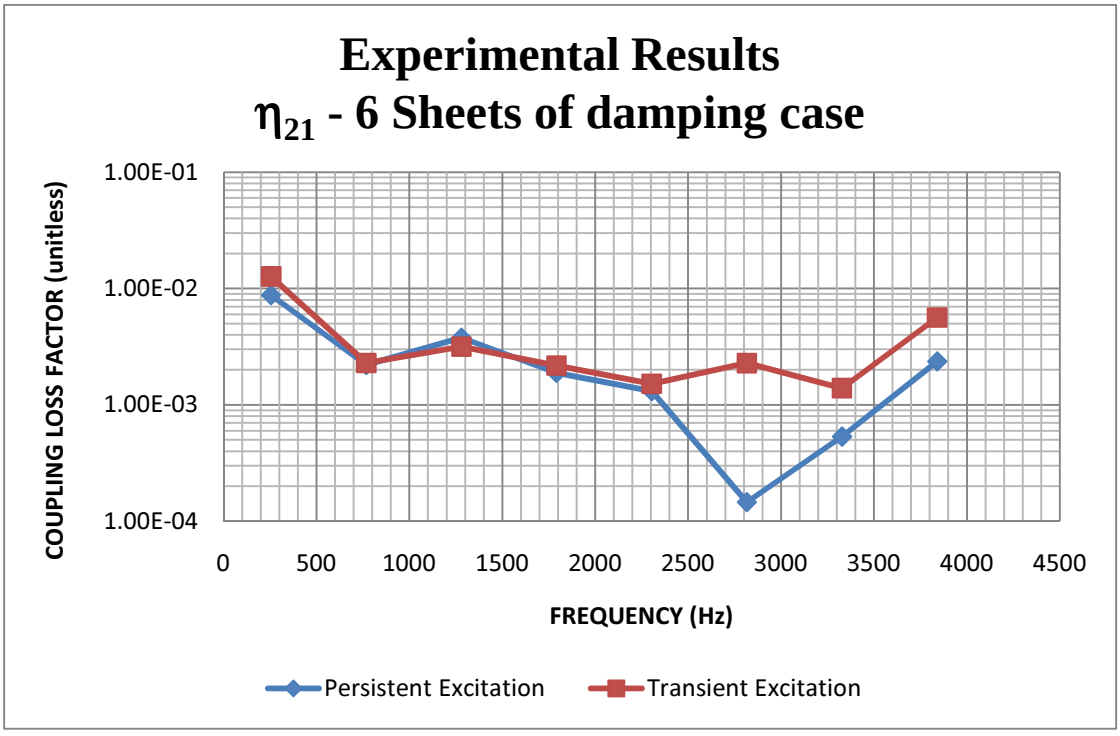

Figure 20 : Experimental Coupling Loss Factor η_{21} - Transient and persistent excitation

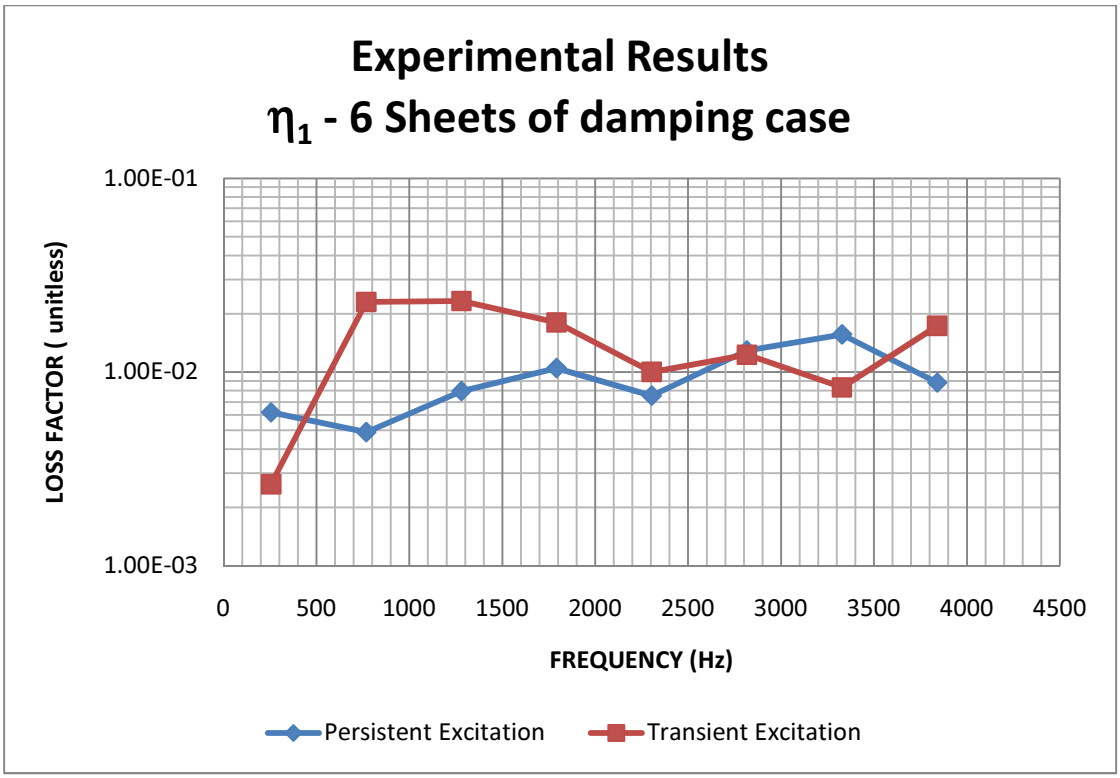

Figure 21 : Experimental Loss Factor η_1 - Transient and persistent excitation

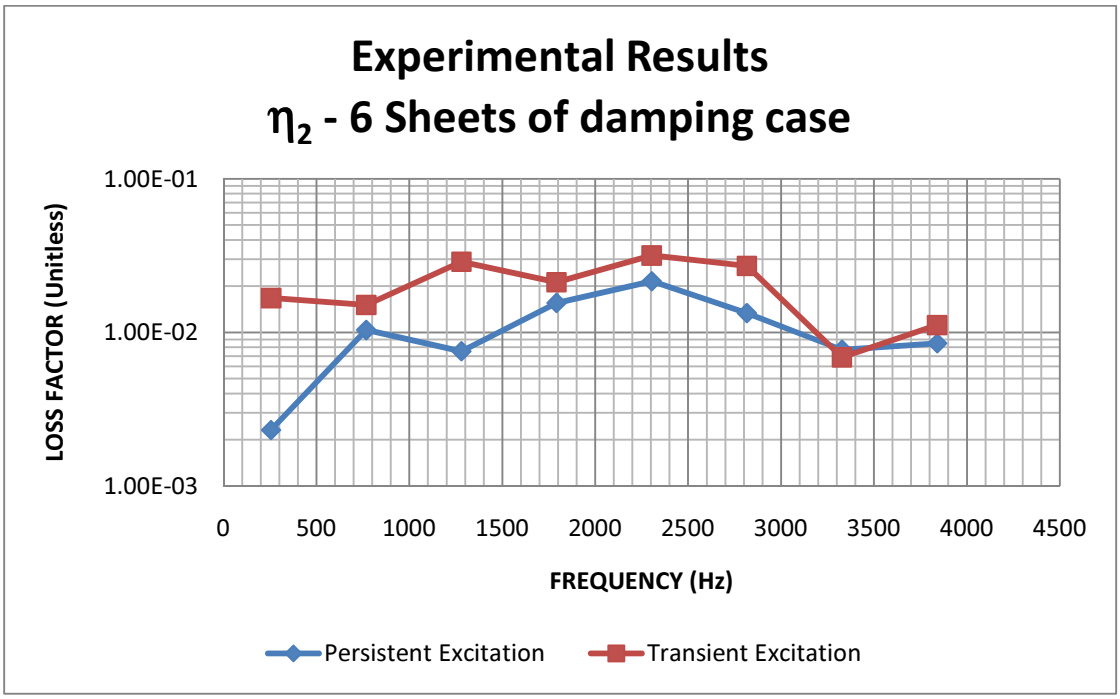

Figure 22 : Experimental Loss Factor η_2 - Transient and persistent excitation

4.3 EFFECT OF DAMPING

One of the primary errors involved in the estimation of loss factors are phase errors in the processing of data into the frequency domain. These phase errors, which are witnessed in cases of low damping, can be minimized by increasing the frequency resolution (decreasing Δf). Near a natural frequency, phase changes occur rapidly and the rate at which those changes occur is directly related to the damping level of the structure involved. The lower the damping of the plate the faster the phase changes occur [1]. As a baseline, experiments were conducted with a constant frequency resolution ($\Delta f = 1Hz$) on the Lai and Soom plates for the 3 damping level cases shown in the Table 3. The loss factors (LF) and coupling loss factors (CLF) thus estimated are plotted in the figures below.

4.3.1 PERSISTENT EXCITATION

It can be seen from Figure 25 and Figure 26 that the change in the damping level of the plates induces a similar change on the estimated loss factor of the plates. As the number of damping sheets attached to the plate increase the loss factor of the plate increases. It can also be noticed that in the bands between 0-2000 Hz the loss factors estimated in the 6 sheets case and the 2 sheets case are very close to one another and in the bands between 2000-4000 Hz the estimated loss factors of the 2 sheets case and the no damping case match. Hence we can deduce that partially damped plates need a larger number of measurement points to correctly determine the damping levels.

On the other hand the effect of damping on the coupling loss factor is not straightforward as seen in Figure 23 and Figure 24. The value of the coupling loss factor increases slightly with

increase in the damping level of the plate. Theoretically speaking, the coupling loss factors should not vary with change in damping levels, but by looking at the experimental results we see that the coupling loss factors show a variation ranging from 10% to 100%. The variation in the experimental coupling loss factors is higher in the lower frequency bands and as the frequency increases the variation decreases, as seen in the bands 7 and 8 (centered at 3584 Hz and 4096Hz). Also it can be seen that AUTOSEA over predicts the CLFs with a variation ranging from about 10% to almost 100%. It can also be seen that as the frequency increases, the variation between the theoretical (AUTOSEA) results and the experimental results decreases. This variation in the results is because the point joint used in AUTOSEA does not correctly describe the physical characteristics of the actual joint between the plates.

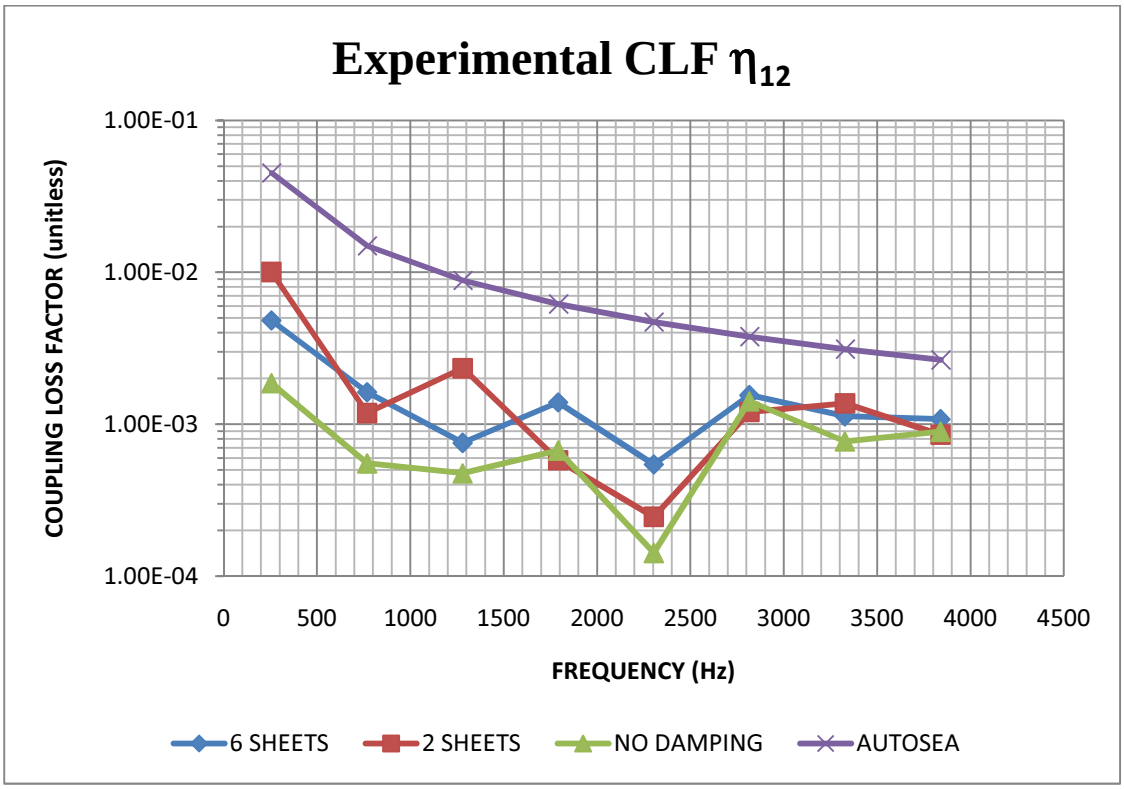

Figure 23 : Effect of damping on the Coupling Loss Factor η_{12}

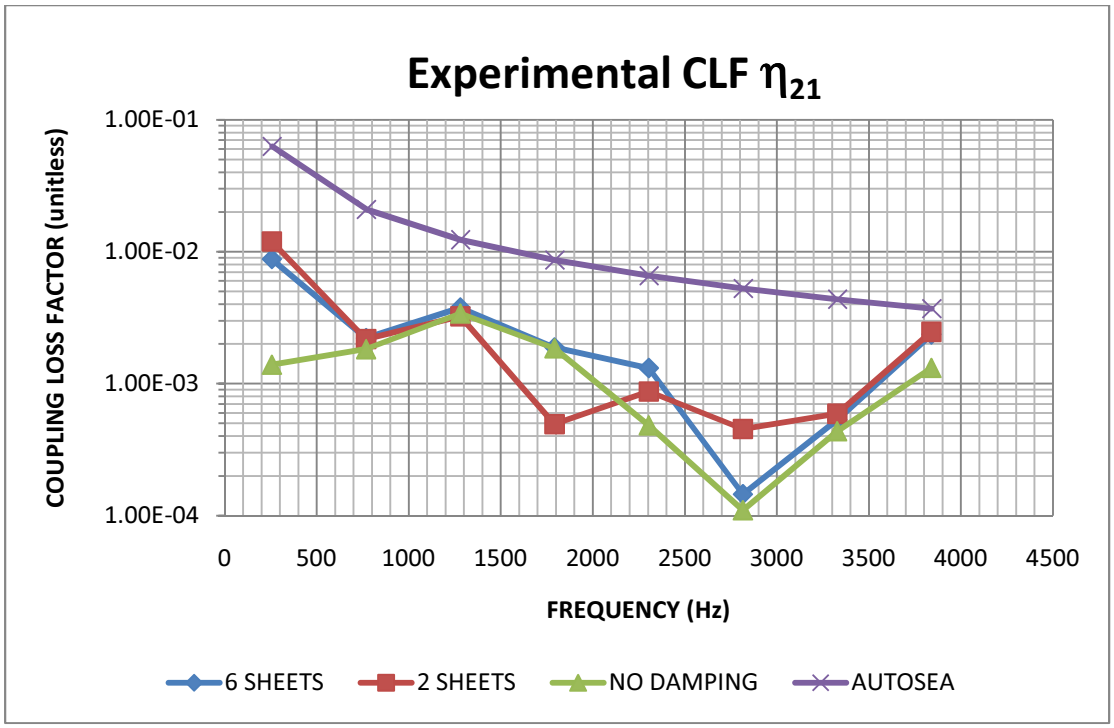

Figure 24 : Effect of damping on the Coupling Loss Factor η_{21}

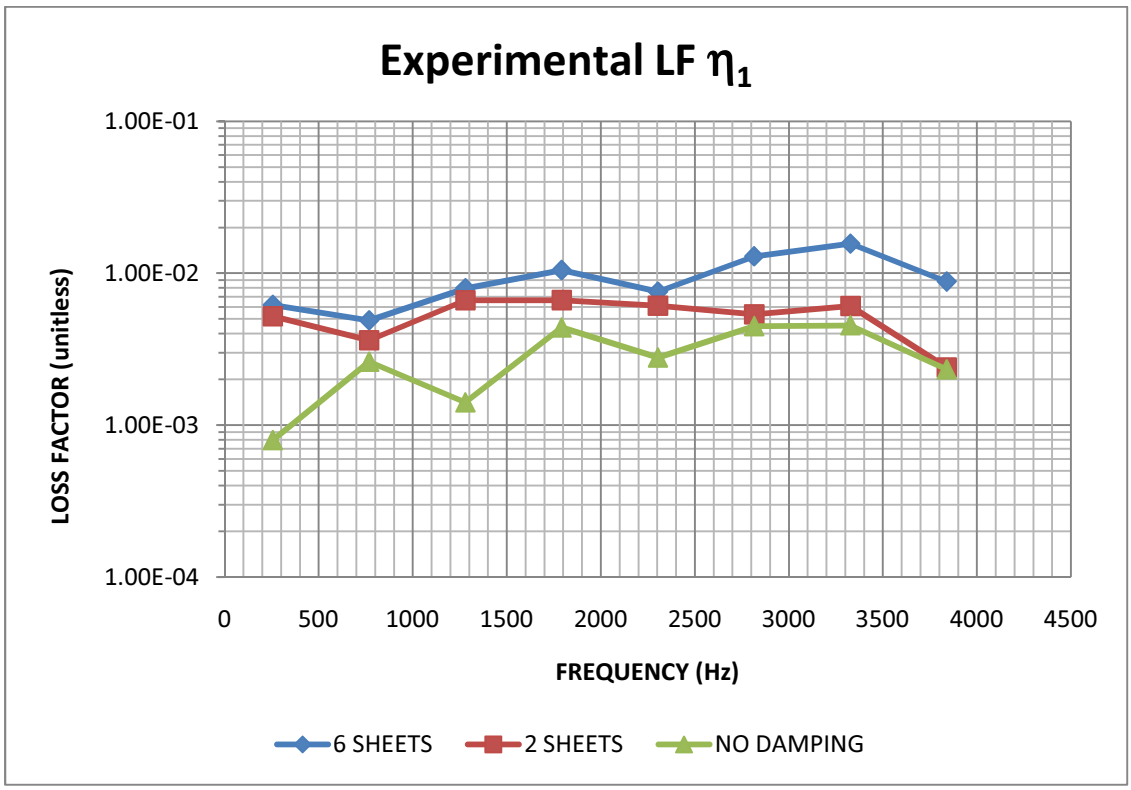

Figure 25 : Effect of damping on the Loss Factor η_1

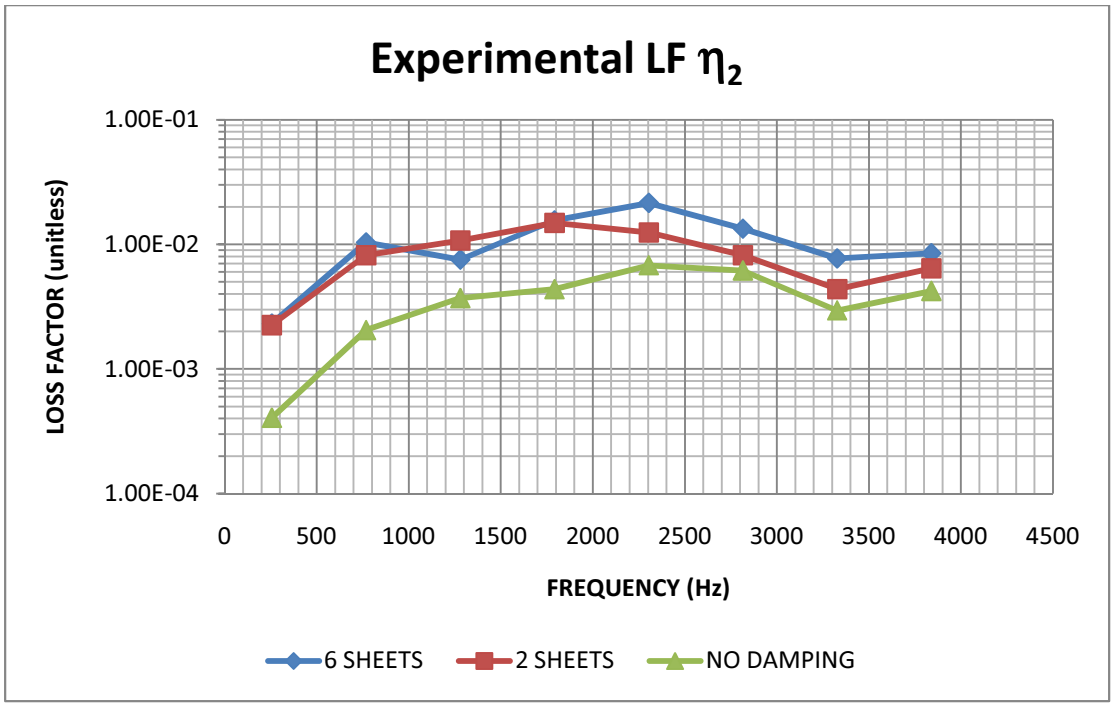

Figure 26 : Effect of damping on the Loss Factor η_2

4.3.2 TRANSIENT EXCITATION

As with the persistent excitation case, the coupling loss factors estimated with an impact hammer as a source of excitation are not directly dependent on the damping. It is seen from Figure 27 and Figure 28 that the coupling loss factors in the “2 sheets” and “no damping” cases are similar in magnitude showing little variation.

It can be seen from Figure 29 and Figure 30 that an increase in damping level of the plate is not correctly represented by the loss factor estimates. The discrepancy in the estimated loss factors could be because of the low number of measurement points on the plates. For the transient hit case, the acceleration is measured only at 3 points on the plate when compared to 9 points in the persistent excitation case.

Comparing the results, it can be inferred that for plates which have partial damping added to them the estimated loss factors can be improved by increasing the number of measurement points and distributing the points throughout the plate.

The estimated coupling loss factors and the estimated loss factors from the “6 sheets” case show a variation of more than an order of magnitude in some frequency bands, seen in Figure 28 and Figure 30. The reason behind the difference probably is that the modes were not properly excited in “6 sheets case”.

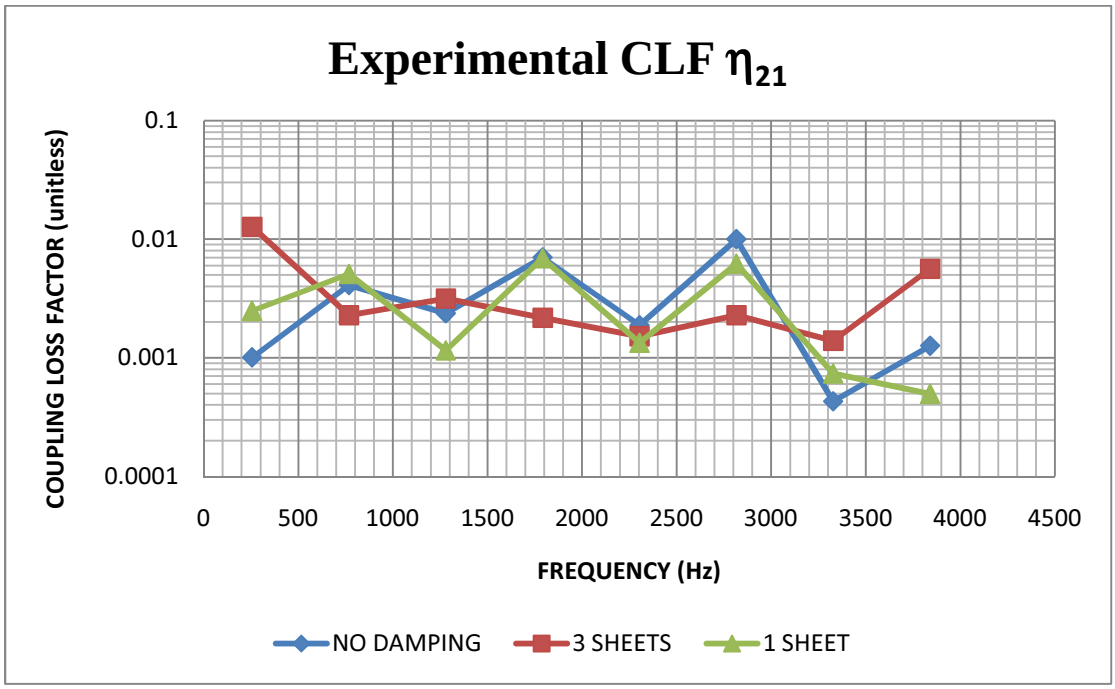

Figure 27 : Effect of damping on the Coupling Loss Factor η_{21}

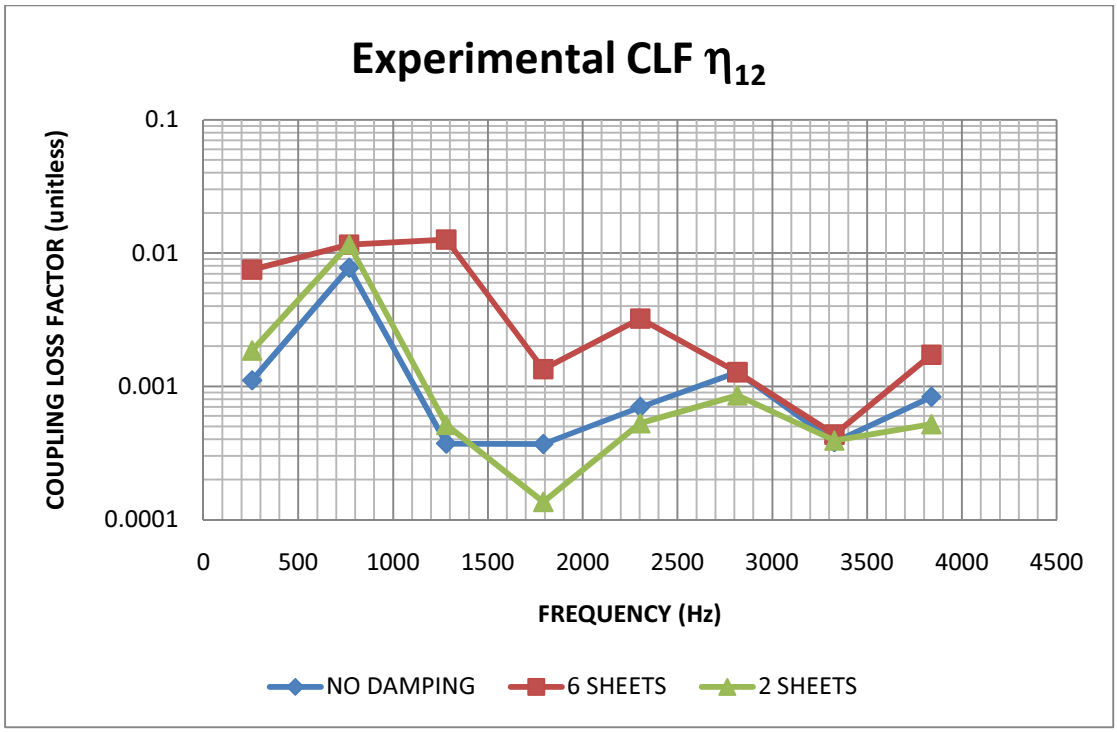

Figure 28 : Effect of damping on the Coupling Loss Factor η_{12}

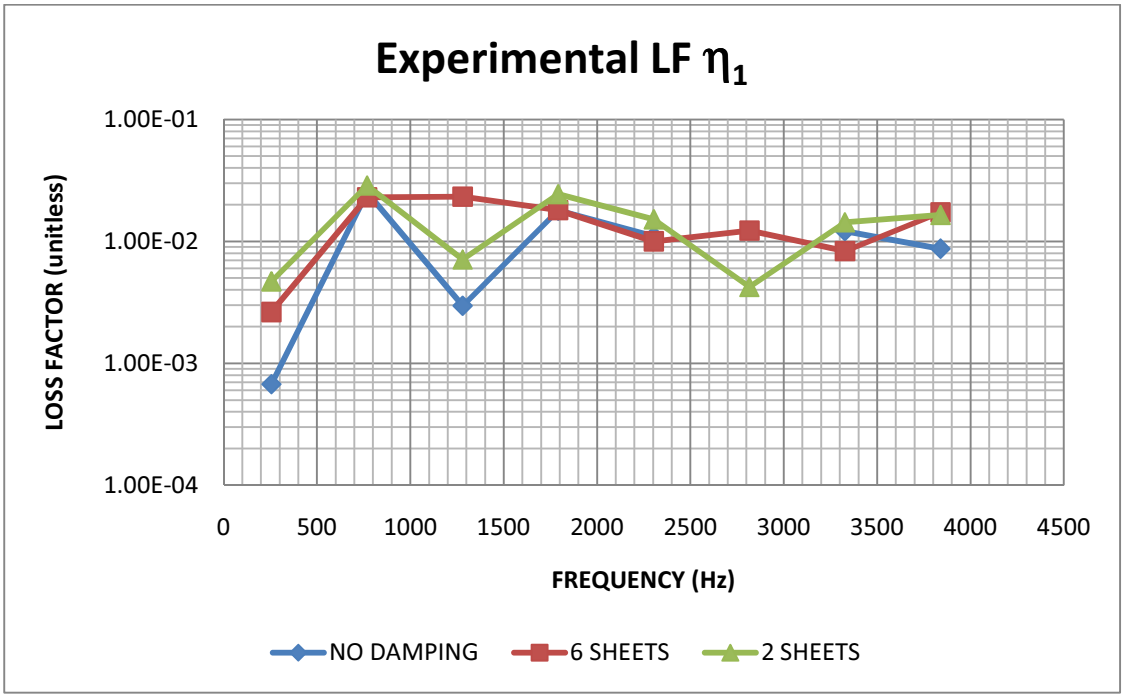

Figure 29 : Effect of damping on the Loss Factor η_1

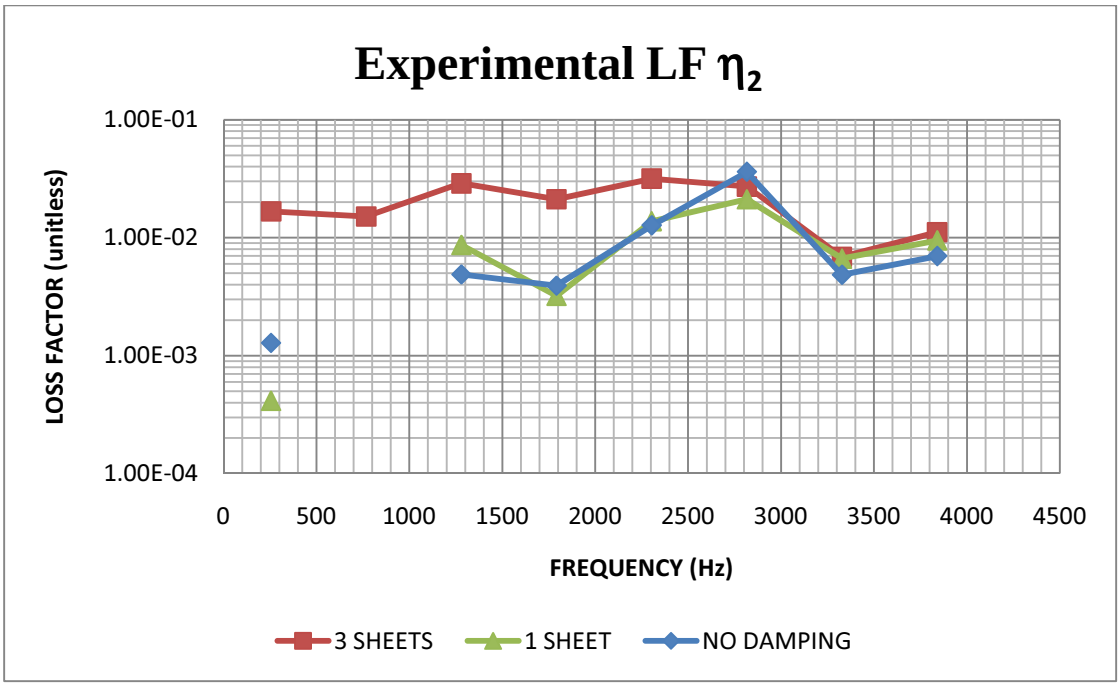

Figure 30 : Effect of damping on the Loss Factor η_2

4.4 MODES IN BAND AND MODAL DENSITY

According to SEA assumptions, each band should have a large (or infinitely many) number of modes. Since it is practically impossible, a band with a large number of modes is generally thought to give better statistical results than a band with less number of modes. Thus both the modes in band and the modal density act as good indicators of the expected quality of the loss factor estimated. The formula to estimate the modal density as given in the book by Lyon and DeJong [1] is

$$< G >_{\omega_c, y_s} = \frac{\pi}{2}\left(\frac{n(\omega)}{M}\right) \tag{4.8}$$

Here, $< G >_{\omega_c, y_s}$ is the conductance or real part of the mobility transfer function in a band with center frequency ω_c and excitation point y_s. M is the mass of the plate and $n(\omega_c)$ is the modal density of the plate. N_{ω_c} is the number of modes in band.

The relationship between modal density and modes in band is given by

$$N_{\omega_c} = n(\omega_c)\Delta\omega_c \tag{4.9}$$

The theoretical formula to calculate the modal density of any flat plate is given by [1] as

$$n(\omega) = \frac{A_p}{4\pi K c_l} \tag{4.10}$$

$K = h/2\sqrt{3}$ is radius of gyration of a plate.

$c_l = \sqrt{E/\rho_m}$ is longitudinal wave speed.

h is the thickness of the plate.

ρ_m is the material density.

E is Young's modulus.

A_p is the surface area of the plate

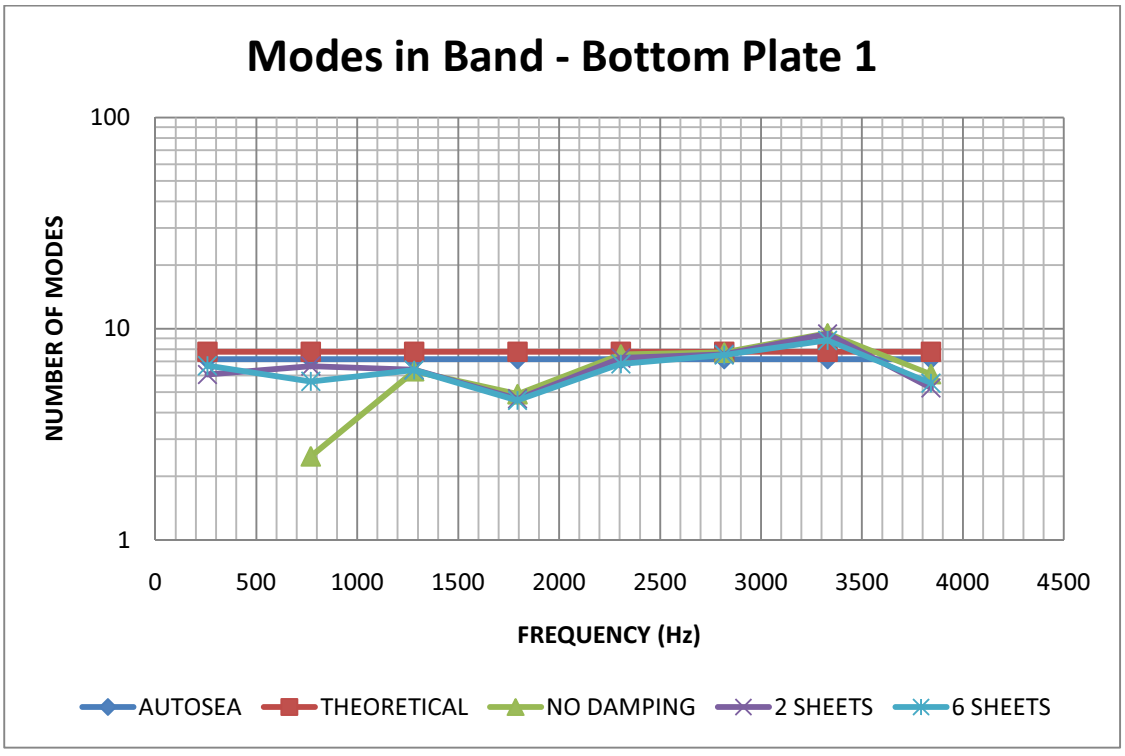

Figure 31 : Modes in band in plate 1

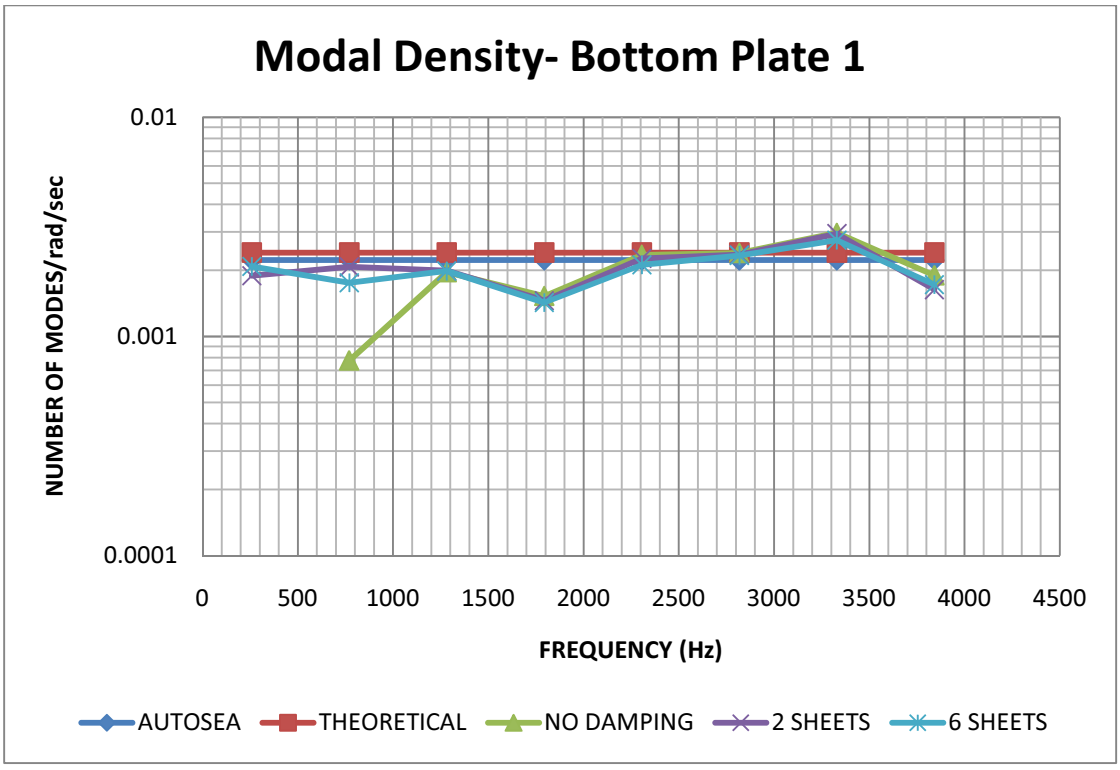

Figure 32 : Modal Density of plate 1

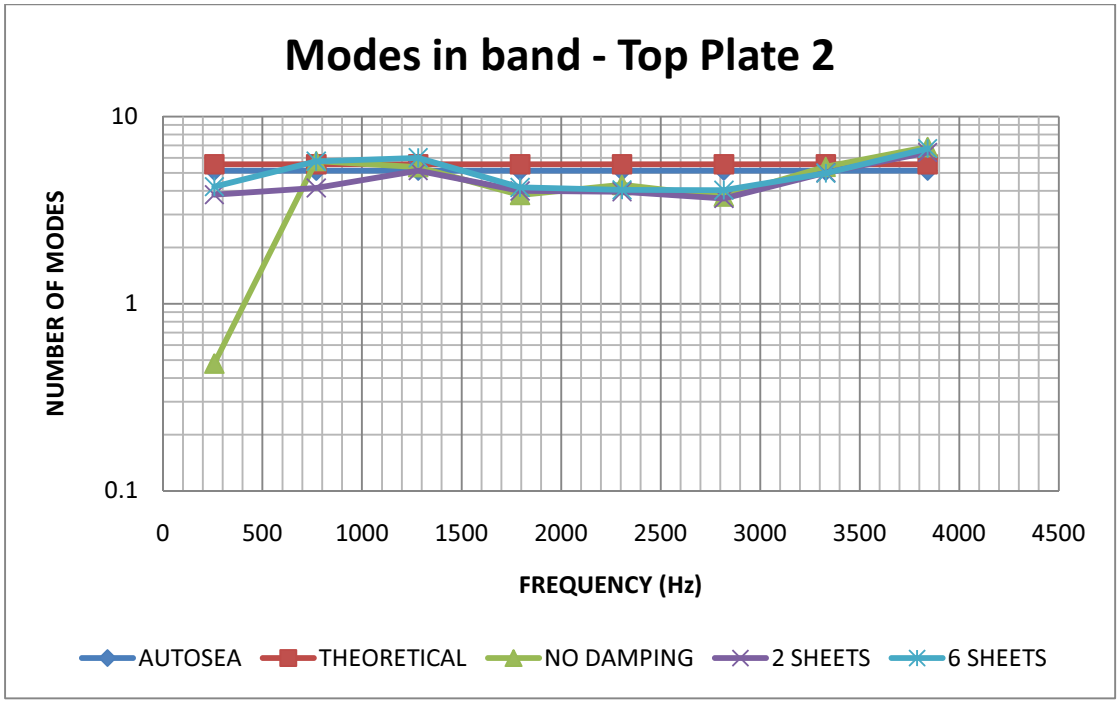

Figure 33 : Modes in band in plate 2

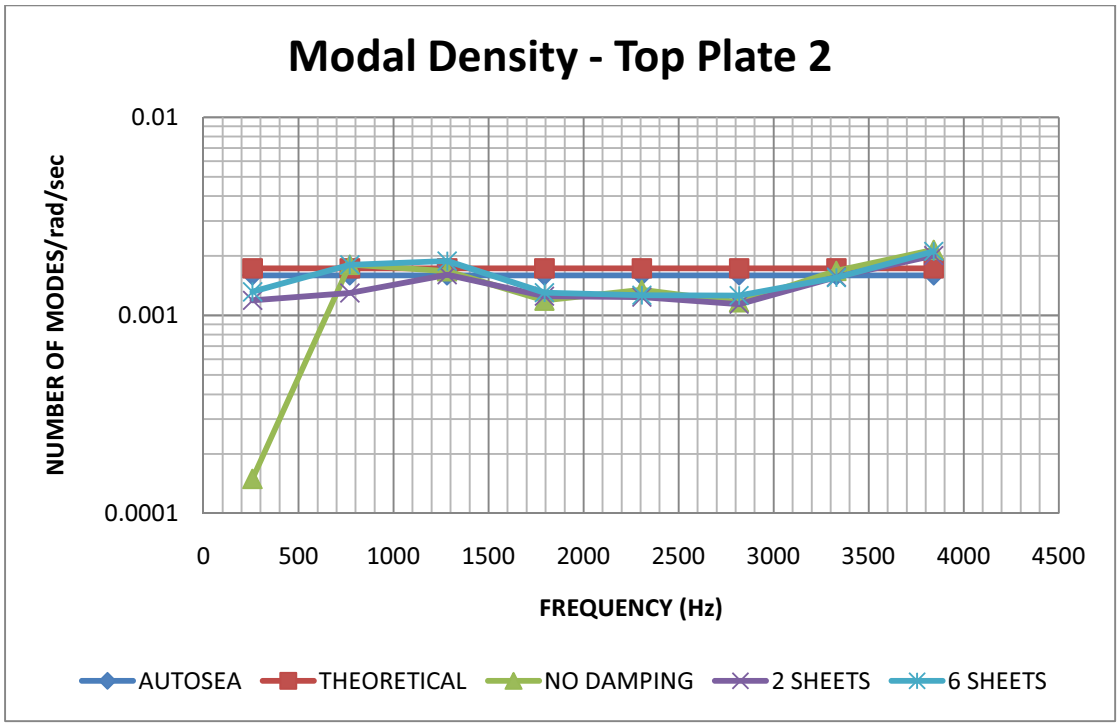

Figure 34 : Modal Density of plate 2

The modes in band and the modal densities are calculated from the experimental FRF's using the formula given by equation (4.8). These values are then compared with the theoretical values computed using the equation (4.10) and with the values calculated by the statistical energy analysis software AUTOSEA^{TM} 2004 sold by the ESI Group.

From Figure 31, Figure 32, Figure 33 and Figure 34 we see that the experimental values of the modes in band and the modal density are in good agreement with both the theoretical values computed and AUTOSEA^{TM} values. Except for the first band in the no damping treatment case, all other bands in all cases match the theoretical values. The first band values can be improved by minimizing phase errors (decreasing Δf). Each frequency band of the bottom plate has an average of 7 modes in it and of the top plate has about 5 modes in it which are statistically sufficiently high number of modes in a band to use SEA techniques appropriately.

4.5 PROCESS PARAMETERS

There are several parameters involved in the estimation of loss factors using the power input method like the number of measurement points, effect of the hammer tip, effect of the frequency resolution and effect of frequency bandwidths to name a few. Experiments were conducted by varying some of those parameters. The loss factors were then estimated using the power input method to check for the effect of the parameters on the estimated loss factors.

4.5.1 EFFECT OF FREQUENCY RESOLUTION

As shown by numerical simulation in section 4.1, the estimated loss factor is dependent on the frequency resolution. Since frequency resolution and the sampling time are inversely proportional, choosing lower frequency resolution (higher numerical value of Δf) means a fewer number of measured data points. This directly affects the quality of the frequency domain data and might introduce phase errors.

Figure 35-Figure 38 show the effect of the frequency resolution on the estimated coupling loss factors and loss factors for the “no damping added” case. A change in frequency resolution from 4 Hz to 0.25 Hz does not affect the estimated loss factor significantly in the frequency bands above 1000 Hz. The effect of the frequency resolution is seen only in the frequency bands below 1000 Hz. This is because higher frequencies have more cycles per second and hence die down quickly when compared to low frequencies thus requiring lesser sampling time to capture the decay. Thus a Δf of even 4Hz correctly predicts the loss factors at higher frequencies.

As the frequency resolution decreases from 0.25Hz to 2Hz, the loss factors in the lower bands start to deviate and are off by a factor of about 3. As the frequency resolution is further decreased the loss factors in the first frequency band become negative and this is consistent with the theory.

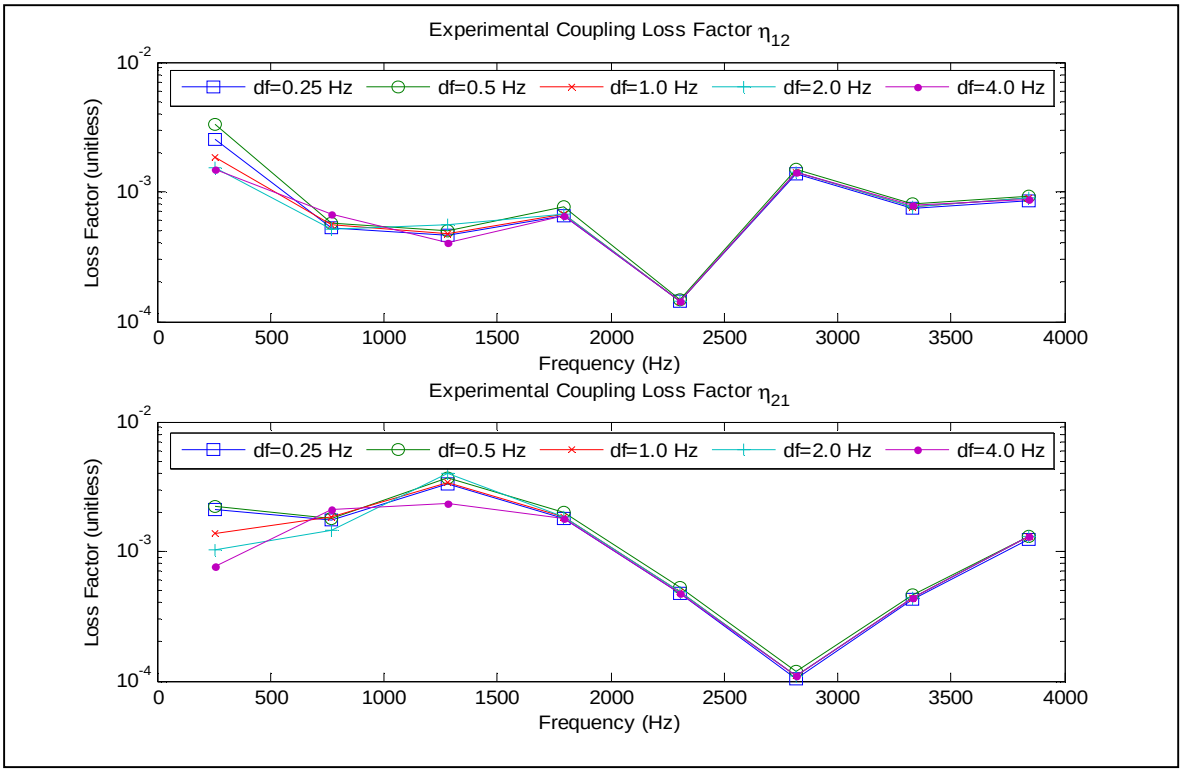

Figure 35 : Effect of frequency resolution on the Coupling Loss Factors (Persistent excitation-No Damping added)

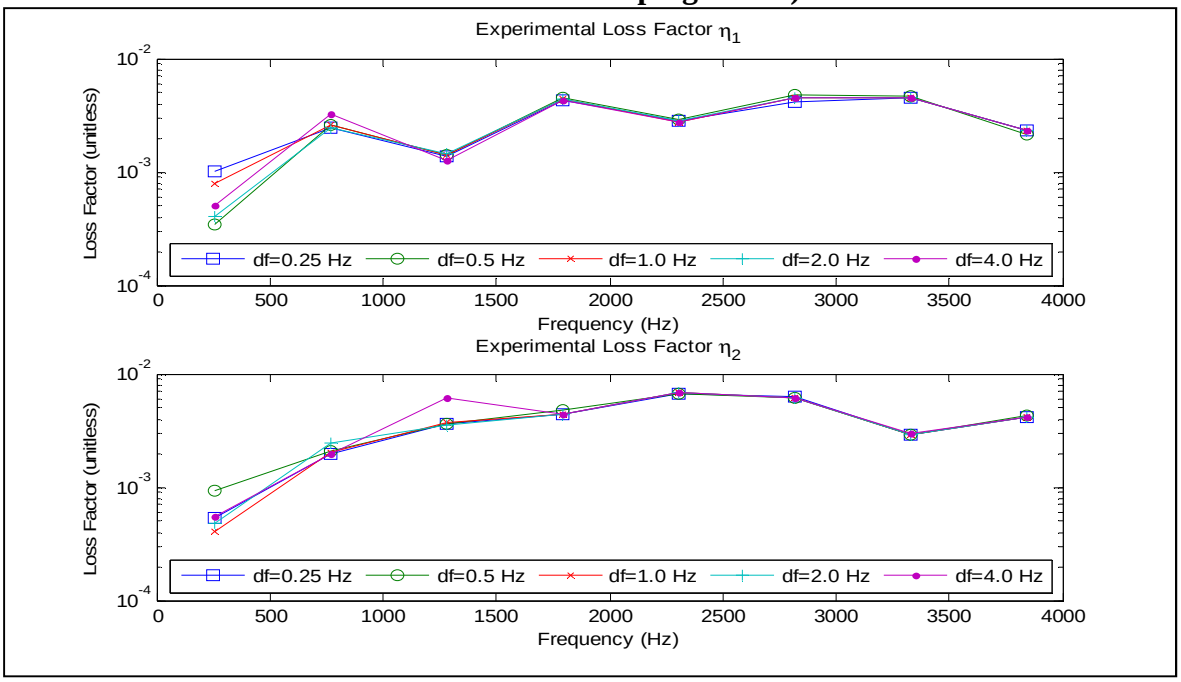

Figure 36 : Effect of frequency resolution on the Loss Factors (Persistent excitation-No Damping added)

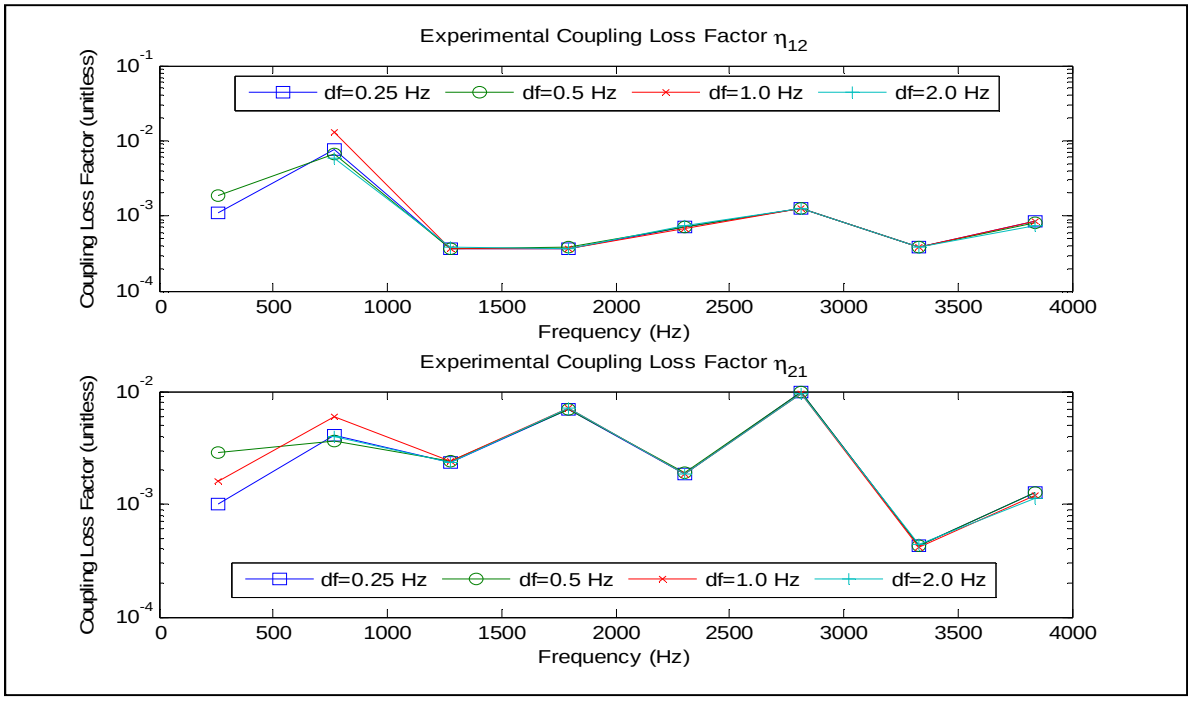

Figure 37 : Effect of frequency resolution on the Coupling Loss Factors (Transient excitation-No Damping added)

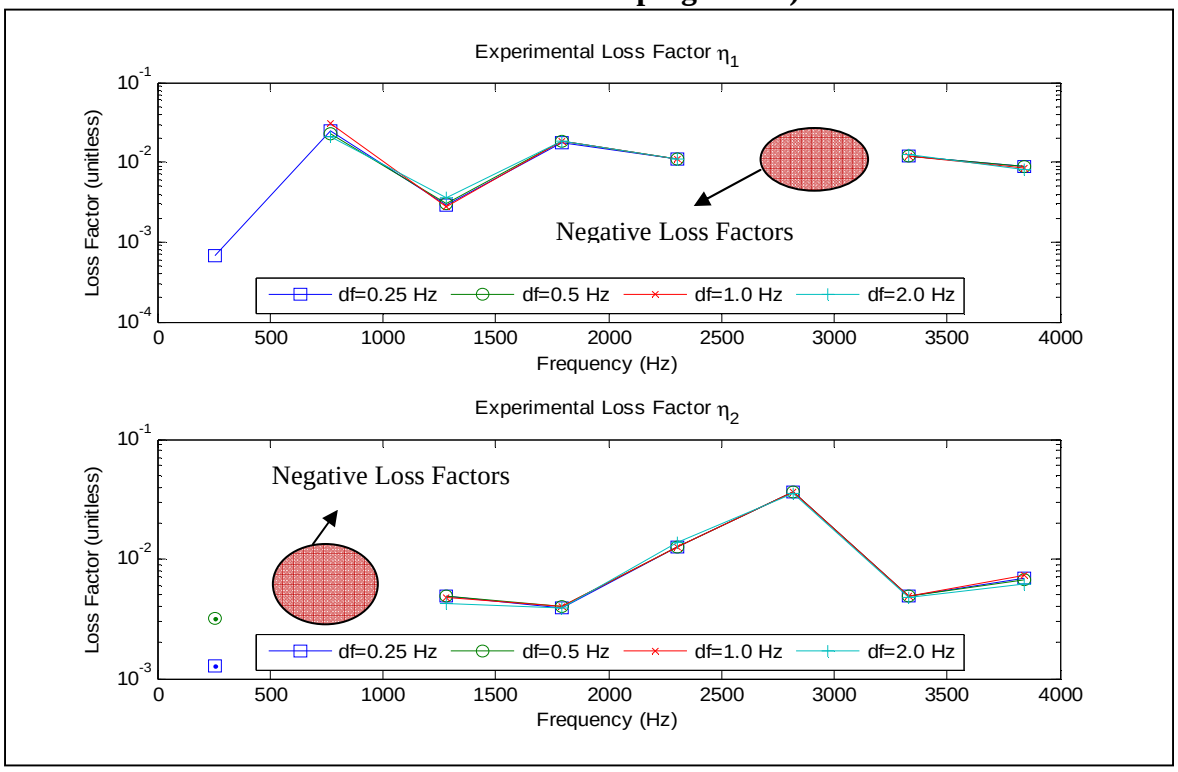

Figure 38 : Effect of frequency resolution on the Loss Factors (Transient excitation-No Damping added)

4.5.2 EFFECT OF FREQUENCY BANDWIDTH

In multi modal systems, loss factor is generally estimated in pre-defined frequency bands like full octave bands, one third octave bands or bands with constant bandwidths. Since transfer of energy and energy losses occur at the natural frequencies the bandwidth should be chosen such that the band has at least a few modes in it so that the loss factor estimated is statistically relevant. In this present study the loss factors are estimated for $1/3^{rd}$ octave bands with full octave bins and compared with the loss factors estimated with constant bandwidths of 512 Hz. The merit in choosing constant bandwidths of 512 Hz over $1/3^{rd}$ octave bands can be seen in Figure 39 to Figure 42 which represent both persistent and transient loading cases with no damping added to the aluminum plates.

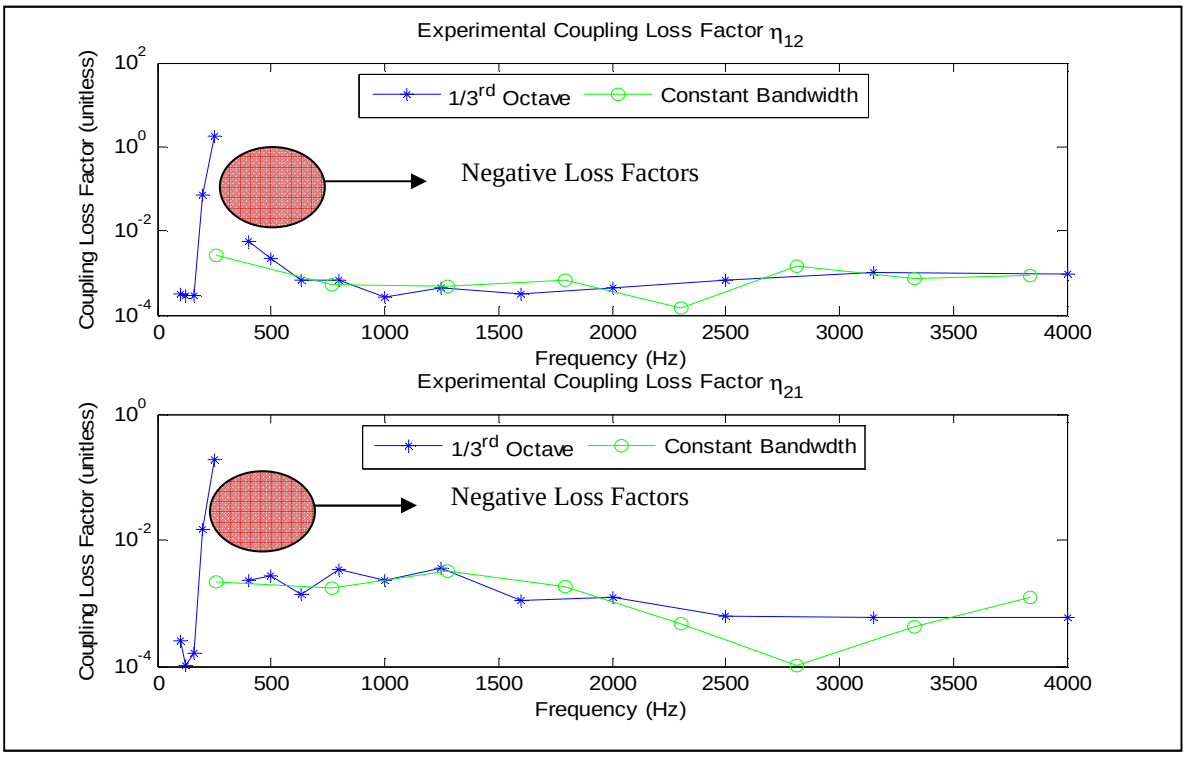

Figure 39 : Effect of frequency bands on the Coupling Loss Factors (No damping added) - Persistent excitation

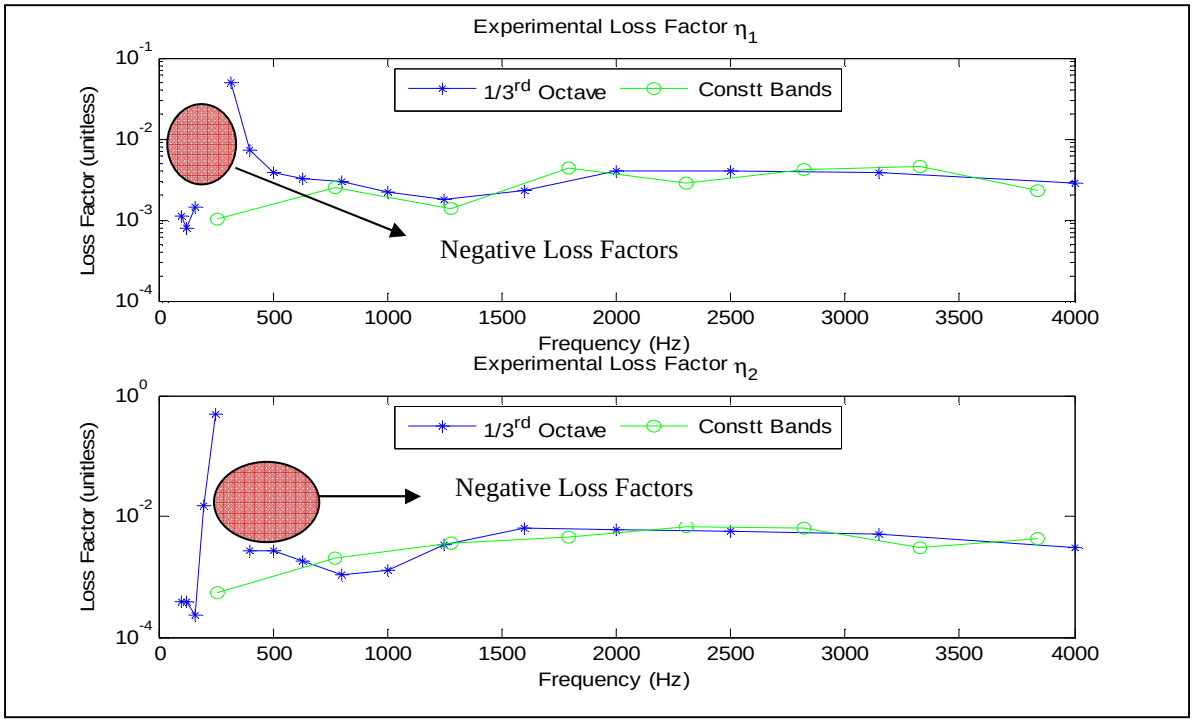

Figure 40 : Effect of frequency bands on the Loss Factors (No Damping added) - Persistent excitation

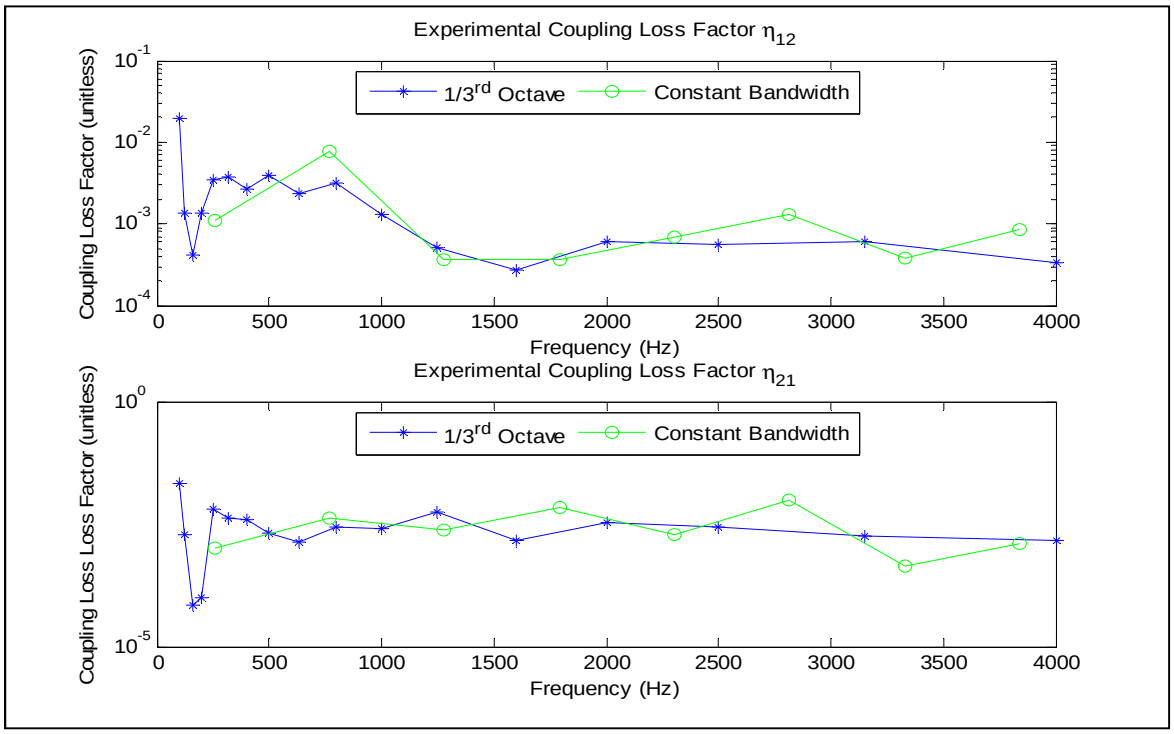

Figure 41 : Effect of frequency bands on the Coupling Loss Factors (No Damping added) - Transient excitation

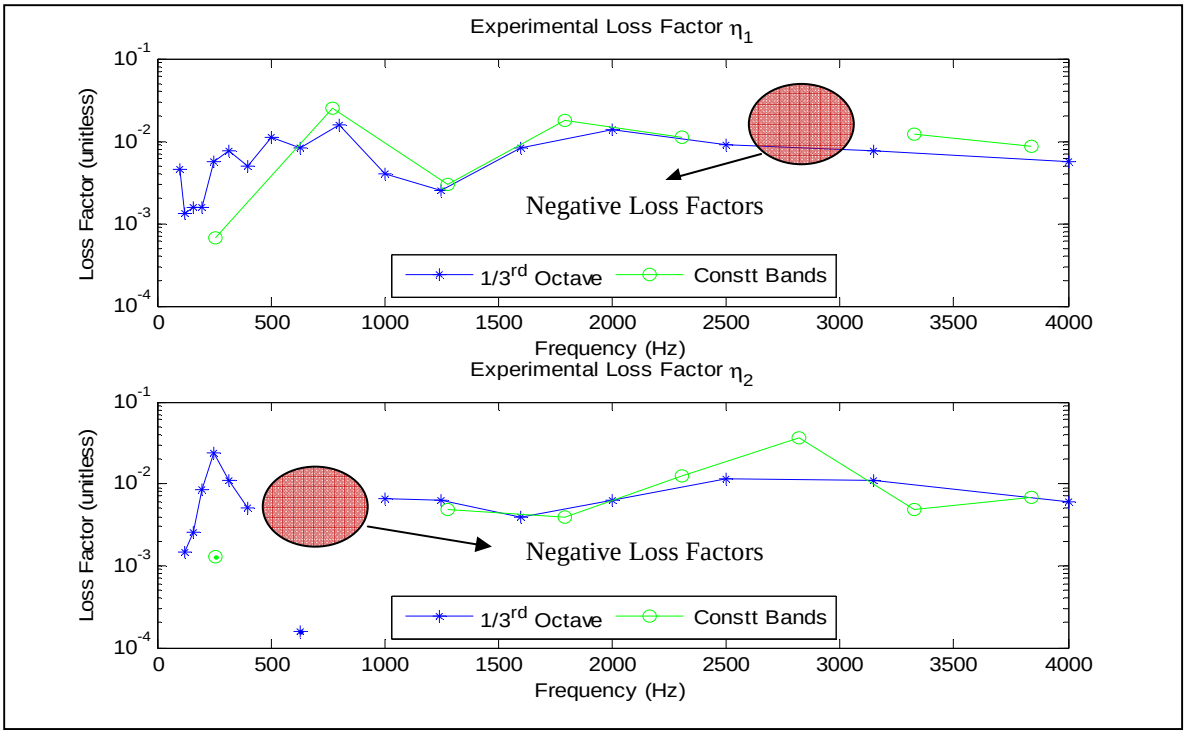

Figure 42 : Effect of frequency bands on the Loss Factors (No Damping added) - Transient excitation

At lower frequencies, between 100 Hz and 1000 Hz), the 1/3rd octave bands are very small, with frequency bandwidths ranging from 70 Hz to 400 Hz. With a modal density of about 0.0016 modes/radians/s, the number of modes per band is between 0.7 to 4 modes in those bands. This means that those bands are not close to the SEA assumption of a large number of modes per band and thus in some of those bands the calculated loss factors are negative, abnormally high or low. In the higher frequency ranges, from 2500 to 4000 Hz, the 1/3rd octave bands are very large and have a large number of modes. For example the band with center frequency 4000 Hz has a bandwidth of almost 1750 Hz. On a side note, these bands, while having a large number of modes might still fail a basic assumption in S.E.A which states that all modes in a band should have almost same modal energies. Large bands also smoothen out the loss factor curves as seen in subplot 2 of Figure 42.

The advantage of 1/3rd octave bands over constant bands can be seen in the bands where negative loss factors are estimated in constant-width bands. In such a case, the 1/3rd octave bands can estimate loss factors which are still a decent approximation of the loss factors at those frequencies. The loss factors under such conditions are underestimated because the bands contain frequency ranges where negative loss factors are estimated.

4.5.3 EFFECT OF NUMBER OF MEASUREMENT POINTS

For the 9 response point case, the accelerometers were placed in a regular pattern as shown in Figure 18. For the 6 points case, 6 accelerometers were distributed arbitrarily over the plate while avoiding the damping sheets and lines of symmetry. In this way, node lines for known, low frequency nodes were avoided. Response and excitation measurements on such node lines are known to bias the loss factor estimations [8]. In the 3 points case, accelerometers situated on the plate diagonals are used for the estimations and for the 1 point case the driving point accelerometer is used for calculations. Figure 43 and Figure 44 give the estimated loss factors for the “No damping added” case with a shaker excitation. It is evident from the figures that there is not much variation in the estimated coupling loss factors and loss factors when the measurement points are between 3 and 9 points. When the loss factors are estimated by just taking acceleration data from a single accelerometer, then the estimated loss factors differ significantly from the other cases.

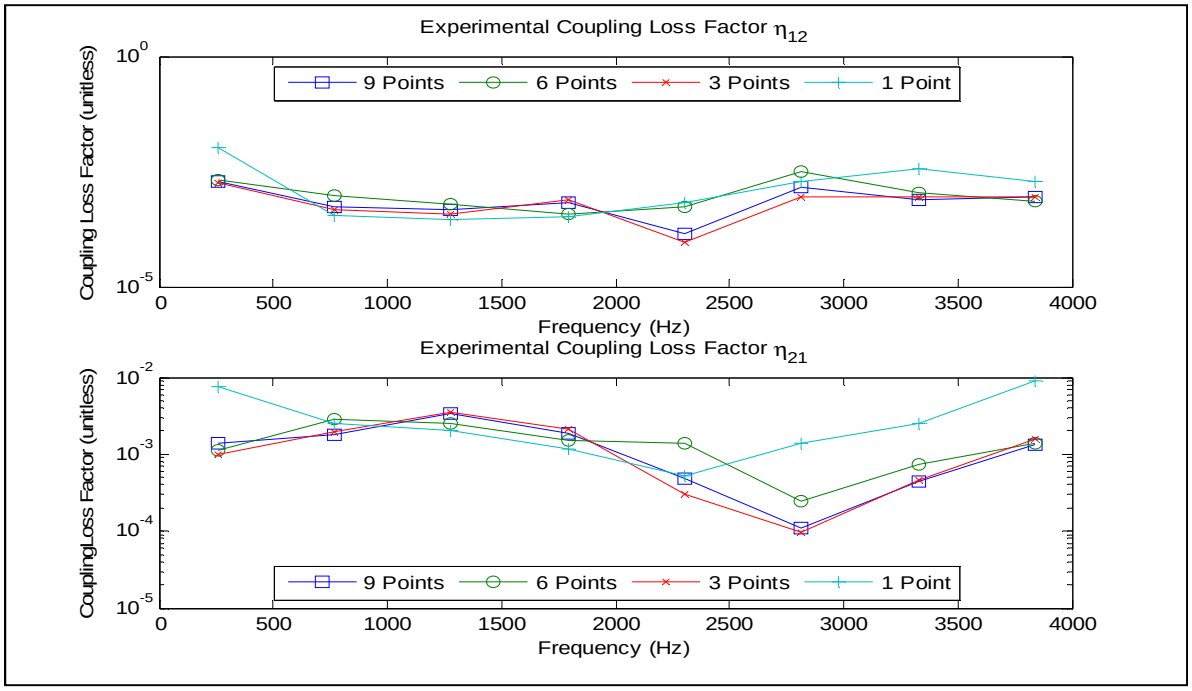

Figure 43 : Effect of number of Measurement points on the Coupling Loss Factors (No Damping added) - Persistent excitation

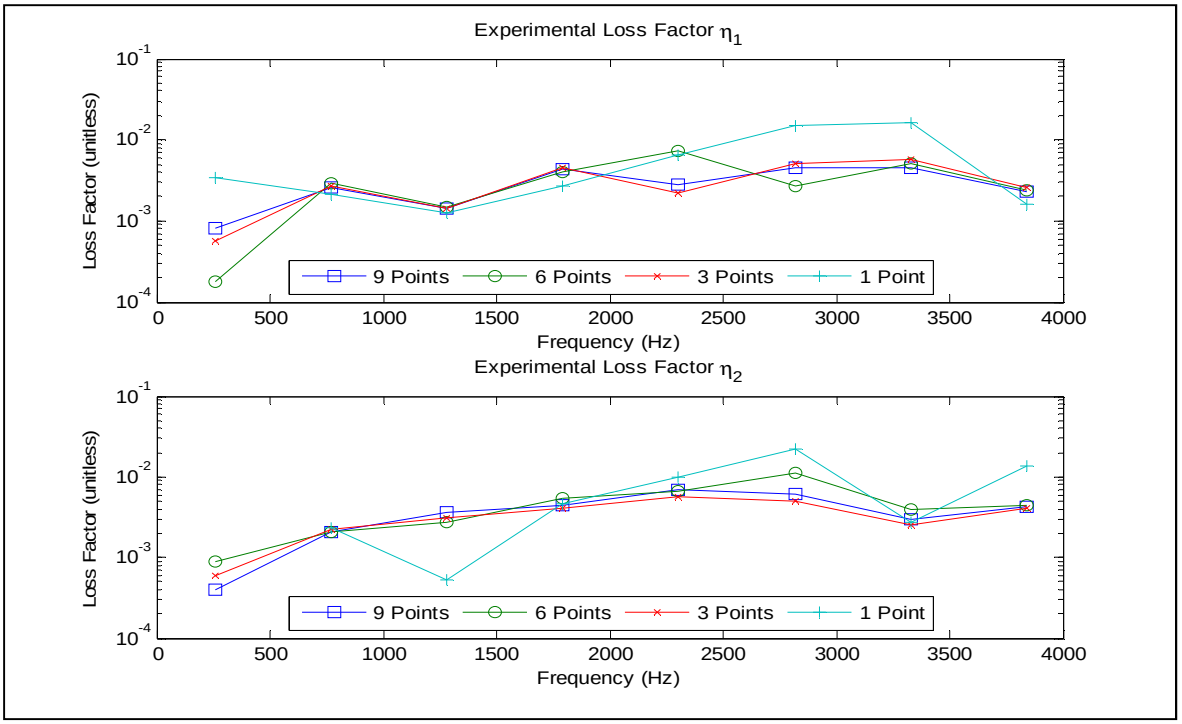

Figure 44 : Effect of number of Measurement points on the Loss Factors (No Damping added case) – Persistent excitation.

From the figures in section 4.3 it is seen that the estimated loss factors in the partially damped case (2 sheets case), where the damping sheets cover less than 15% of the surface area, are of similar magnitude as those from the no damping case. A possible reason might be the low discretization of the plates, as only 3 measurement points were chosen. Thus, for partially damped cases the number of measurement points has to be increased and distributed over the whole plate covering both the damping sheets and exposed areas of the plate.

4.5.4 EFFECT OF HAMMER TIP

For transient excitation, a modally-tuned PCB impact hammer is used to excite the Lai and Soom plates. This study concentrates on the effect of the hammer tip on the maximum frequency excited in the structure and thus on the loss factor estimated. Three different hammer tips were used experimentally – the steel tip, the plastic tip, and the soft tip. The time domain plot of the hits with different tips is shown below. The duration of the hit for the steel tip is about 0.4 ms, the plastic tip is about 0.6 ms and the soft tip is about 9.0 ms to successfully excite the entire structure. The duration of hit for the soft tip can be decreased to about 1.0 ms but upon doing that the magnitude becomes so low that the energy is transferred into the structure does not excite the structure and the accelerometers do not pick up any significant motion.

The maximum frequency excited by a hit can be inferred from auto-spectrum of the input force and is the frequency at which the auto-spectrum hits the noise floor. The subplot 1 of Figure 46 shows the maximum frequencies excited by the soft, plastic and steel tips to be about 1250 Hz, 3300 Hz and above 4000 Hz respectively.

The hammer tip is chosen based on the frequency range of interest. For low frequencies a soft tip is used and for high frequencies a steel tip or a plastic tip can be used. This is because of the relative difficulty in getting a good hit while using the steel tip when compared to a soft tip. For the steel tip and the plastic tip as the duration of the hit is about 0.5 ms the probability of getting a good hit is very low and it depends a lot on the skill of the person handling the hammer. Thus choosing the correct tip can save a lot of experimental time.

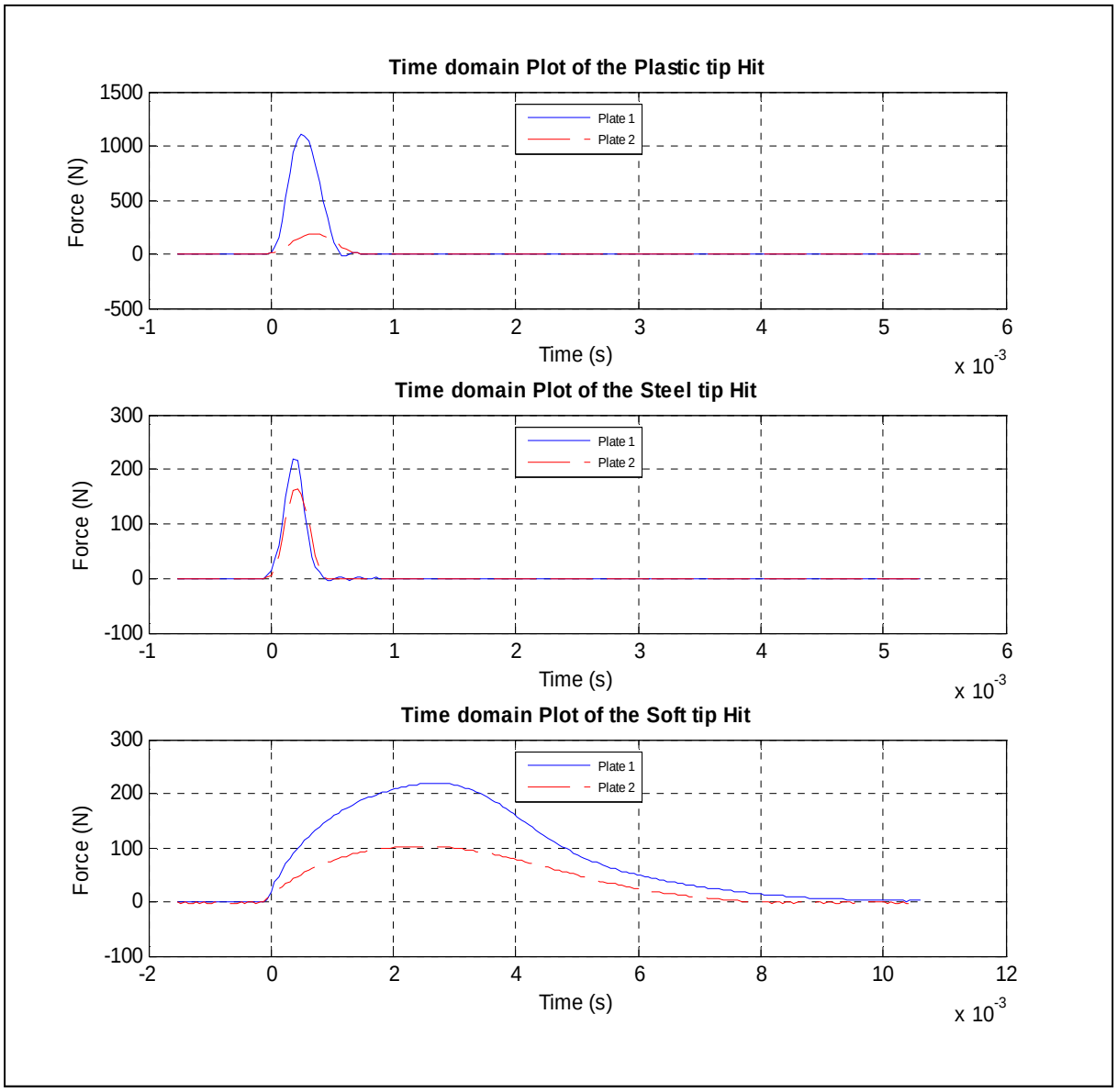

Figure 45 : Time domain plot of the hammer hit with different tips

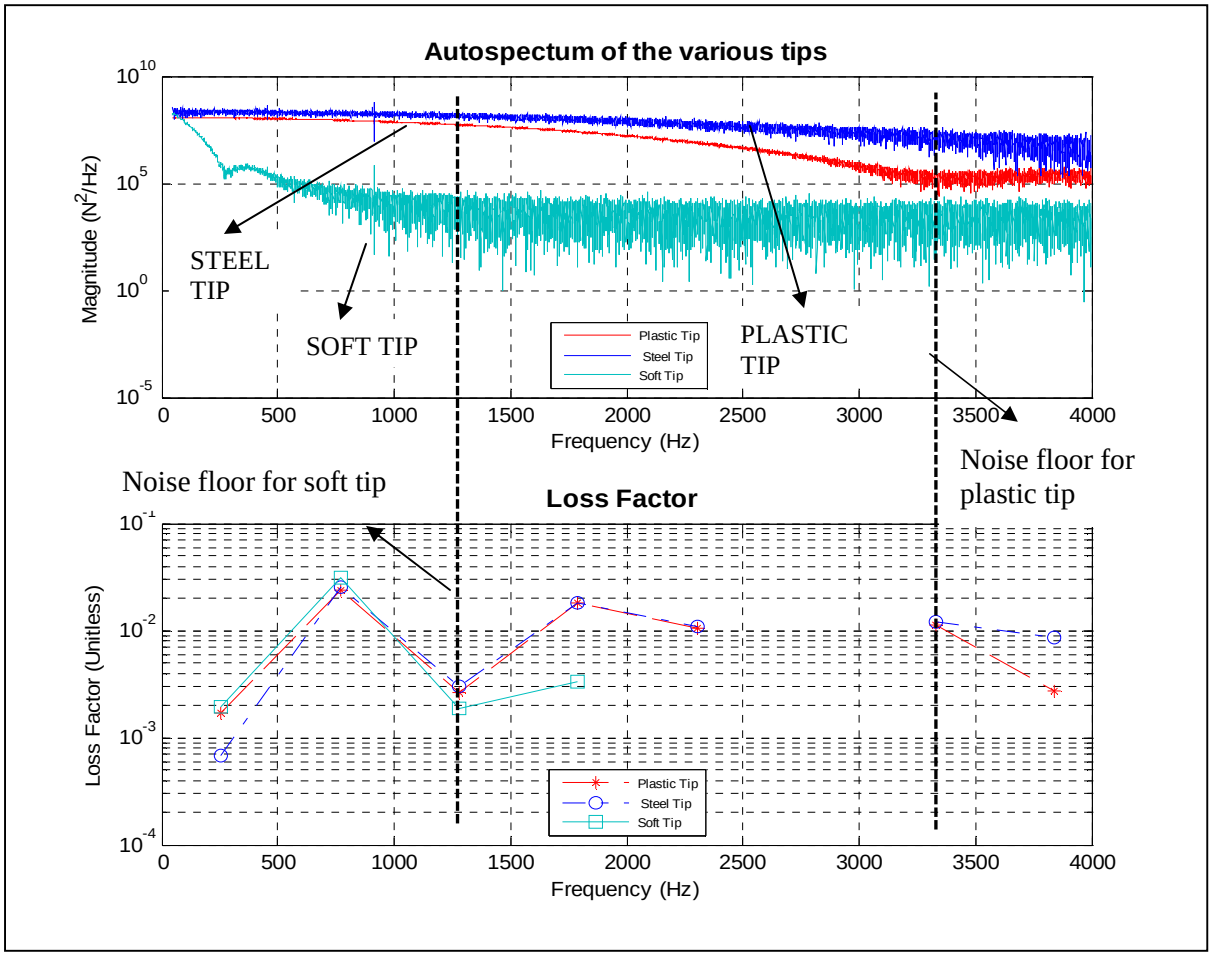

Figure 46 : Effect of the hammer tip on the estimated loss factors (no damping case)

On the comparison of the estimated loss factors and coupling loss factors excited by the various tips, we can notice from Figure 46 and Figure 47 that the loss factor curves deviate once the auto-spectrum hits the noise floor. For example the soft tip excites the structure until about 1250 Hz which falls in band 3, centered at 1280 Hz, and the plastic tip excites the structure until about 3300 Hz which falls in the band 7, centered at 3330 Hz. The coupling loss factor and the loss factor curves from the Figure 46 and Figure 47 show that the estimated loss factors, coupling loss factors deviate after band 3 in the soft tip case and after the band 7 in the plastic tip case. Thus, the auto-spectrum can also be used as an indicator to check for errors in the estimated loss factors and coupling loss factors.

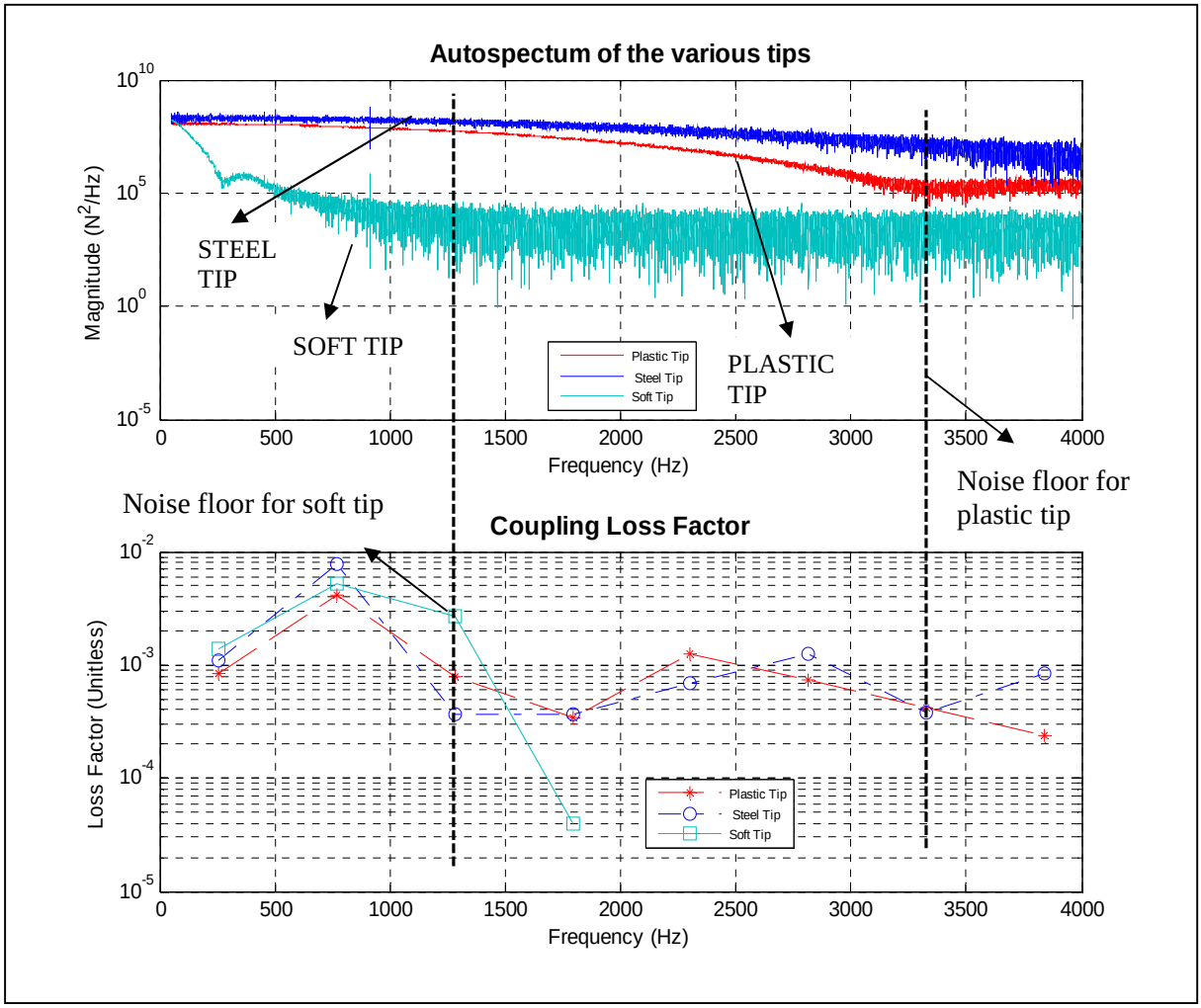

Figure 47 : Effect of the hammer tip on the estimated Coupling Loss Factors (no damping)

5.0 ESTIMATION OF LOSS FACTORS USING THE TRANSIENT STATISTICAL ENERGY ANALYSIS METHOD

The main aim of using the transient statistical energy analysis method to estimate the loss factors in this thesis was to interpret the results by M. L. Lai in [26] and [14], to determine the practical limitations of the method and to establish the degree of agreement of the asymptotic loss factor estimations with respect to the power input method. The numerical simulations performed here are similar to the ones performed in reference [26].

5.1 NUMERICAL SIMULATION OF A SIMPLE 2-DOF SYSTEM

The main purpose of the numerical simulations is to show that in a transient case the damping coefficients, hence the loss factors, vary with time. Substituting a steady state loss factor for transient excitations, as done by Manning and Lee [20], might not fully explain the physics behind the problem and the new "apparent time varying coupling loss factors" introduced by Lai and Soom in [14] correctly represent the energy losses in the system under a transient load. These time varying loss factors are then used to develop a new method (TSEA method) to analyze transient load cases.

Consider the 2-DOF system with a spring coupling between the oscillators as shown in the Figure 13. The equation of motion for the whole system is given by the equation (2.19). Decoupling the matrix form and writing the equations of motion for the individual oscillators gives us

$$M_1\ddot{x}_1 + C_1\dot{x}_1 + (K_1 + K_g)x_1 - K_g x_2 = F_1 \tag{5.1}$$

$$M_2\ddot{x}_2 + C_2\dot{x}_2 + (K_2 + K_g)x_2 - K_g x_1 = F_2 \tag{5.2}$$

The above 2 equations are the force balance equations. Multiplying (5.1) by $\dot{x}_1$ and (5.2) by $\dot{x}_2$ gives us the power balance equations as

$$M_1\ddot{x}_1\dot{x}_1 + C_1\dot{x}_1^2 + (K_1 + K_g)\dot{x}_1 x_1 - K_g\dot{x}_1 x_2 = F_1 x_1 \tag{5.3}$$

$$M_2\ddot{x}_2\dot{x}_2 + C_2\dot{x}_2^2 + (K_2 + K_g)\dot{x}_2 x_2 - K_g\dot{x}_2 x_1 = F_2 x_2 \tag{5.4}$$

Using the identities

$$\begin{aligned} \frac{1}{2}\frac{d\dot{x}_1^2}{dt} &= \ddot{x}_1\dot{x}_1 \\ \frac{1}{2}\frac{dx_1^2}{dt} &= \dot{x}_1 x_1 \end{aligned} \tag{5.5}$$

Equations (5.3), (5.4) can be reduced to

$$\frac{d}{dt}\left(\frac{1}{2}M_1\dot{x}_1^2 + \frac{1}{2}(K_1 + K_g)x_1^2\right) + C_1\dot{x}_1^2 = F_1 x_1 + K_g\dot{x}_1 x_2 \tag{5.6}$$

$$\frac{d}{dt}\left(\frac{1}{2}M_2\dot{x}_2^2 + \frac{1}{2}(K_2 + K_g)x_2^2\right) + C_2\dot{x}_2^2 = F_2 x_2 + K_g\dot{x}_2 x_1 \tag{5.7}$$

We can further simplify the above equations. The total energy is the sum of potential energy and kinetic energy. Hence,

$$E_1 = \frac{1}{2}\left(\left(K_1 + K_g\right)x_1^2\right) + \frac{1}{2}\left(M_1\dot{x}_1^2\right) \tag{5.8}$$

The power is dissipated through the inherent damping in the oscillator and hence the term containing the damping coefficient is the power dissipated term

$$\pi_{diss}^1 = C_1\dot{x}_1^2 \tag{5.9}$$

Power input is due to the external forces acting on the system, so the power input is given by

$$\pi_{in}^{1} = F_1 \dot{x}_1 \tag{5.10}$$

The remaining terms in equations (5.7) and (5.6) define the power transferred between the oscillators

$$\pi_{tr}^{12} = K_g \dot{x}_1 x_2 \tag{5.11}$$

Combining the equations (5.6), (5.7), (5.8), (5.9), (5.10), (5.11) we get

$$\begin{aligned} \frac{d}{dt} E_1 &= \pi_{in}^{1} - \pi_{diss}^{1} - \pi_{tr}^{12} \\ \frac{d}{dt} E_2 &= \pi_{in}^{2} - \pi_{diss}^{2} - \pi_{tr}^{21} \end{aligned} \tag{5.12}$$

Integrating the above equation (5.12), results in the energy balance equations

$$\begin{aligned} \frac{d}{dt} \varepsilon_1(t) &= E_{in}^{1}(t) - E_{diss}^{1}(t) - E_{tr}^{12}(t) \\ \frac{d}{dt} \varepsilon_2(t) &= E_{in}^{2}(t) - E_{diss}^{2}(t) - E_{tr}^{21}(t) \end{aligned} \tag{5.13}$$

Oscillator 2 is excited by a rectangular step force of magnitude $\frac{(\delta(t) - \delta(t - \Delta t))}{\Delta t}$ and duration 0.001 s to simulate transient conditions. δ is the Dirac-delta function.

A simple 2-DOF problem is numerically solved using the state matrix method shown in section 4.1. The properties of the sample 2-DOF system are as follows. The masses M_1 and M_2 are 1 Kg each. The natural frequencies ω_{n1} and ω_{n2} are 149.8 radians/s and 200.1 radians/s respectively. The spring stiffness K_1 and K_2 are 22500N/m and 40000N/m respectively. The spring coupling K_c is 1000N/m. The blocked natural frequencies of the oscillators are ω_1=150 radians/s and ω_2=200 radians/s respectively. The input loss factor of both the oscillators is 0.075.

The transferred energies, transferred power, integrated kinetic energies, integrated total energies, kinetic energies, total energies can be calculated from the formulae given above.

The new "apparent time varying coupling coefficient" is given by equation (2.39) and is restated here

$$E_{tr}^{12}(t) = 2C_{12}(t)\left(\varepsilon_1^k(t) - \varepsilon_2^k(t)\right) \tag{5.14}$$

The energy input and the blocked period of oscillation are used to non-dimensionalize the energy terms. The energy input term is given by

$$E_{in}(t) = \int_{-\infty}^{\infty} F_t(\tau) v_{ft}(\tau) d\tau \tag{5.15}$$

Here,

F_t is the truncated force up to time t and is defined as

$F_t(\tau) = F(t)$ when $\tau \le t$

and $F_t(\tau) = 0$ when $\tau > t$

$v_{ft}(\tau)$ is the velocity of the oscillator which is excited by the force $F(t)$.

The results are plotted in the figures below. Figure 48 and Figure 49 show the velocities of the oscillators 1 and 2 of the simple 2-DOF problem. Since oscillator 2 is directly excited by the external rectangular impulse force we can see a nice decay in its response whereas the oscillator 1, which is excited by the spring coupling and the energy flowing in it, does not have a smooth decay.

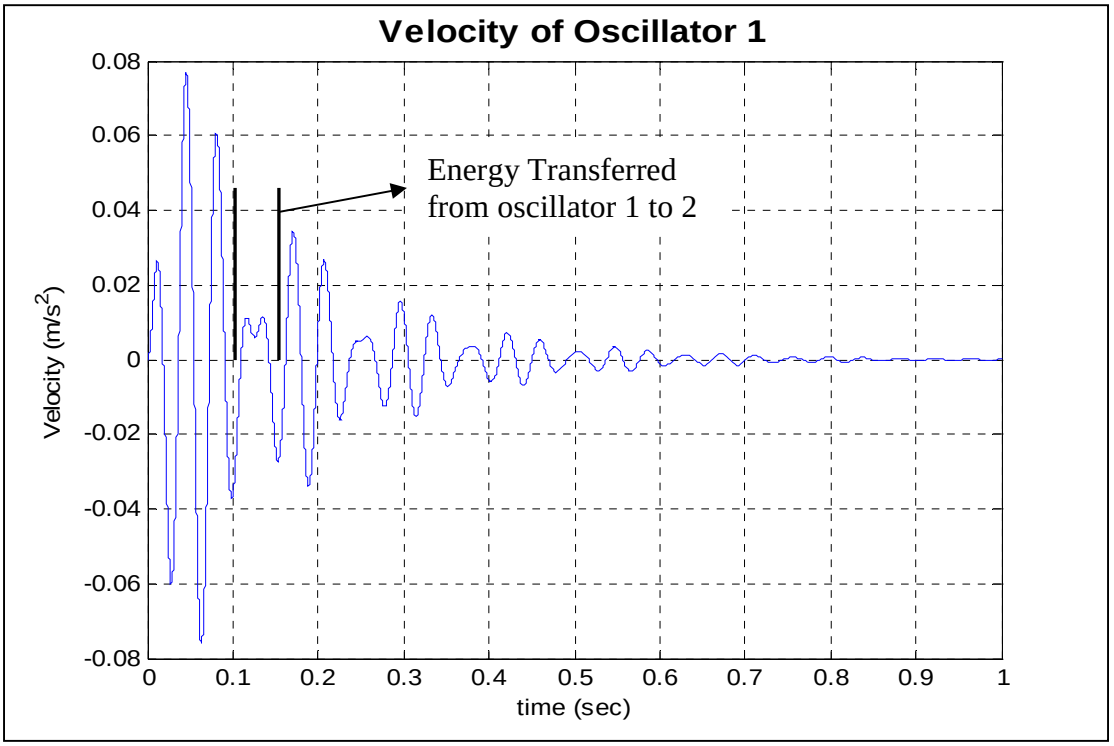

Figure 48 : Velocity of oscillator 1 of the simple 2-dof system

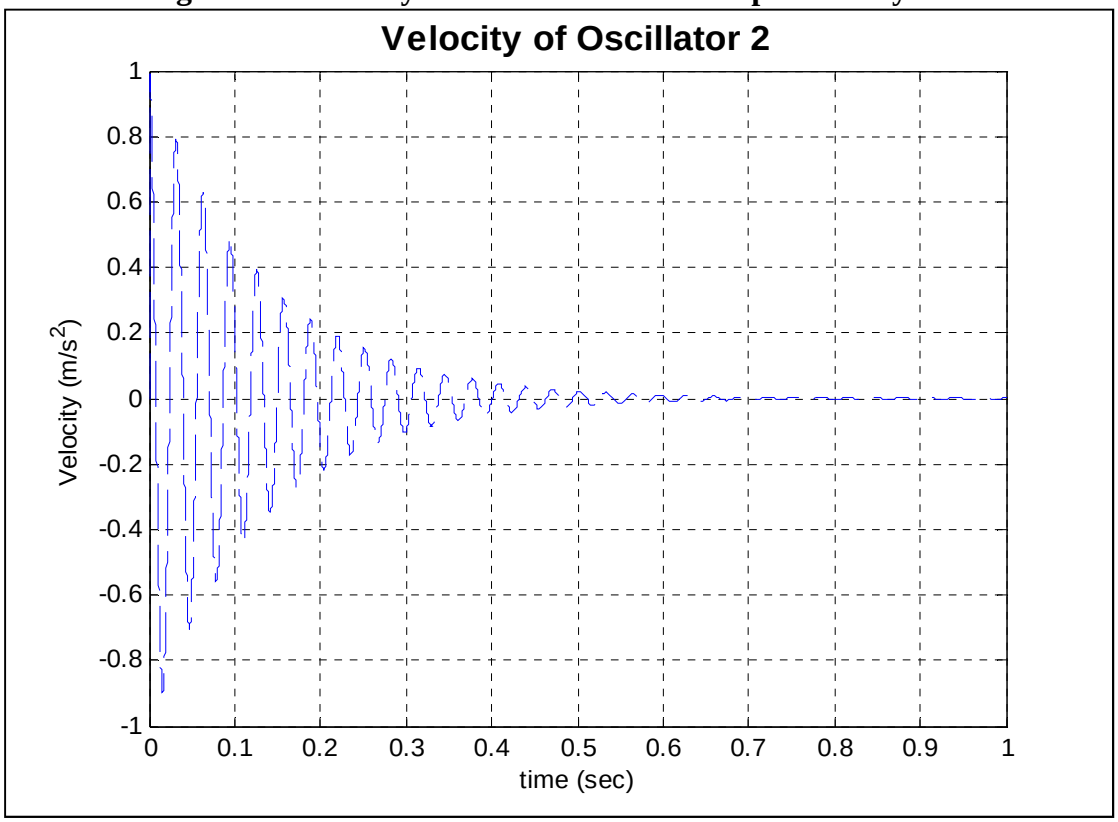

Figure 49 : Velocity of oscillator 2 of the simple 2-dof system

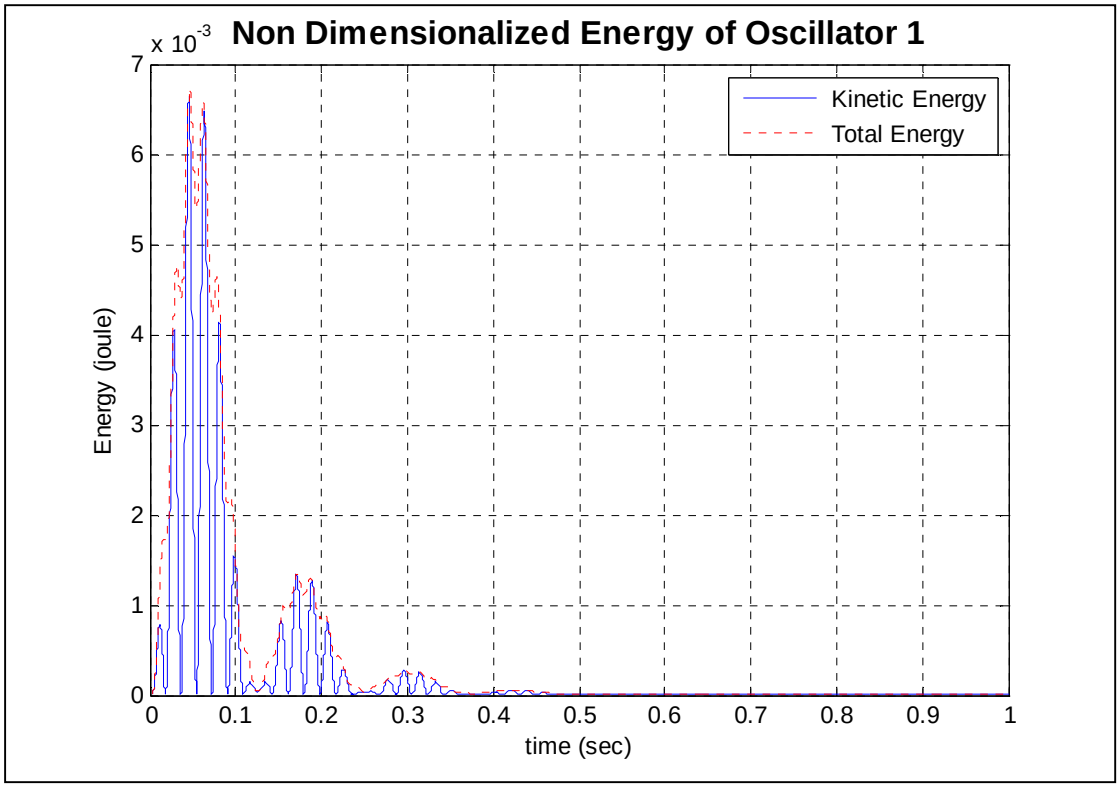

Figure 50: Total energy and Kinetic energy of oscillator 1

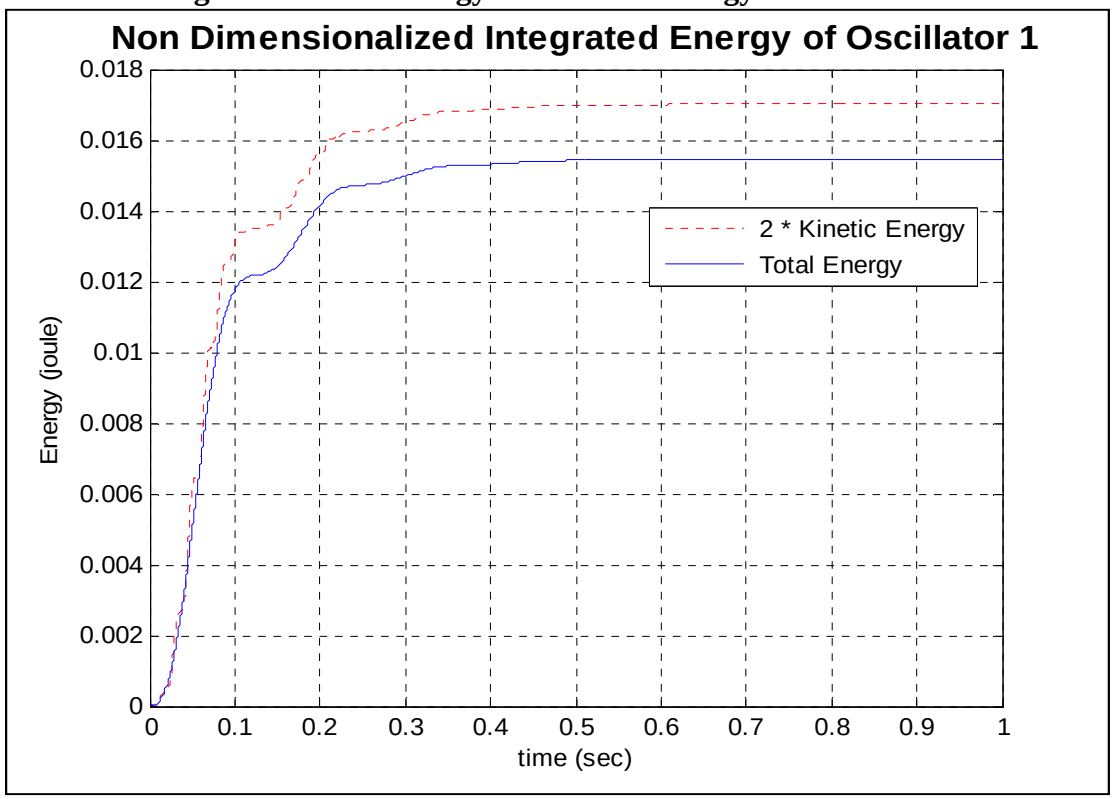

Figure 51 : Integrated energy of oscillator 1

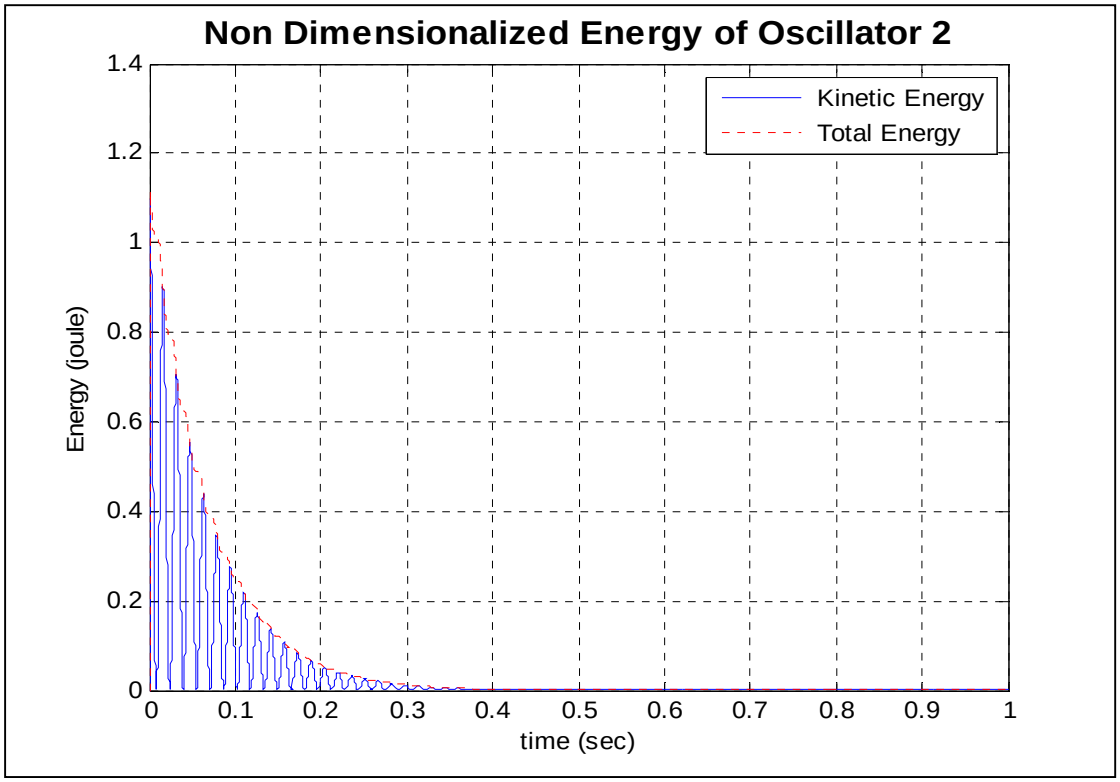

Figure 52 : Total energy and Kinetic energy of oscillator 2

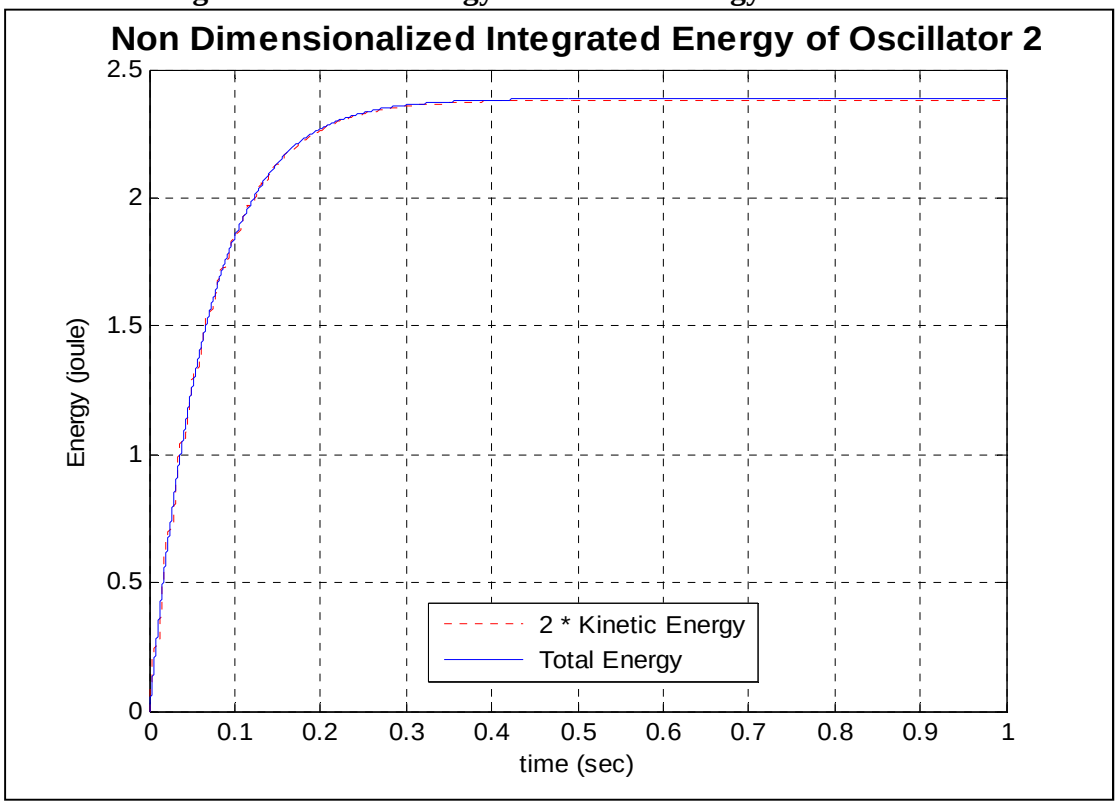

Figure 53 : Integrated energy in oscillator 2

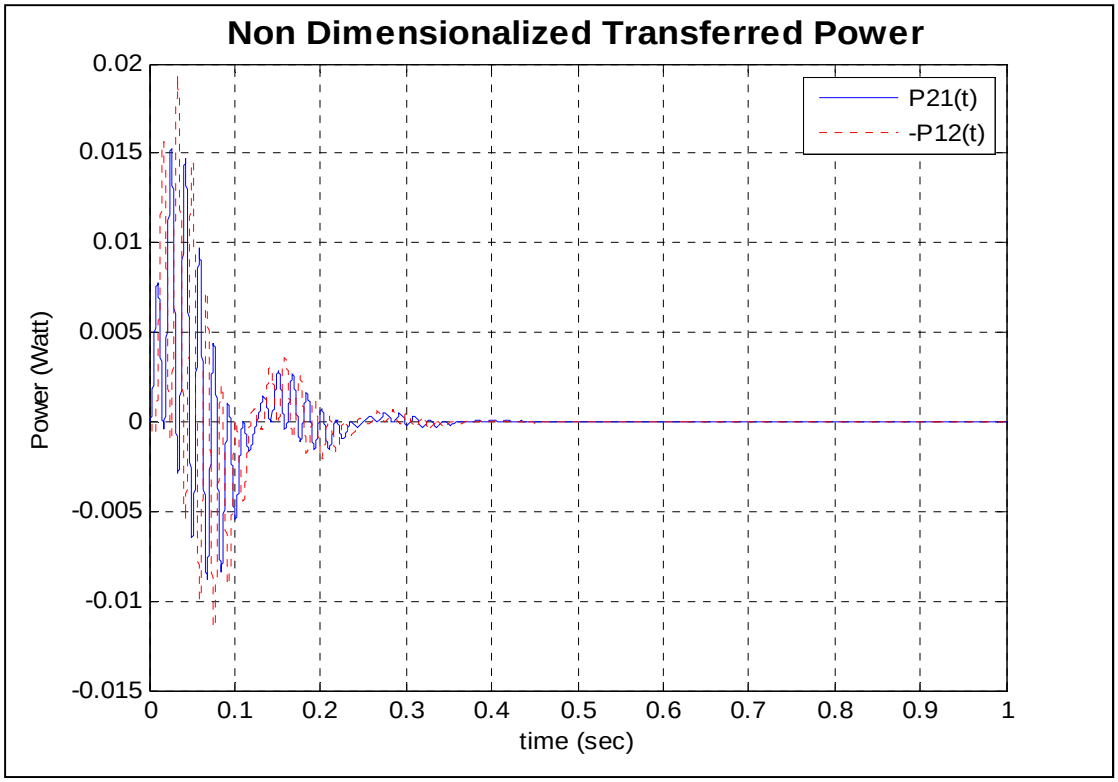

Figure 54 : Transferred power between the 2 oscillators

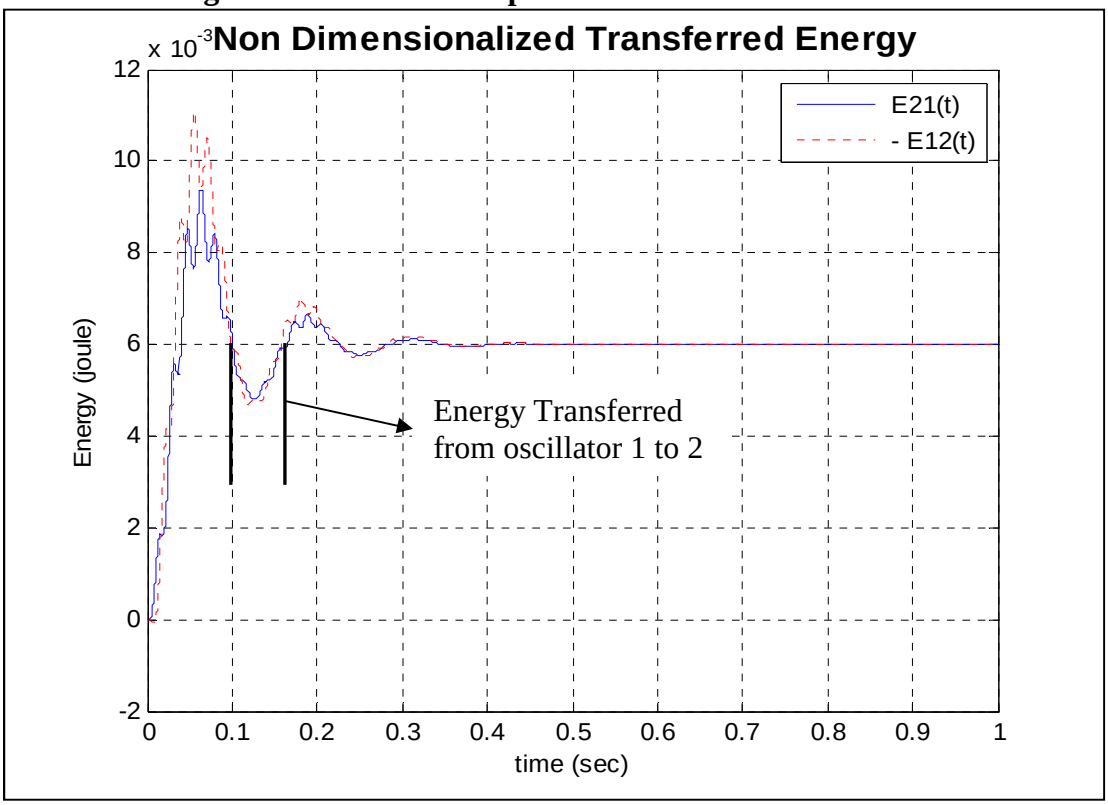

Figure 55 : Transferred energy between the 2 oscillators

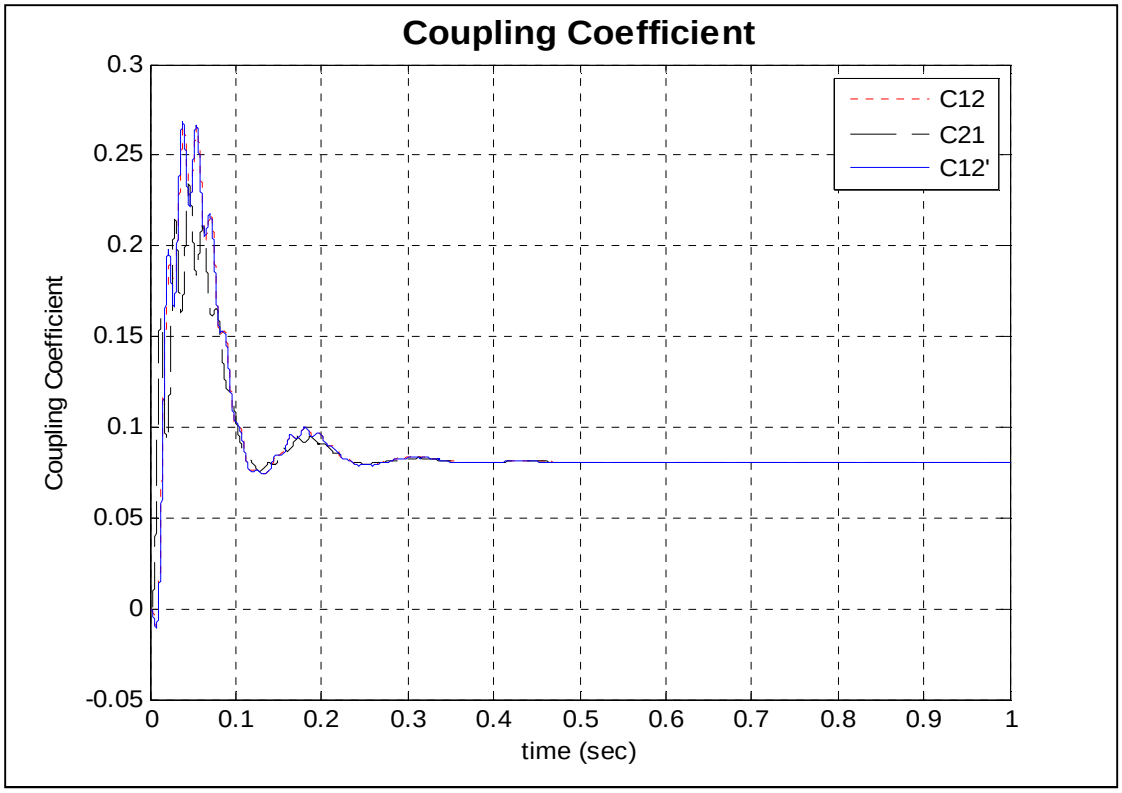

Figure 56 : Apparent time varying coupling coefficient

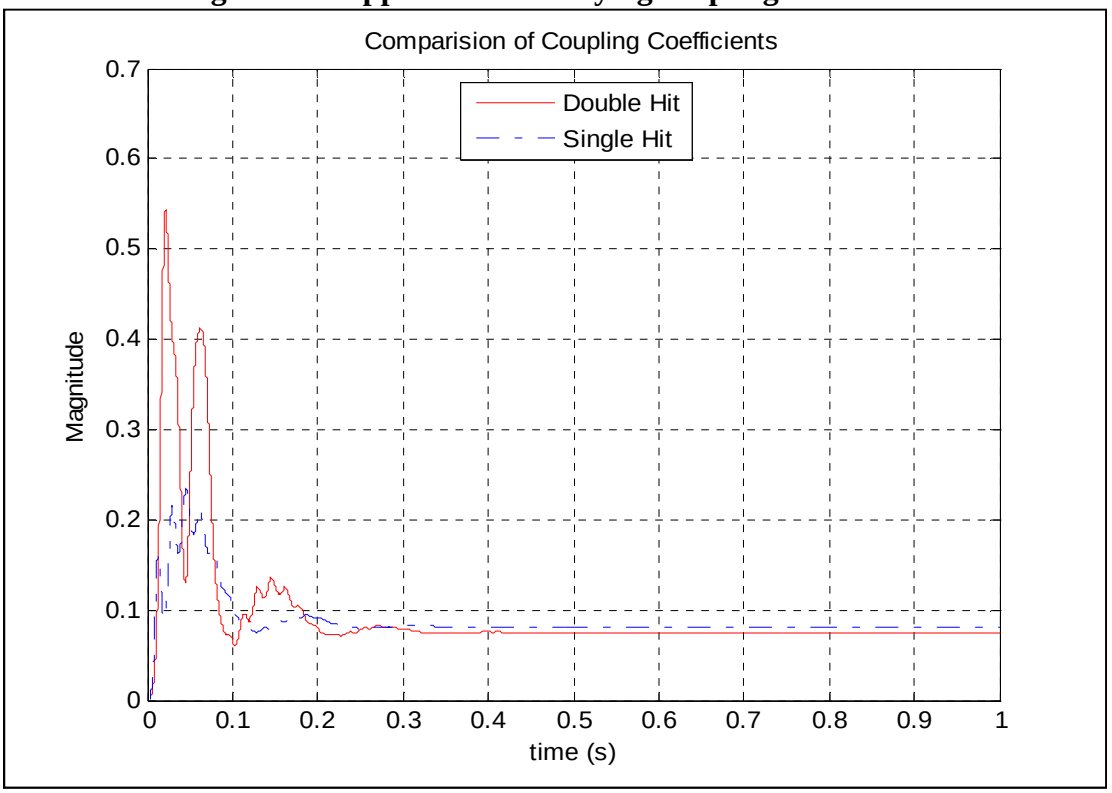

Figure 57 : Comparison of coupling coefficients

On comparing Figure 48 and Figure 55 we can see that the increase in the velocity of oscillator 1 corresponds to the time where energy is transferred from oscillator 2 to oscillator 1 and the decrease in the velocity corresponds to the time where energy is transferred from oscillator 1 to 2. There is no substantial effect on the response of oscillator 2 because of the vast (2 orders of magnitude) difference in the magnitude of the velocity and the energy transferred.

Figure 53 shows that twice the integrated kinetic energy for oscillator 2 is approximately equal to the integrated total energy which proves the assumption used in the derivation of the T.S.E.A. method. The slight difference between the integrated energies in Figure 51 occurs at a time when the energy is transferred from oscillator 1 to 2 and when the displacement of the oscillator 1 reaches a minimum value, from time t=0.1s to 0.15s as marked in the plots. Comparing the plots in Figure 51 and Figure 53 it can be noted that the integrated energy curves in oscillator 2 have the same magnitude but the integrated energy curves in oscillator 1 have a variation of about 10%. This difference can be neglected because of the difference in the energy levels of the 2 oscillators is almost 2 orders of magnitude.

Figure 50 and Figure 52 show the change in energy levels of the 2 oscillators with respect to time and the time at which they stop oscillating. Oscillator 2, which is directly excited, shows a nice decay in its energy curve whereas the energy curve of the oscillator 1, which is excited by the coupling joint, looks like a sinusoidal curve with multiple maximums and minimums.

Figure 54 and Figure 55 show the power and energy transfer characteristics between the 2 oscillators. The energy transferred is always positive and slowly reaches an asymptotic value as the vibration decays down. The transferred power on the other hand is an instantaneous quantity and is both positive and negative depending on the direction of the energy flow between the

oscillators. Once the oscillators come to an equilibrium state we see that both the transferred energy and transferred power reach an asymptotic value, which is 0 for transferred power.

Figure 56 shows the coupling coefficient between the 2 oscillators. The plot actually shows that the coupling coefficient is dependent on time and slowly reaches a value which is equal to the steady state coupling coefficient. Since, C_{12} (t) and C_{12}' (t) are calculated using the transferred energy term E_{12} (t) and C_{21} (t) is calculated using E_{21} (t) the variations in the coupling coefficient terms are because of the differences in the energy terms.

The values in Figure 48 to Figure 56 match exactly with the values calculated by M. L. Lai in [14], the sole exception being the duration of the hit. Lai stated that the duration of hit was 0.075 seconds. But upon performing a numerical study with that hit duration it was found that the integrated total energy and integrated kinetic energy terms depend on the duration of the hit. They were off by about 150% and thus the coupling coefficients estimated were also off by about 150%. Experimentally such a hit is called a bad hit or a double hit. This is one of the reasons why double hits are not acceptable experimentally.

5.2 EXPERIMENTAL RESULTS FOR THE LAI AND SOOM PLATES

The experimental setup and test settings used to calculate loss factors using the power input method were used to estimate the coupling loss factors using the T.S.E.A method. A force transducer is used to connect the 2 plates and it measures the force transferred between the two plates. The input force is also measured to filter out double hits and out of range hits.

Small holes are drilled into the plates at the top right corner on the bottom plate and at the bottom right corner on the top plate. The force transducer is then bolted into the two plates and this creates a physical point joint between the plates. Any force transfer that happens between the 2 plates happens through the force transducer. To maintain consistency with and compare results with Lai and Soom results the plate dimensions, measurement points and the hit points are similar to the ones used in [26].

Figure 58- Figure 63, are the plots of the apparent time varying coupling loss factors in the various bands for different levels of damping on the Lai and Soom plates. Comparing the band 1 and band 2 results from the below 6 figures it is clear that as the damping level increases the number of negative loss factor estimations decrease.

Comparing the individual bands in the figures below, we can also notice that in bands at higher frequencies, i.e. band 3 and above, the time varying loss factors converge to an asymptotic value quickly when compared to the lower frequency bands, i.e. band 1 and 2. This is because at higher frequencies, as the system vibrates with more cycles per second, more energy is lost per second and hence reaches a steady state quickly when compared to the lower frequency bands.

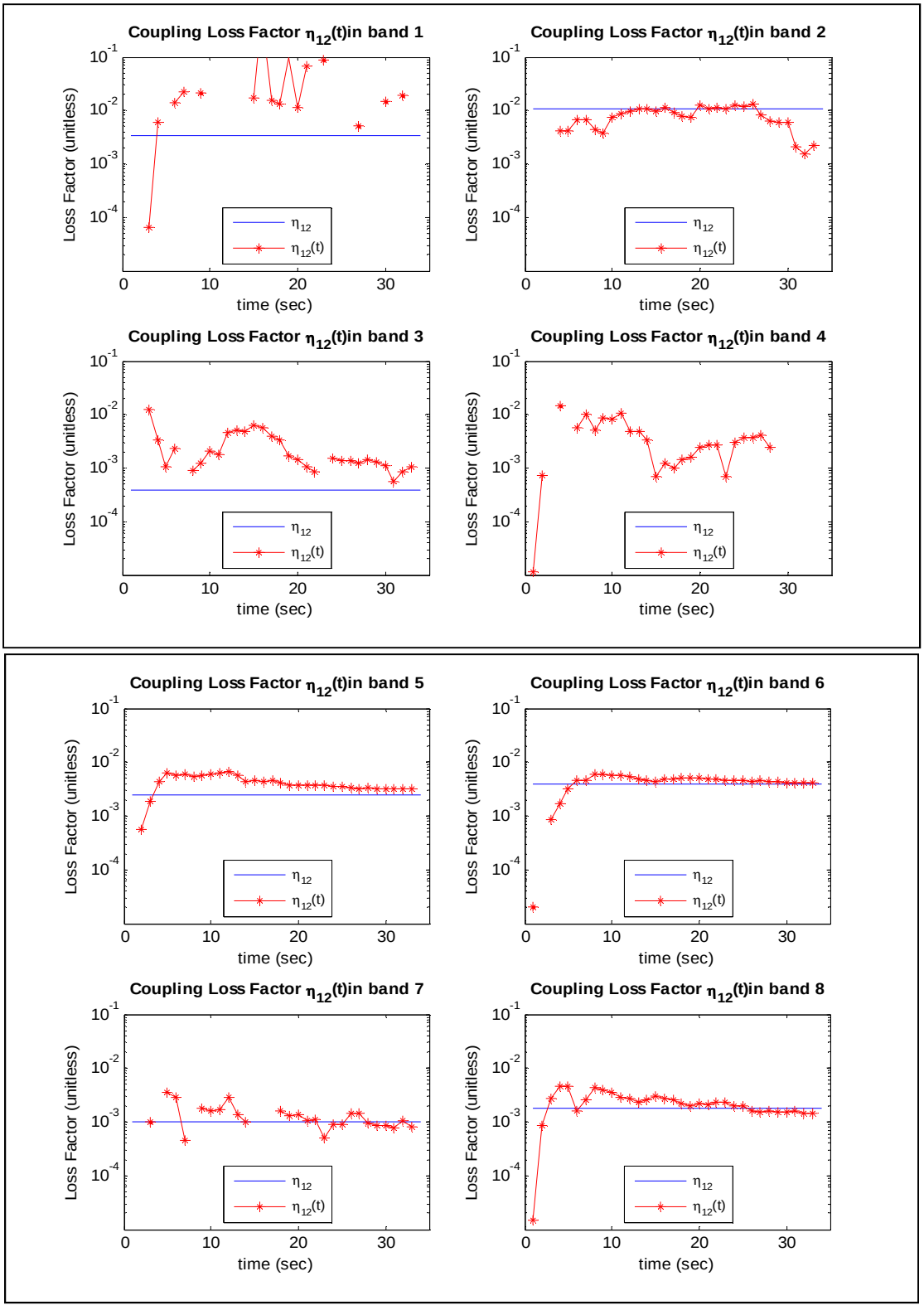

Figure 58 : Apparent Coupling Loss Factor η_{12} of the Lai and Soom plates with no damping added.

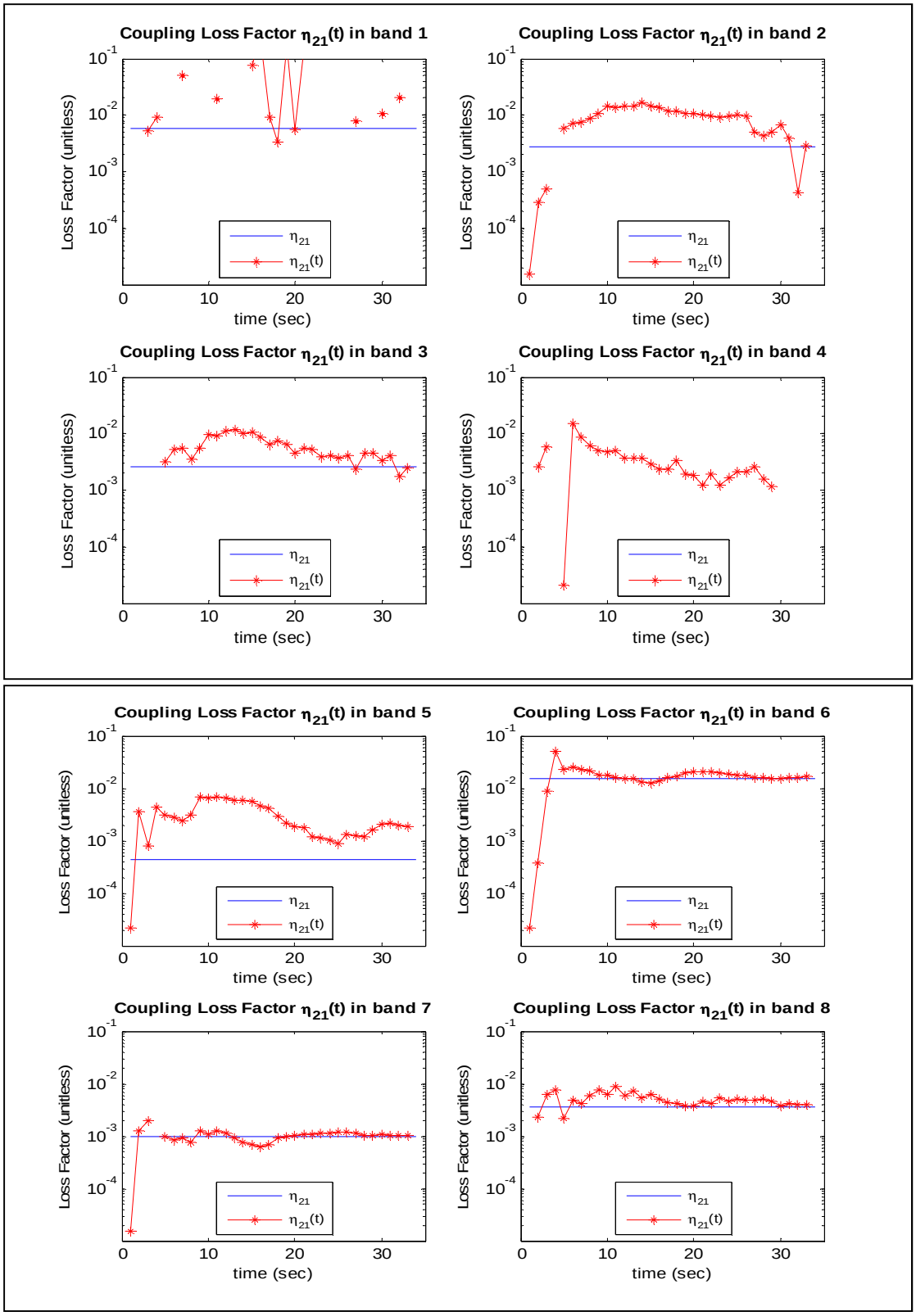

Figure 59 : Apparent Coupling Loss Factor η_{21} of the Lai and Soom plates with no damping added.

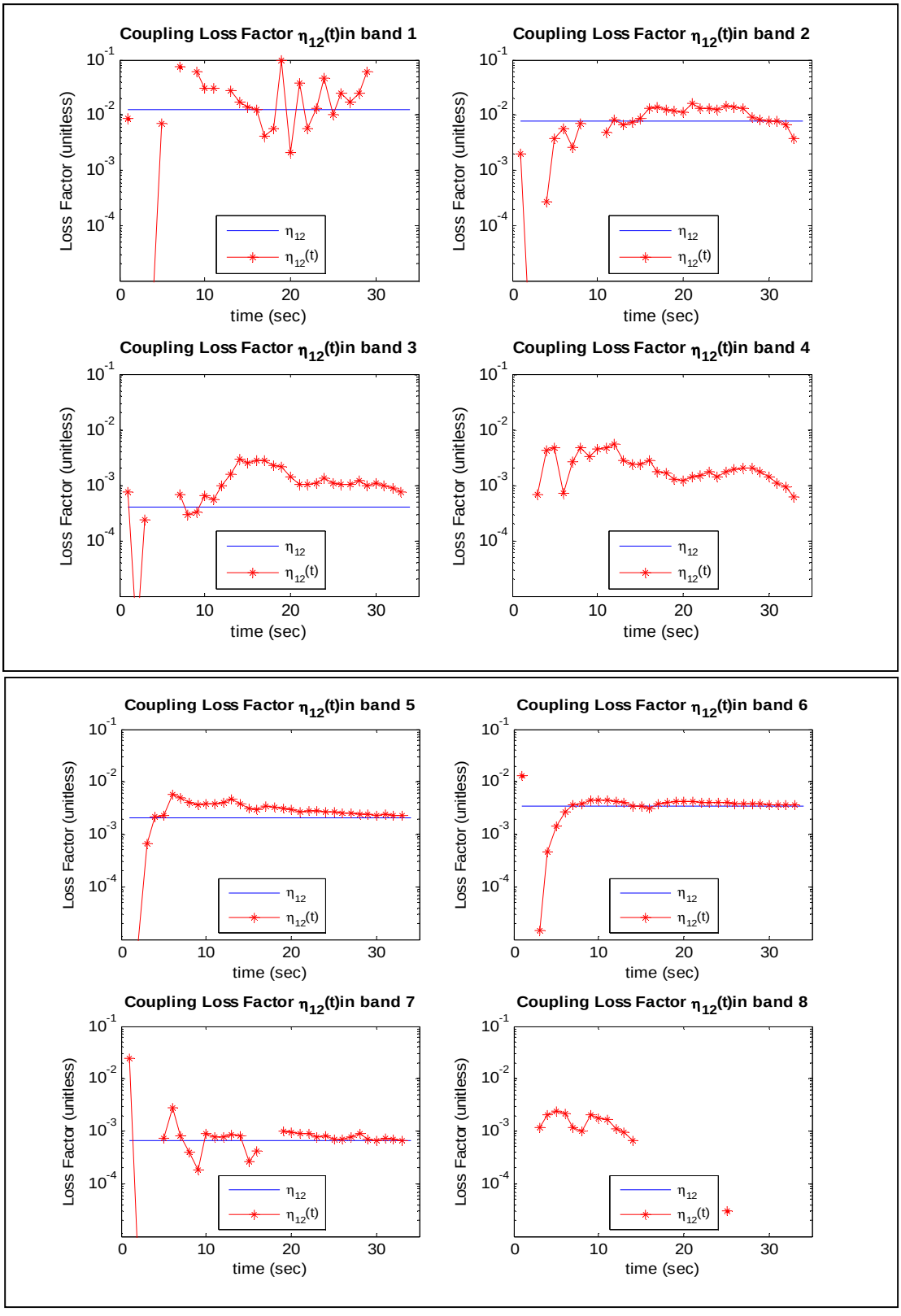

Figure 60 : Apparent Coupling Loss Factor η_{12} of the Lai and Soom plates with 2 sheets of damping added

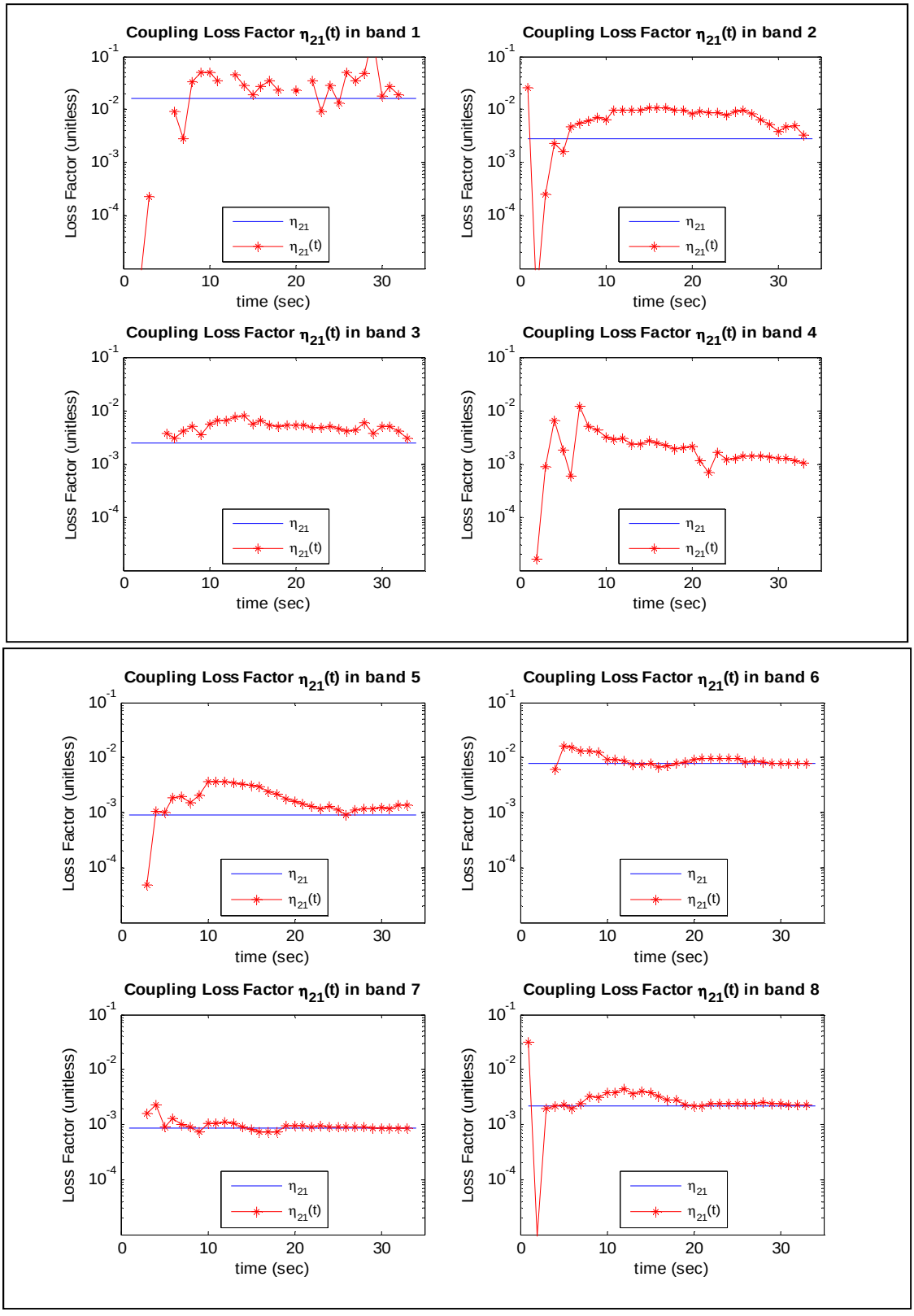

Figure 61 : Apparent Coupling Loss Factor η_{21} of the Lai and Soom plates with 2 sheets of damping added

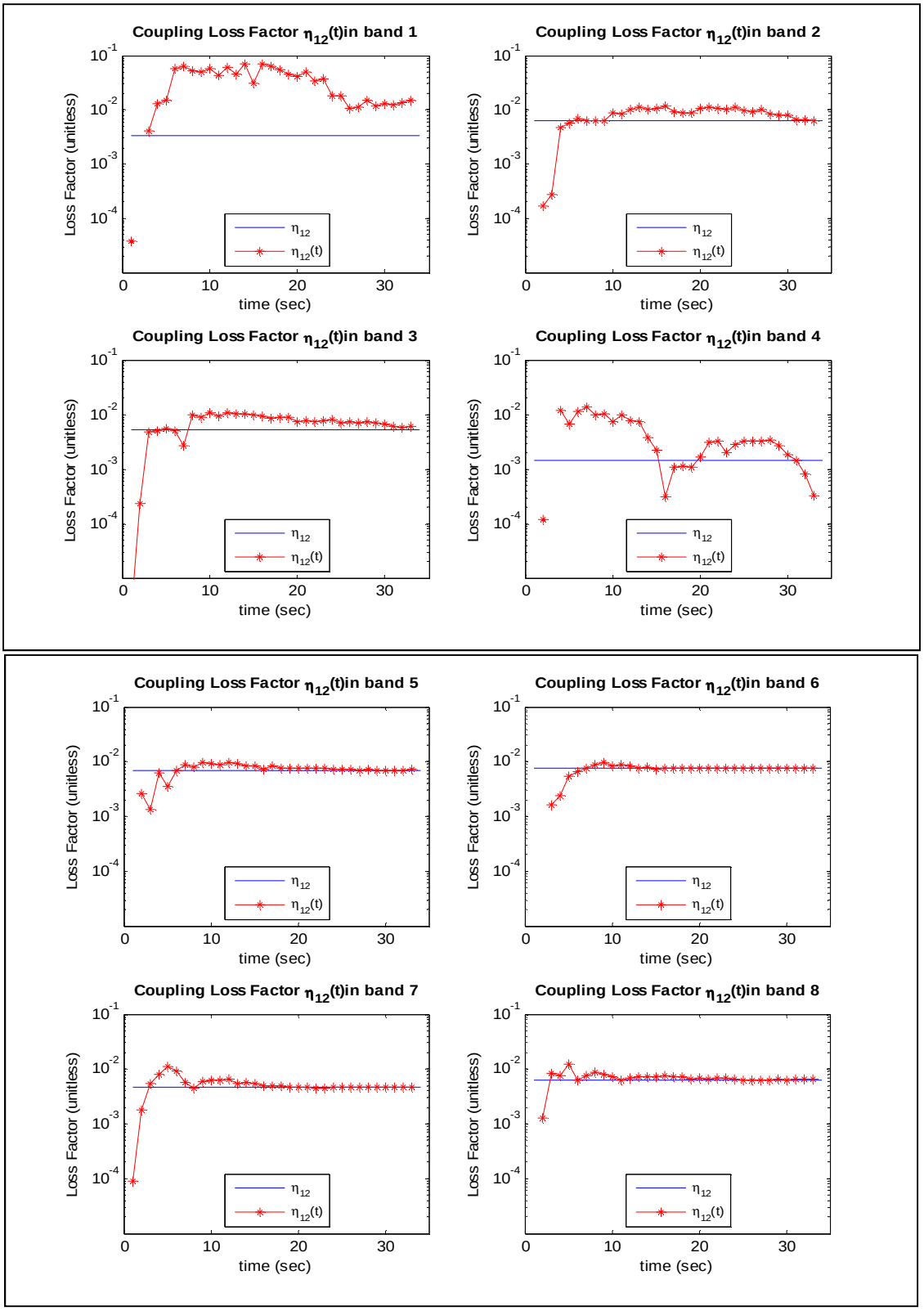

Figure 62 : Apparent Coupling Loss Factor η_{12} of the Lai and Soom plates with 6 sheets of damping added

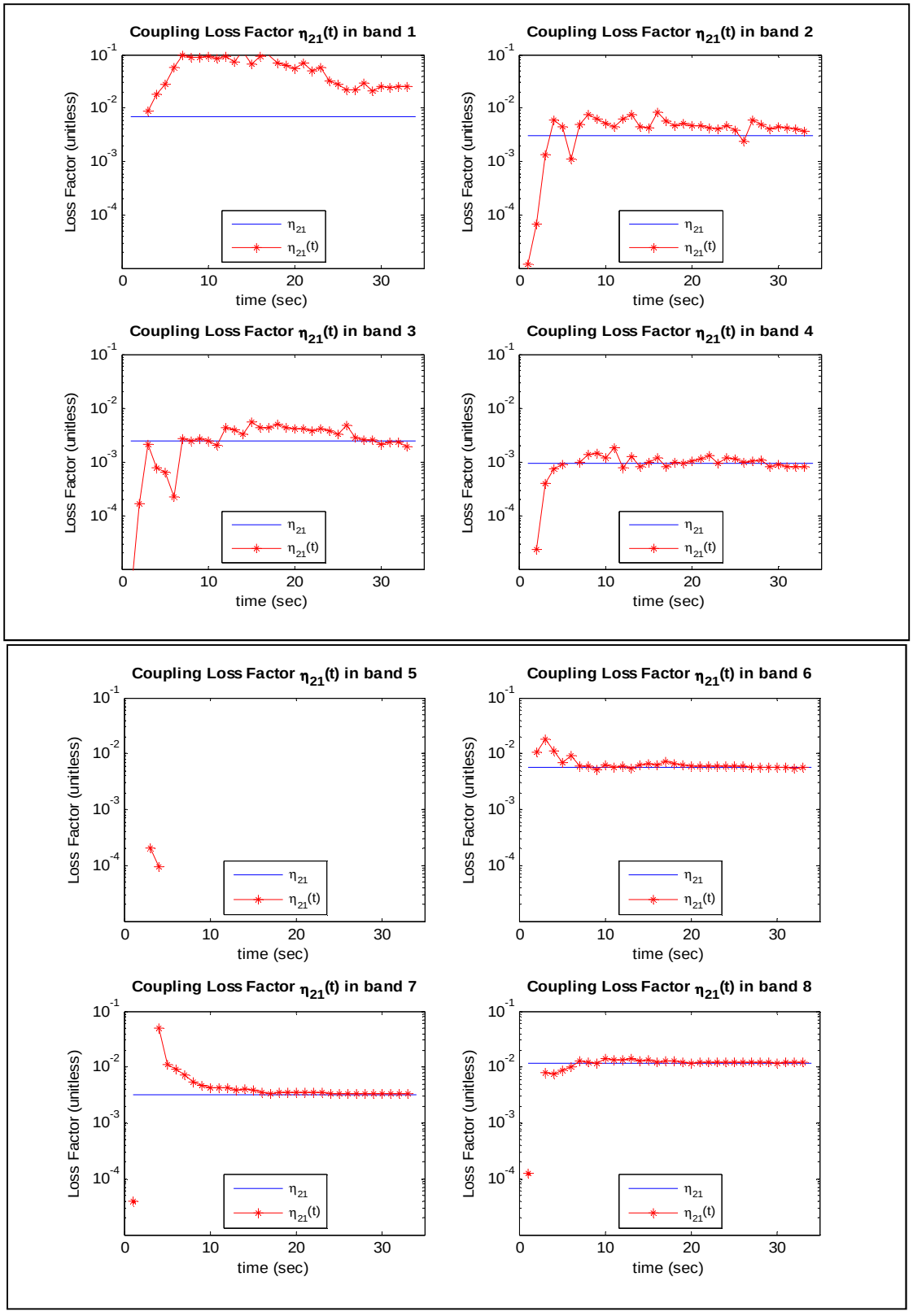

Figure 63 : Apparent Coupling Loss Factor η_{21} of the Lai and Soom plates with 6 sheets of damping added

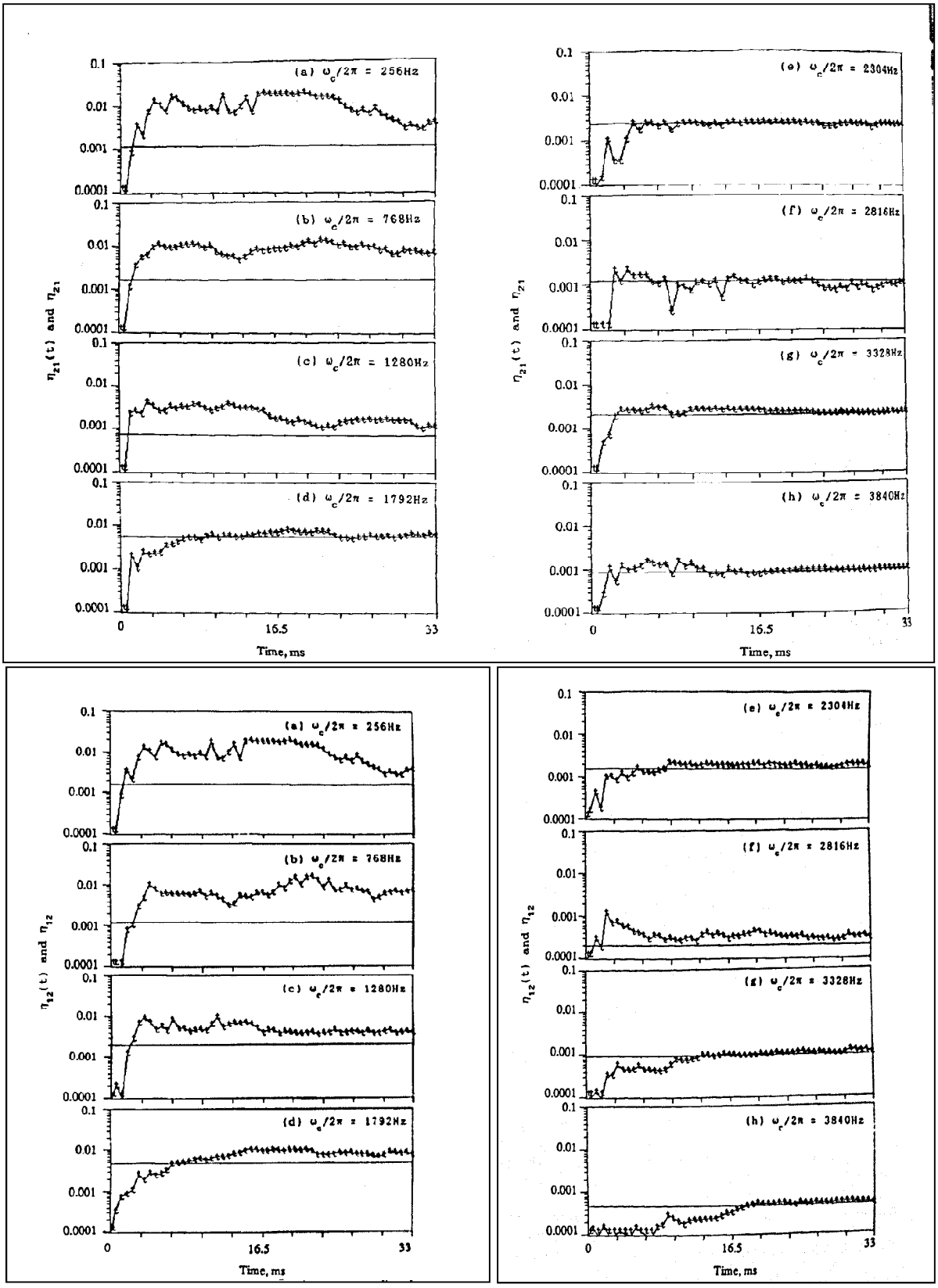

Figure 64 : Time varying Coupling Loss Factors from [14]

As the damping of the system increases the energy losses per cycle increase hence the system reaches a steady state position quickly. This means that the "apparent time varying coupling coefficient", as shown in Figure 56, also reaches the asymptotic value quickly. Since the coupling coefficient and the loss factor are related by the equation given below the "apparent time varying loss factor" will attain the asymptotic value quickly. From the figures above this relationship is also proved experimentally.

$$\eta_{12}(t,\omega_c) = \frac{C_{12}(t,\omega_c)N_2}{\omega_c} \tag{5.16}$$

5.2.1 NEGATIVE ASYMPTOTIC COUPLING LOSS FACTORS

In Table 4, which summarizes experimental results using the T.S.E.A. method it can be noticed that the asymptotic loss factors are negative in a few bands like the 4th band in the 2 sheets of damping added case and the 5th band in the 6 sheets of damping added case to name a few. Investigations were performed to find out the cause of these negativities.

Table 4 : Table comparing asymptotic coupling loss factor estimations

Bands	L&S[26]		No Damping		2 Sheets		6 Sheets	
	η_{12}	η_{21}	η_{12}	η_{21}	η_{12}	η_{21}	η_{12}	η_{21}
1	0.002	0.002	0.000621	0.001509	0.002181	0.001851	0.003389	0.007008
2	0.001	0.002	0.007178	0.00165	0.006927	0.00268	0.00635	0.003012
3	0.002	0.0008	0.000365	0.00233	0.000385	0.002469	0.005279	0.002375
4	0.005	0.006	-0.00217	-0.00177	-0.00066	-0.00025	0.001425	0.000937
5	0.002	0.003	0.002435	0.000433	0.002072	0.000866	0.006787	-0.00452
6	0.0002	0.0015	0.003908	0.015416	0.00349	0.007924	0.007509	0.005557
7	0.001	0.002	0.000935	0.000929	0.000663	0.000848	0.004665	0.003153
8	0.0005	0.0009	0.001779	0.003638	-0.00031	0.002153	0.006387	0.011483

Figure 65 and Figure 66 show the transferred power between plates 2 and 1 when plate 1 is excited and when plate 2 is excited respectively in the frequency range of 1500 Hz to 4000 Hz. The transferred power $P_{21,1}$ which has to be negative (as the plate 1 is excited) is positive at frequencies 1700 Hz, 3815 Hz and 3870 Hz. Similarly the transferred power $P_{21,2}$ which has to be positive is negative at 1700 Hz, 2000 Hz and 2350 Hz. It is because of these negativities in the transferred power that the asymptotic loss factors are negative in band 4 and band 8.

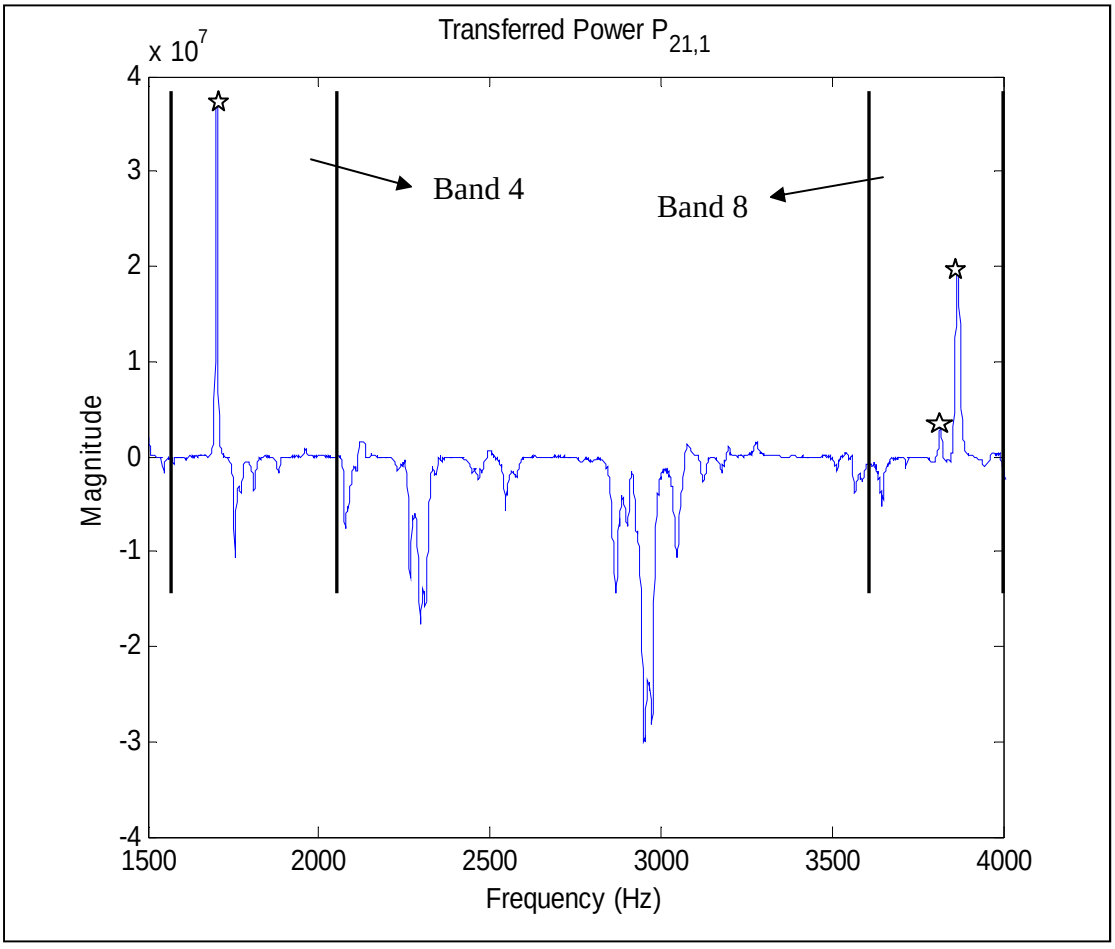

Figure 65 : Power transferred $P_{21,1}$, Bands 3-8, 2 Sheets of damping case

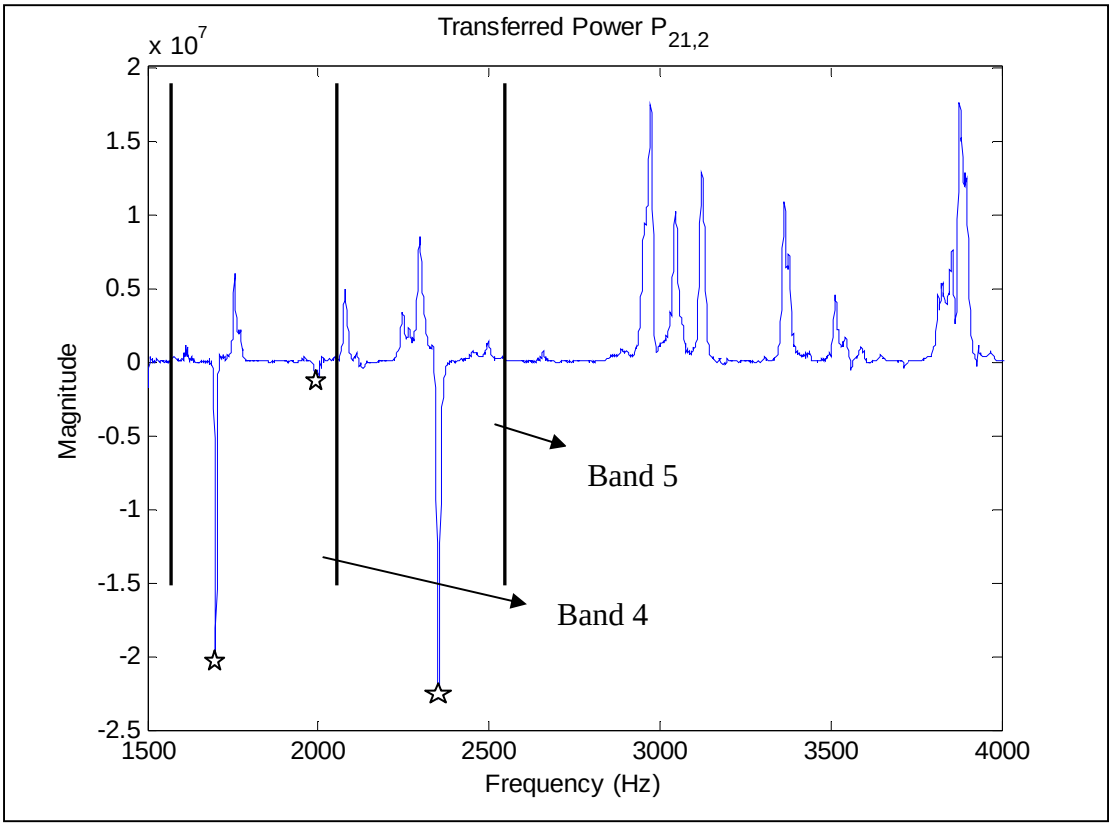

Figure 66 : Power transferred $P_{21,2}$, Bands 3-8, 2 Sheets of damping case

A modal analysis was performed on the Lai and Soom plates using a PSV Laser Vibrometer, which measures and saves velocity data from various points in the plates, and a shaker to excite the structure. The mode shapes at the above mentioned frequencies are plotted below.

From the figures below it is seen that at the frequencies at which the transferred power is negative the mode shapes have a particular similarity. A closer look at the point junction where the two plates are joined shows that at those frequencies the 2 plates are vibrating out phase with one another. At equilibrium the plates are so positioned in the mode shape plots that the 2 plates are on the same plane. But at the above shown mode shapes there is a Gap along the through the thickness dimension between the two plates at the junction. It is also noticed that a large gap transforms itself into a bigger negative peak in the Transferred power spectrum. This out of

phase motion of the 2 plates makes the force transducer at the junction to measure force contrary to the expected direction of power flow.

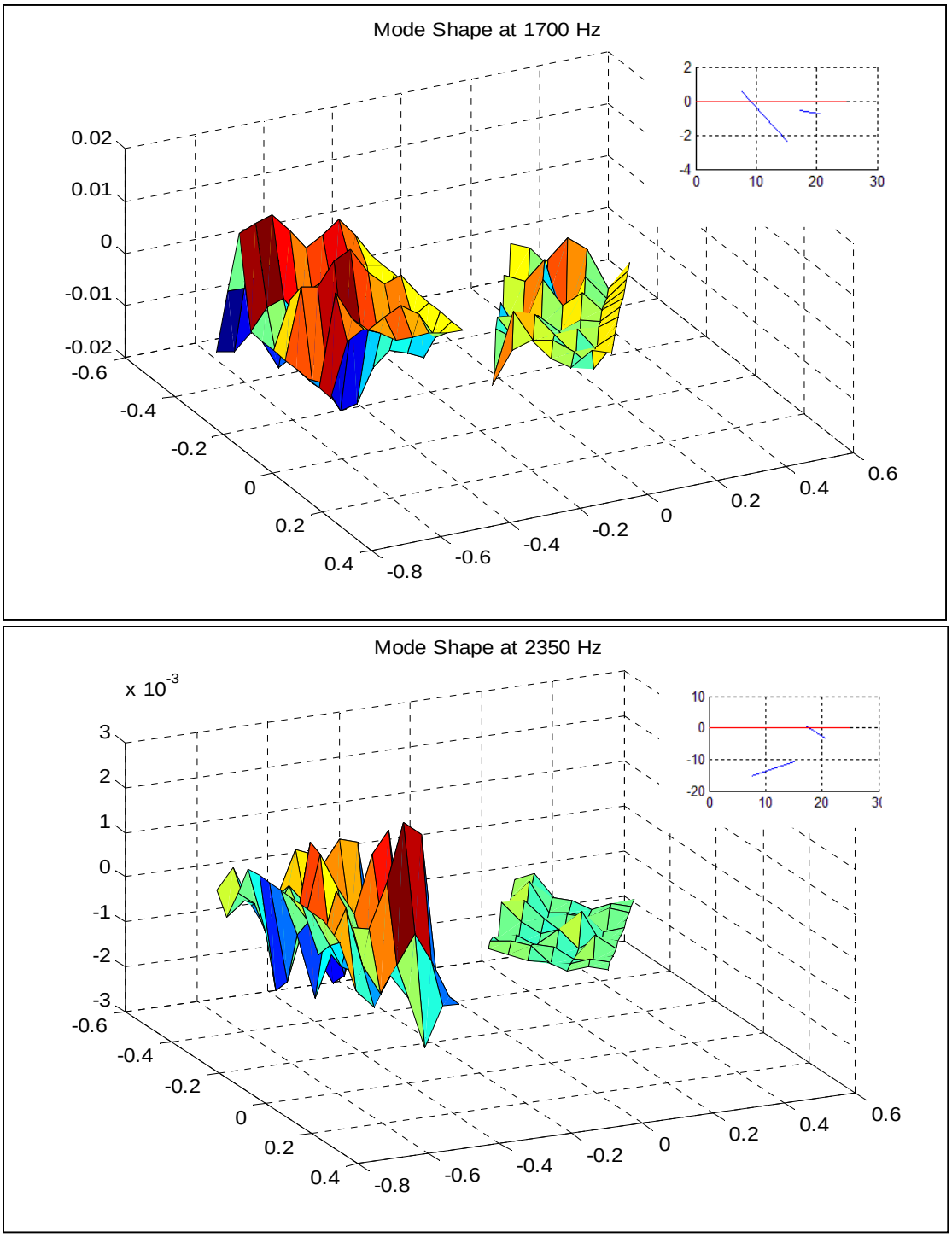

Figure 67 : Mode shapes at 1700 Hz and 2350 Hz

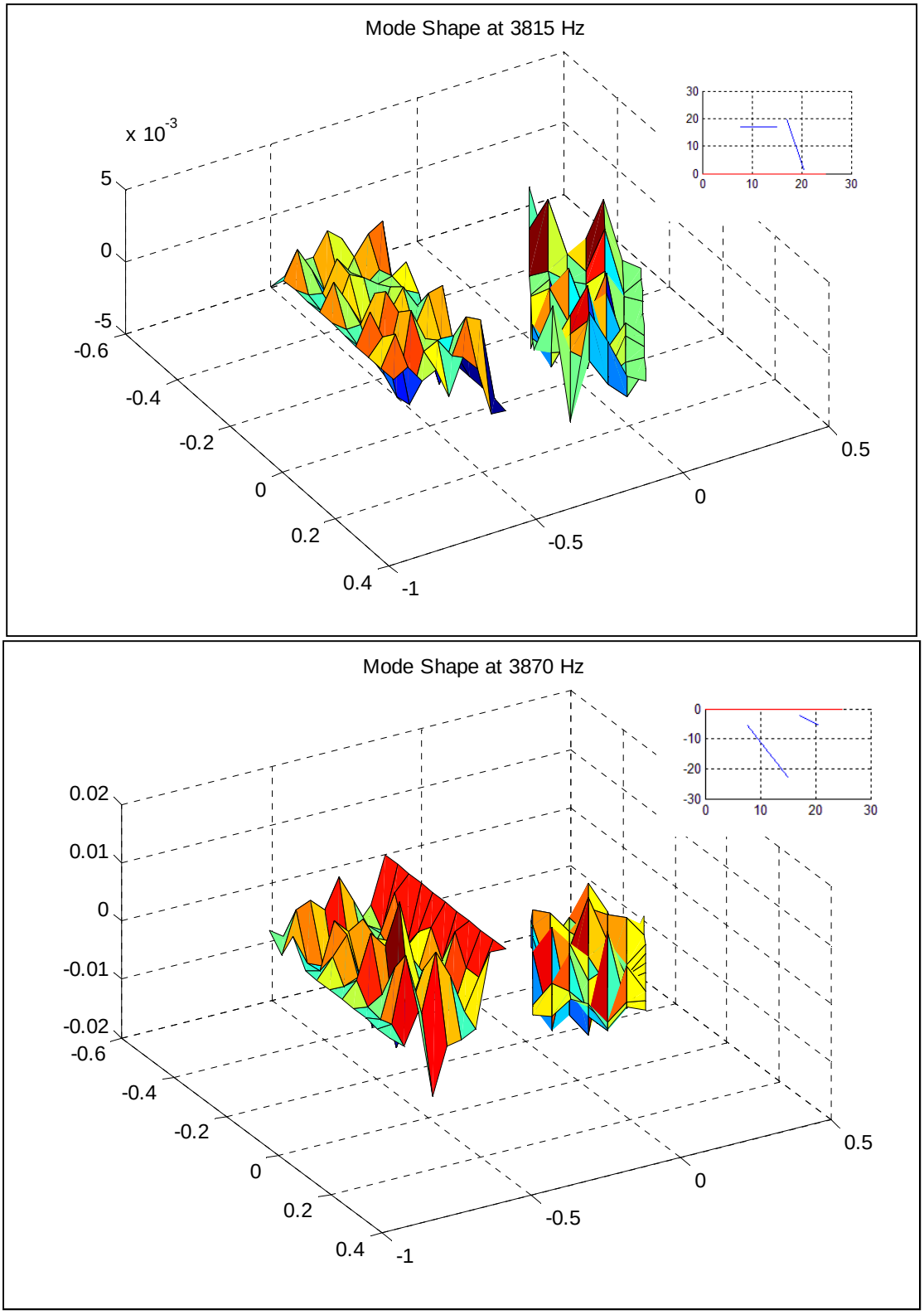

Figure 68 : Mode shapes at 3815 Hz and 3870 Hz

Comparing the results generated by Lai in [26] with the experimental results from this thesis we can infer

- All apparent time varying coupling loss factors are negative for the initial 2-3 ms and this is seen in the experimental results both in this thesis and appears to be as well in Lai's dissertation [26].
- Apparent time varying coupling loss factors are negative in the lower frequency bands and those negativities decrease as the damping level of the plate increases.
- The negative asymptotic coupling loss factors are due to the flexibility at the joint. The type of joint used to join the plates is not mentioned in [26]. Flexibility at the bolted joint has caused the negativities in the experimental results.

5.3 INFLUENCE OF LEVEL OF DAMPING ON ESTIMATION

Experiments were conducted on the Lai and Soom plates with damping added in the form of constrained layer damping. 3 different levels of damping were tested, No damping added case, 2 sheets of damping added and 6 sheets of damping added. From the figures below it can be noticed that the asymptotic coupling loss factor is not related to the damping level of the plates unlike the "apparent time varying coupling loss factor". It can also be noticed from the figures below that the values of the coupling loss factors improves slightly as the damping is increased. When compared with the analytical loss factor estimated using AUTOSEA^{TM} 2004 it can be noticed that the loss factors are under predicted at frequencies below 2000 Hz. For frequencies above 2000 Hz the experimental loss factors tend toward the predicted values.

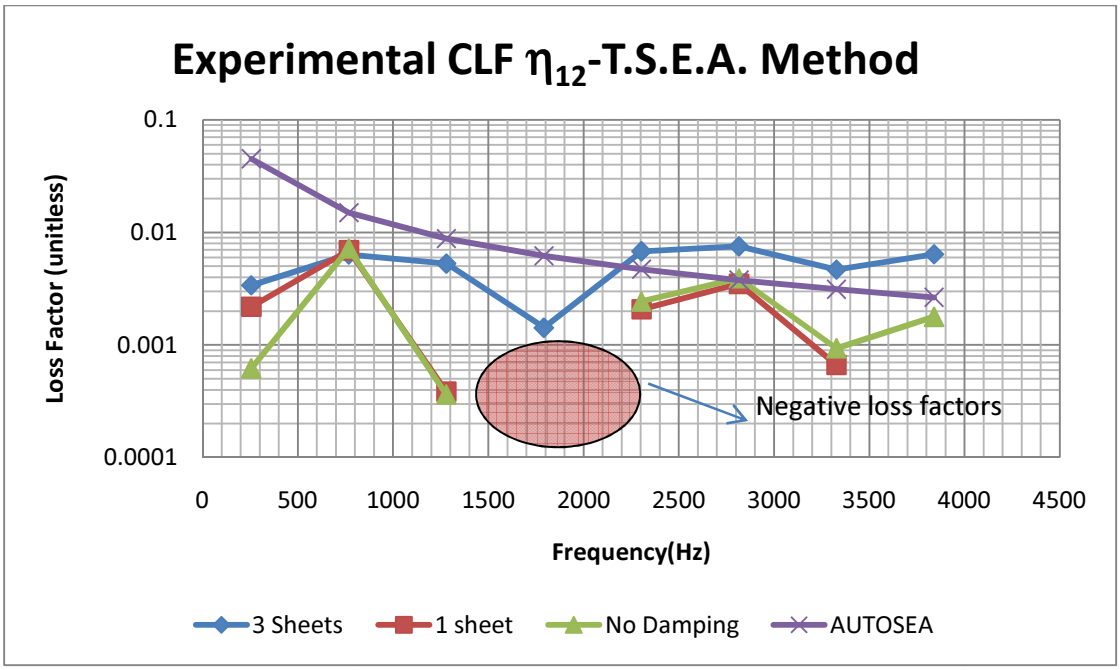

Figure 69 : Effect of damping on the asymptotic coupling loss factor η_{12}

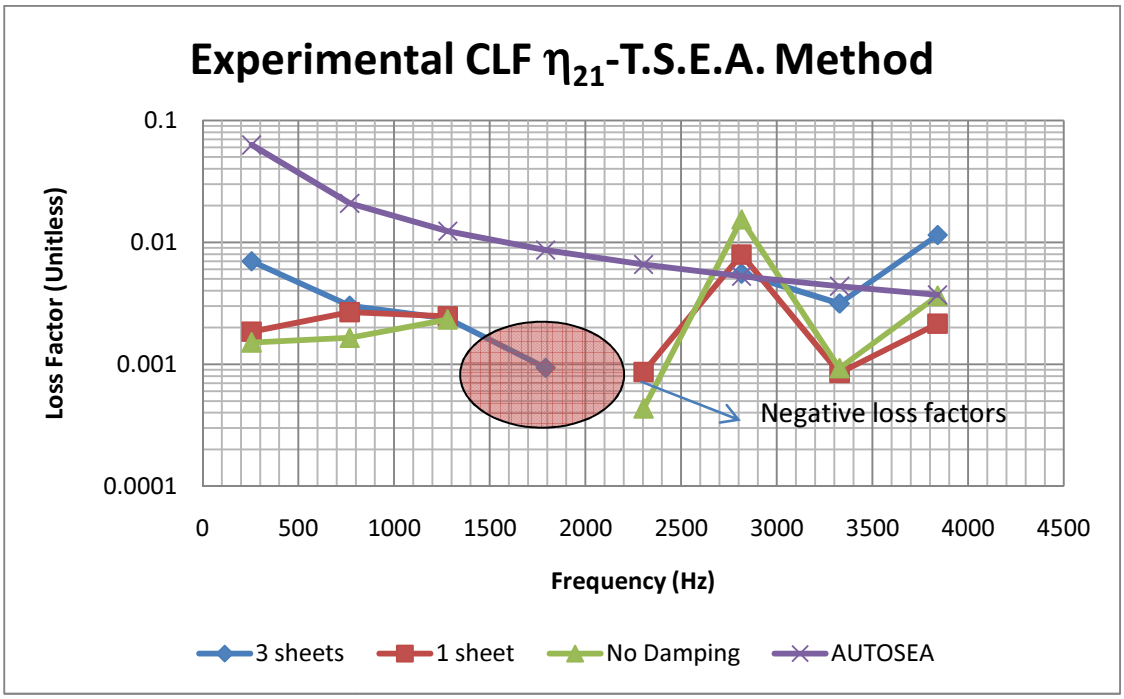

Figure 70 : Effect of damping on the asymptotic coupling loss factor η_{21}

5.4 PROCESS PARAMETERS

5.4.1 EFFECT OF FREQUENCY RESOLUTION

Frequency resolution is an important parameter which affects the quality of the data acquired in an experiment especially the resolution of phase in the cross-spectrum. Experiments performed with wrong frequency resolution can result in incorrect loss factors and a waste of experimental time. Since frequency resolution is inversely proportional to the sampling time, any changes made to the frequency resolution directly affect the number of data points and thus the length of the data record.

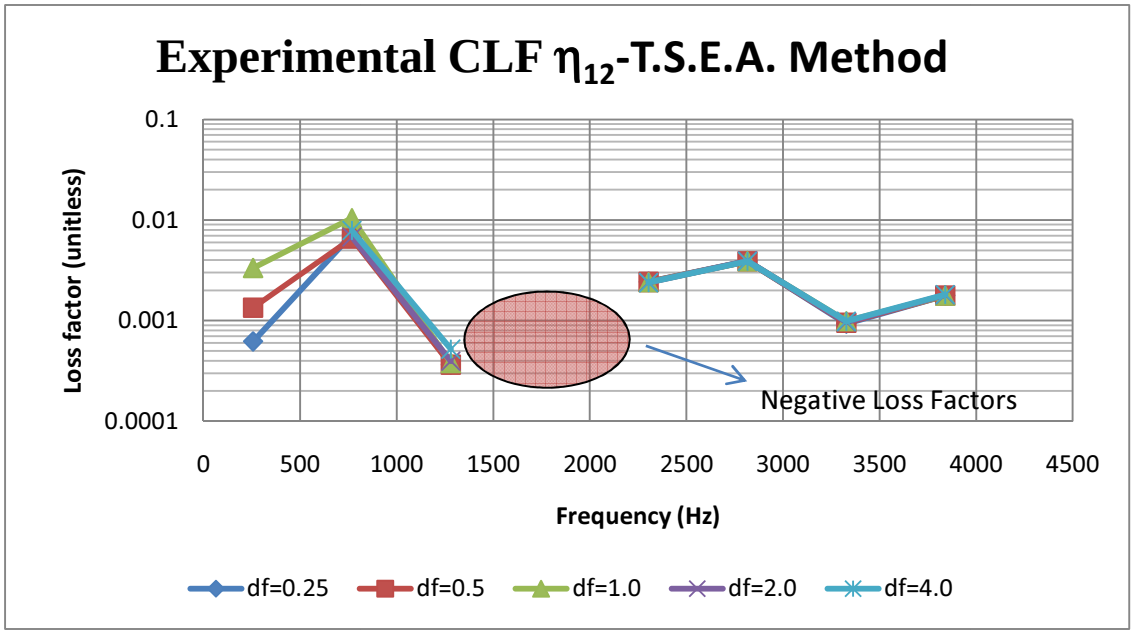

Figure 71 : Effect of frequency resolution on the Asymptotic Coupling Loss Factor η_{12} (No Damping added)

Experiments were conducted on the Lai and Soom plates with a frequency resolution of 0.25 Hz. The experimental data was then decimated so that the loss factors could be calculated with frequency resolutions 0.5 Hz, 1 Hz, 2 Hz and 4 Hz. Higher frequencies have more cycles

per second than lower frequencies and hence damp out faster. Hence the effect of the change in frequency resolution can be first seen on the lower frequency bands. With a frequency resolution of 4 Hz only frequencies below 1000 Hz are affected. As the frequency resolution is lowered the loss factors in the first band, centered at 256 Hz, start to deviate and as the frequency resolution is further lowered negative loss factors are estimated.

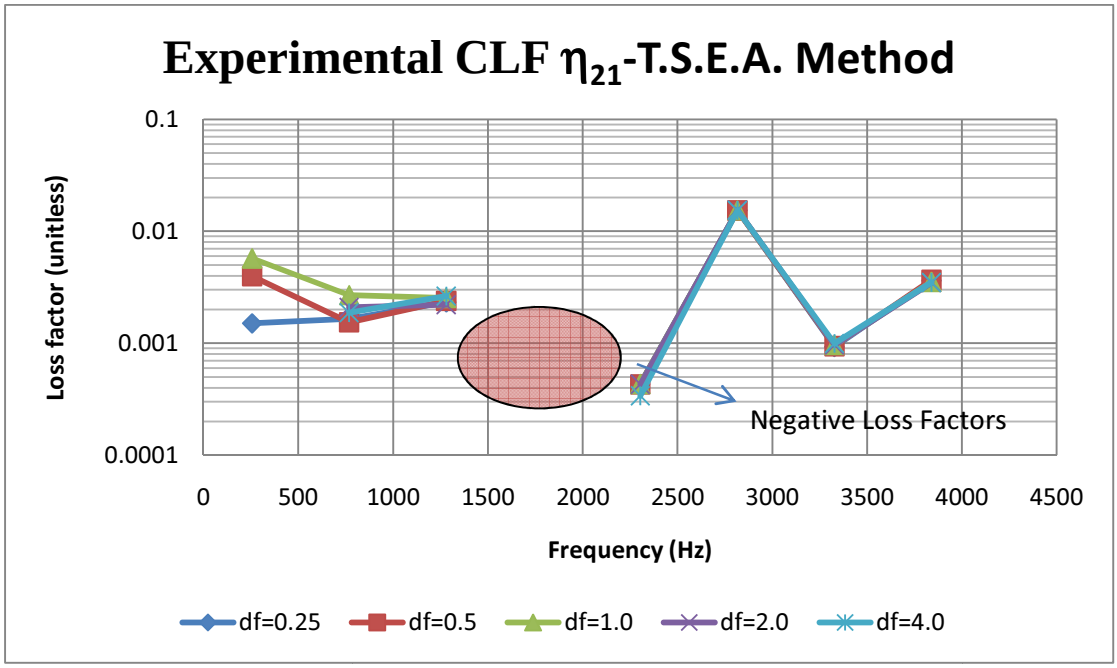

Figure 72 : Effect of frequency resolution on the Asymptotic Coupling Loss Factor η_{21} (No Damping added)

5.4.2 EFFECT OF FREQUENCY BANDWIDTH

In this thesis all the work presented was calculated in constant bandwidths of 512 Hz. The effect of bandwidths on the loss factor is studied by comparing the loss factor estimated with standard 1/3rd octave bands and full octave bins with the loss factor estimated with constant bandwidths of 512 Hz. As seen Figure 73 and Figure 74 the effect of frequency bands on the loss factor estimated by the T.S.E.A. method is similar to the effect on the Power Input Method. Choosing constant bands is particularly helpful in predicting loss factors in the lower frequency

ranges as 1/3rd octave bands in the lower frequency ranges, i.e. below 500 Hz, are very narrow bands in which there may be no natural frequencies at all.

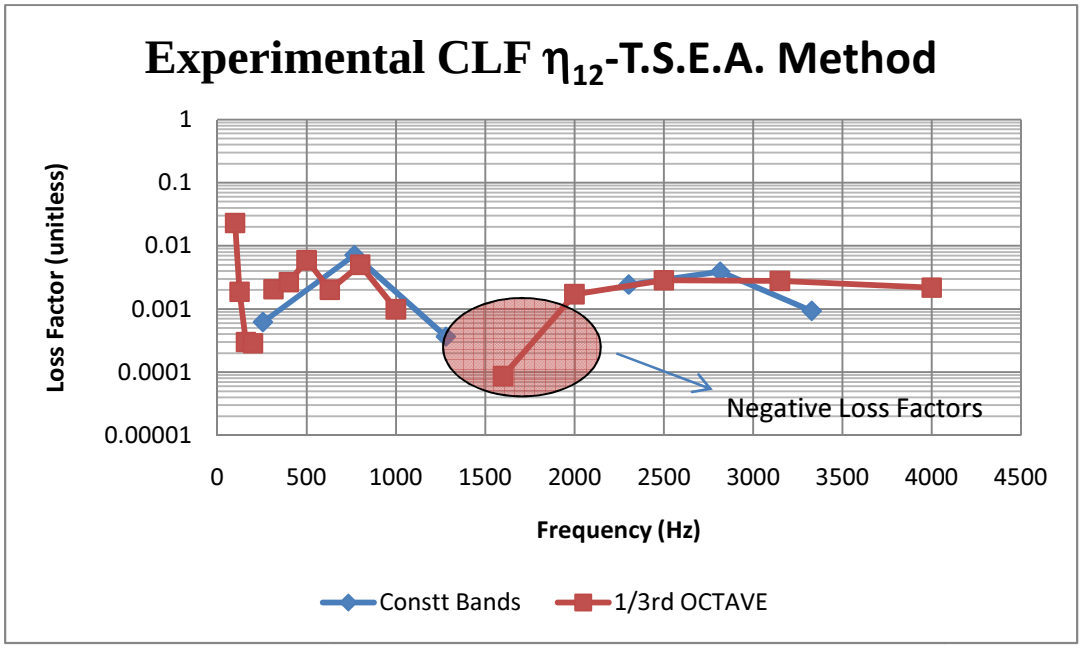

Figure 73 : Effect of frequency bandwidth on the asymptotic coupling loss factor η_{12} (No Damping added)

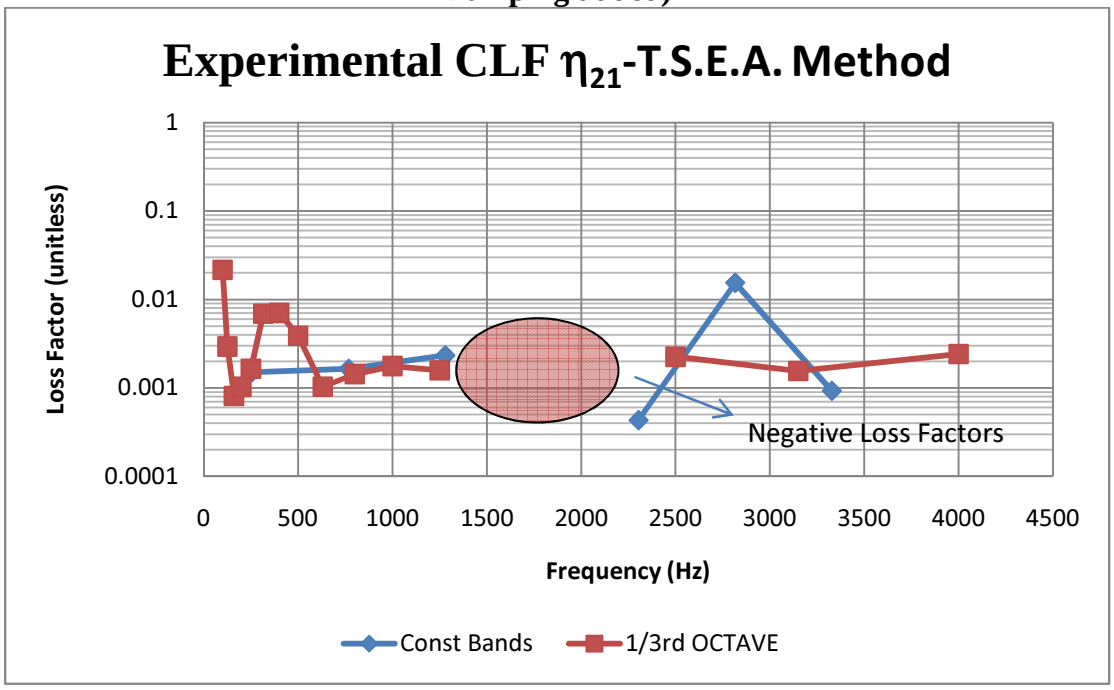

Figure 74 : Effect of frequency bandwidth on the asymptotic coupling loss factor η_{21} (No Damping added)

6.0 CLOSURE

6.1 CONCLUSIONS

6.1.1 POWER INPUT METHOD

- Numerical Simulations have shown that the loss factors estimated from the power input method are dependent on the frequency resolution used. Lightly damped systems need a high frequency resolution to avoid negative estimations, whereas high damping level estimations are not that dependent on the frequency resolution.
- Experimental results on lightly damped, coupled plates show that the negativities in the estimated loss factors are reduced or removed by increasing the frequency resolution. Increased frequency resolution (low Δf) provides better estimates of the *phase* of the only cross-spectra needed, that is, the cross-spectra between the input force and the driving point responses.
- Experiments on plates with varying levels of damping but with the same coupled junction have shown that the coupling loss factor is independent of the damping of the plates.
- Loss factors estimated using the power input method have shown good agreement between the results with both shaker and hammer excitation.
- Experiments conducted with different hammer tips have shown the importance of considering effective bandwidth. This can be seen by computing the auto-spectrum of the input force. The estimated loss factors start to become invalid once the input auto-spectrum hits the noise floor.
- Experiments conducted by changing the number of measurement points have shown that for lightly damped plates a minimum 3 points distributed on the plate are needed to estimate loss factors reliably.

6.1.2 TRANSIENT STATISTICAL ENERGY ANALYSIS METHOD

- Experiments conducted on plates coupled at a point have shown that the estimated loss factors are extremely dependent on the joint flexibility. Flexibility at the joint may lead to negative loss factors.
- Experiments have shown that an increase in the damping of the coupled plates decreases the negativities in the “apparent time varying loss factor” curves.
- An increase in the damping level also results in the “apparent time varying coupling loss factor” attaining an asymptotic value quickly.
- Numerical simulations have shown that if a transient force (example: from an impulse hammer) duration is longer than the natural period of the oscillator then the coupling coefficients may be off by more than 150%.
- Experiments have shown that an increase in damping does not have any effect on the asymptotic coupling loss factor.
- Experimental results show that a decrease in the frequency resolution results in negative asymptotic coupling loss factors and apparent time varying coupling loss factors.

6.2 FUTURE WORK

- The exact relationship between the estimated loss factor and the frequency resolution has to be determined.
- Future work on the Power Input Method can be concentrated on determining the reasons for the slight disagreements between the shaker-excited loss factors and hammer-excited loss factors.
- T.S.E.A. method must be applied to plates with different joints like riveted, bonded, and bolted to determine the effect of various kinds of point joints on the estimated coupling loss factors.
- The concept of the apparent coupling coefficients must be further developed so that time varying loss factors can be estimated even at joints where the transferred energy cannot be directly measured.
- Further work on T.S.E.A method can be concentrated on determining the correct damping range where T.S.E.A. method can be applied.
- The effect of the stiffness of the force gauge (both lateral and rotational inertia) on the estimated coupling loss factor using T.S.E.A. method has to be determined.
- Further work can be directed towards using the Power Input Method in a computational sense, that is, based on the finite element model, to characterize the effects of using a massive, flexible force gauge at the joint in the experimental investigation to represent the theoretical mass-less point junction.

REFERENCES

[1] R. H. Lyon and R. G. DeJong, *Theory and Application of Statistical Energy Analysis*: Elsevier Science & Technology Books, 1995.

[2] S.S.Rao, *Mechanical Vibrations*: Prentice Hall, 2004.

[3] Nashif.A.D., *et al.*, *Vibration Damping*: Wiley, John & Sons, 1985.

[4] C. W. De Silva, *Vibration : Fundamentals and practice*: CRC Press, 1999.

[5] W. Liu, "*Experimental and Analytical Estimation of damping in beams and plates with damping treatments*," Doctor of Philosophy, Aerospace Engineering, University of Kansas, Lawrence, 2008.

[6] Maidanik.G, "*A definition of a loss factor is unique, some definitions are not*," *Journal of Acoustical Society of America*, vol. 106, pp. 2179-2179, 1999.

[7] H. Dande, "*Homework #2, AE 790, Structural Acoustics, Spring 2009*," 2009.

[8] W. Liu and M. S. Ewing, "*Experimental and Analytical Estimation of Loss Factors by the Power Input Method*," *AIAA Journal*, vol. 45, No. 2, pp. 477-484, 2007.

[9] H. Dande, "*Panel Damping Loss Factor Estimation using the Random Decrement Technique*," Master of Science, Aerospace Engineering, University of Kansas, Lawrence, 2009.

[10] M. S. Ewing, *et al.*, "*Validation of Panel Damping Loss Factor Estimation Algorithms Using a Computational Model*," presented at the 50th AIAA/ASME/ASCE/AHS/ASC structures Structural Dynamics and Materials Conference, 2009.

[11] K. Vatti, "*Damping Estimation of Plates for Statistical Energy Analysis*," Master of Science, Aerospace Engineering, University of Kansas, Lawrence, 2010.

[12] J. He and Z.-F. Fu, *Modal Analysis*: Butterworth-Heinemann, 2001.

[13] B. Bloss and M. D. Rao, "*Measurement of Damping In Structures by the power input method* " *Experimental Techniques*, vol. 26, pp. 30-33, 2002.

[14] M. L. Lai and A. Soom, "*Prediction of Transient Vibration Envelopes Using Statistical Energy Analysis Techniques*," *Journal of Vibration and Acoustics*, vol. 112, pp. 127-137, 1990.

[15] F. J. Fahy, "*Statistical Energy Analysis: A Critical Overview*," *Philosophical Transactions: Physical Sciences and Engineering*, vol. 346, pp. 431-447, 1994.

[16] R. H. Lyon and Maidanik.G, "*Power Flow between Linearly Coupled Oscillators*," *Journal of Acoustical Society of America*, vol. 34, pp. 623-639, 1962.

[17] J. E. Manning, "*SEA Coupling Factors for Regular and Irregular Structures* " presented at the International Union of Theoretical and Applied Mechanics, University of Southampton.

[18] E. E. Ungar, "*Statistical Energy Analysis of Vibrating Systems*," *Trans. ASME Journal of Engineering for Industry*, pp. 626-632, 1967.

[19] W. Gersch, "*Average power and Power exchange in oscillators*," *Journal of Acoustical Society of America*, vol. 46, pp. 1180-1185, 1968.

[20] J. E. Manning and K. Lee, "*Predicting Mechanical Shock Transmission*," *Shock and Vibration Bulletin*, vol. 37, No 4, pp. 65-70, 1968.
[21] R. E. Powell, "*Statistical Energy Analysis of Transient Vibration*," presented at the Winter Annual Meeting of the American Society of Mechanical Engineers, Boston, Massachusets, 1987.
[22] C. A. Mercer, *et al.*, "*Energy flow between two weakly coupled oscillators subject to transient excitation*," *Journal of Sound and Vibration*, vol. 15, pp. 373-379, 1971.
[23] R. J. Pinnington and D. Lednik, "*Transient Statistical Energy Analysis of an Impulsively Excited two Oscillator System*," *Journal of Sound and Vibration*, vol. 189, pp. 249-264, 1996.
[24] A. J. Keane and W. G. Price, *Statistical Energy Analysis An overvier, with applications in structural dynamics*. Cambridge: Cambridge University Press, 1994.
[25] R. H. Lyon, *Statistical Energy Analysis of dynamic systems: theory and applications*. Cambridge: M.I.T. Press, 1975.
[26] M. L. Lai, "*Modeling of Transient Vibrations with Statistical Energy Analysis Techniques*," Doctor of Philosophy, Mechanical and Aerospace Engineering, University of New York at Buffalo, Buffalo, 1988.
[27] D. A. Bies and S. Hamid, "*In situ determination of loss and coupling loss factors by the power injection method*," *Journal of Sound and Vibration*, vol. 70, pp. 187-204, 1980.
[28] M. Carfagni and M. Pierini, "*Determining the Loss Factor by the Power Input Method (PIM), Part 2: Experimental Investigation with Impact Hammer Excitation*," *Journal of Vibration and Acoustics*, vol. 121, pp. 422-428, 1999.
[29] A. L. Libardi and P. S. Vartoto, "*Experimental Determination of Loss Factors on Coupled Structures Using the Power Injection Method*," presented at the 2004 IMAC-XXII: Conference & Exposition on Structural Dynamics, Dearborn, Michigan, 2004.
[30] M. Carfagni, *et al.*, "*Determining Loss Factors using the power input method with Shaker Excitation*," *Proceedings of the 16th International Modal Analysis Conference*, vol. 1, pp. 585-590, 1998.
[31] R. Panuszka, *et al.*, "*Experimental Assessment of Coupling Loss Factors of Thin Rectangular Plates*," *Archives of Acoustics*, vol. 30, pp. 533-551, 2005.
[32] Jocobsen and Finn, "*Measurement of structural loss factors by the power input method*," Technical University of Denmark,1986.
[33] J. A. Wolf Jr., "*The influence of mounting stiffness on frequencies measured in a vibration test*," *Society of Automotive Engineers*, vol. SAE Paper 840480, 1984.
[34] D. J. Inman, *Engineering Vibration Second Edition*. New Jersey: Prentice-Hall, 2001.

APPENDIX A. CODES

1 TRUE RANDOM FORCE PROGRAM

```
%%% Random Force Generator Code
clc
clear all
close all
FAmplitude=1; % Force Amplitude
F=5000; % Sampling Frequency
T=20;  % time of the sample
N=F*T; % Number of Samples
df=F/N; % Frequency Resolution
f_low=1; % Defining limits of the Frequency Band
f_high=5000; % Highest Freqeuency
band=f_high-f_low; % Force Band
f_cutoff_low=ceil(f_low/df);   % generating array indices - lower limit
f_cutoff_high=ceil(f_high/df);  % generating array indices - upper limit
So=FAmplitude/band;
P=zeros(N/2+1,1);
P(f_cutoff_low:f_cutoff_high,1)=So*ones(f_cutoff_high-f_cutoff_low+1,1);
N1=length(P);
level=P/2;
level=N*(N*df)*level;
level=sqrt(level);
phase=2*pi*rand(N1,1);
Fw=level.*(cos(phase)+1i*sin(phase));
Fw(N+1:2*(N-1))=conj(flipud(Fw(2:N-1)));% appending complex conjugate Force
force=real(ifft(Fw)); % Random Force
```

2 SIMULATED ENERGY FLOW PROGRAM FOR A 2 DOF-SYSTEM.

```
% Divided by e0 and Non Dimentionalized
close all
clear all
clc
global M1 M2 Mc K1 K2 Kc C1 C2 f2 G f1 t2
M1=input('Input the value of M1: ');
M2=input('Input the value of M2: ');
Mc=input('Input the value of Mc: ');  % only spring coupling
w1=input('Input the value of w1: ');
w2=input('Input the value of w2: ');
K1=w1^2;
K2=w2^2;
```

```
Kc=input('Input the value of Kc: ');
wn1=input('Input the value of wn1: ');
wn2=input('Input the value of wn2: ');
C1=0.075*wn1;
C2=0.075*wn2;
G=input('Input the value of G: ');
f1=input('Input the value of f1:0 ');
f2=input('Input the value of f2:1 ');
t2=input('Input the value of t2:duration of the pulse ');
d=input('Input the value of d:d is the array in the e0 array after the force
is removed ');
xo=[0;0;0;0];
ts=linspace(0,1,10000);
[xspan,y]=ode45(@f,ts,xo);
figure(100)
plot(xspan,y(:,1));
grid on
figure(101)
plot(xspan,y(:,2),'--');
grid on
figure(102)
plot(xspan,y(:,3));
title('Velocity of Oscillator 1','FontWeight','bold','FontSize',14);
grid on
ylabel('Velocity (m/s^2)');
xlabel('time (sec)');
figure(103)
plot(xspan,y(:,4),'--');
title('Velocity of Oscillator 2','FontWeight','bold','FontSize',14);
grid on
ylabel('Velocity (m/s^2)');
xlabel('time (sec)');
%%
w2=200; % Blocked Natural Frequency of Plate 2
T2=2*pi/w2;
dt=1/10000;
step=1:1:length(xspan);
Matr=zeros(length(step),7);
e0=zeros(length(step),1);
F2=zeros(length(step),1);
for i=2:1:length(xspan)-1
    F2(i)=(heaviside(xspan(i))-heaviside(xspan(i)-t2))/t2;
    e0(i,1)=e0(i,1)+(F2(i)*y(i,4));                    % e0
    e0(i+1,1)=e0(i,1);
end
e0=e0*dt;
% INTEGRATION
for i=1:1:length(xspan)-1
    Matr(i,2)=Matr(i,2)+(2*M1*y(i,3)^2/2);                  % Ek1
    Matr(i,3)=Matr(i,3)+((M1*y(i,3)^2/2)+(K1*y(i,1)^2/2));  % E1
    Matr(i,4)=Matr(i,4)+(2*M2*y(i,4)^2/2);                  % Ek2
    Matr(i,5)=Matr(i,5)+((M2*y(i,4)^2/2)+(K2*y(i,2)^2/2));  % E2
    Matr(i,6)=Matr(i,6)+(Kc*y(i,2)*y(i,3));                 % E21
    Matr(i,7)=Matr(i,7)-(Kc*y(i,1)*y(i,4));                 % E12
    Matr(i+1,:)=Matr(i,:);
end
Matr=Matr*dt;
```

```
step=step*dt;
C=zeros(length(step),3);
for i=2:1:length(xspan)
    C(i,1)=-Matr(i,7)/(Matr(i,2)-Matr(i,4));          %C12
    C(i,2)=Matr(i,6)/(Matr(i,4)-Matr(i,2));           %C21
    C(i,3)=-Matr(i,7)/(Matr(i,3)-Matr(i,5));          %C12'
end
for i=1:1:length(xspan)
    Matr(i,2)=Matr(i,2)/(e0(d,1)*T2);
    Matr(i,3)=Matr(i,3)/(e0(d,1)*T2);
    Matr(i,4)=Matr(i,4)/(e0(d,1)*T2);
    Matr(i,5)=Matr(i,5)/(e0(d,1)*T2);
    Matr(i,6)=Matr(i,6)/e0(d,1);
    Matr(i,7)=Matr(i,7)/e0(d,1);
end
%Plotting
figure(11)
hold on
title('Non Dimensionalized Integrated Energy in Oscillator
1','FontWeight','bold','FontSize',14);
plot(step,Matr(:,2),':r');
plot(step,Matr(:,3));
grid on
box on
ylabel('Energy (joule)');
xlabel('time (sec)');
legend(' 2 * Kinetic Energy',' Total Energy');
hold off
figure(12)
hold on
title('Non Dimensionalized Integrated Energy in Oscillator
2','FontWeight','bold','FontSize',14);
plot(step,Matr(:,4),':r');
plot(step,Matr(:,5));
grid on
box on
ylabel('Energy (joule)');
xlabel('time (sec)');
legend(' 2 * Kinetic Energy',' Total Energy');
hold off
figure(13)
hold on
title('Non Dimensionalized Transferred Energy
','FontWeight','bold','FontSize',14);
plot(step,Matr(:,6));
plot(step,Matr(:,7),':r');
grid on
box on
ylabel('Energy (joule)');
xlabel('time (sec)');
legend(' E21(t)',' - E12(t)');
hold off
figure(110)
hold on
title('Coupling Coefficient','FontWeight','bold','FontSize',14);
plot(step,C(:,1),':r');
plot(step,C(:,2),'--k');
```

```
plot(step,C(:,3));
grid on
box on
ylabel('Coupling Coefficient');
xlabel('time (sec)');
legend('C12','C21','C12''');
hold off
save('hit_plate_2_1.mat','xspan','y');
%
Matr=zeros(length(step),7);
for i=1:1:length(xspan)-1
    Matr(i,6)=Matr(i,6)+(Kc*y(i,2)*y(i,3));                % E21
    Matr(i,7)=Matr(i,7)-(Kc*y(i,1)*y(i,4));                % E12
end
save('hit_plate_2_2.mat','xspan','y','Matr');
```

3 SIMULATED POWER FLOW PROGRAM FOR A 2 DOF-SYSTEM.

```
% Divided by e0 and Non Dimentionalized
close all
clear all
clc
global M1 M2 Mc K1 K2 Kc C1 C2 f2 G f1 t2
M1=input('Input the value of M1: ');
M2=input('Input the value of M2: ');
Mc=input('Input the value of Mc: ');  % only spring coupling
w1=input('Input the value of w1: ');
w2=input('Input the value of w2: ');
K1=w1^2;
K2=w2^2;
Kc=input('Input the value of Kc: ');
wn1=input('Input the value of wn1: ');
wn2=input('Input the value of wn2: ');
C1=0.075*wn1;
C2=0.075*wn2;
G=input('Input the value of G: ');
f1=input('Input the value of f1:0 ');
f2=input('Input the value of f2:1 ');
t2=input('Input the value of t2:duration of the pulse ');
d=input('Input the value of d:d is the array in the e0 array after the force
is removed ');
xo=[0;0;0;0];
ts=linspace(0,1,10000);
[xspan,y]=ode45(@f,ts,xo);
figure(100)
plot(xspan,y(:,1),xspan,y(:,2),'--');
figure(101)
plot(xspan,y(:,3),xspan,y(:,4),'--');
%%
w2=200; % Blocked Natural Frequency of Plate 2
```

```
dt=1/10000;
T2=2*pi/w2;
step=1:1:length(xspan);
e0=zeros(length(xspan),1);E1k=zeros(length(xspan),1);E1=zeros(length(xspan),1
);
E2k=zeros(length(xspan),1);E2=zeros(length(xspan),1);
P21=zeros(length(xspan),1);P12=zeros(length(xspan),1);
F2=zeros(length(step),1);
for i=1:1:length(step)
    F2(i)=(heaviside(xspan(i))-heaviside(xspan(i)-t2))/t2;
    e0(i,1)=e0(i,1)+(F2(i)*y(i,2));                % e0
    e0(i+1,1)=e0(i,1);
end
e0=e0*dt;
for i=1:1:length(xspan)
    E1k(i,1)=E1k(i,1)+(M1*y(i,3)^2/2);
    E1(i,1)=E1(i,1)+(M1*y(i,3)^2/2)+(K1*y(i,1)^2/2);
    E2k(i,1)=E2k(i,1)+(M2*y(i,4)^2/2);
    E2(i,1)=E2(i,1)+(M2*y(i,4)^2/2)+(K2*y(i,2)^2/2);
    P21(i,1)=P21(i,1)+(Kc*y(i,2)*y(i,3));
    P12(i,1)=P12(i,1)-(Kc*y(i,1)*y(i,4));
end
for i=1:1:length(step)
    E1k(i,1)=E1k(i,1)/e0(d,1);
    E1(i,1)=E1(i,1)/e0(d,1);
    E2k(i,1)=E2k(i,1)/e0(d,1);
    E2(i,1)=E2(i,1)/e0(d,1);
    P21(i,1)=P21(i,1)*T2/e0(d,1);
    P12(i,1)=P12(i,1)*T2/e0(d,1);
end
figure(7)
hold on
title('Non Dimensionalized Energy in Oscillator
1','FontWeight','bold','FontSize',14);
plot(xspan,E1k(:,1));
plot(xspan,E1(:,1),':r');
ylabel('Energy (joule)');
xlabel('time (sec)');
legend(' Kinetic Energy',' Total Energy');
grid on
box on
hold off
figure(8)
hold on
title('Non Dimensionalized Energy in Oscillator
2','FontWeight','bold','FontSize',14);
plot(xspan,E2k(:,1));
plot(xspan,E2(:,1),':r');
ylabel('Energy (joule)');
xlabel('time (sec)');
legend(' Kinetic Energy',' Total Energy');
grid on
box on
hold off
figure(9)
hold on
```

```
title('Non Dimensionalized Transferred
Power','FontWeight','bold','FontSize',14);
plot(xspan,P21(:,1));
plot(xspan,P12(:,1),':r');
ylabel('Power (Watt)');
xlabel('time (sec)');
legend('P21(t)','-P12(t)');
grid on
box on
hold off
```

ODE SOLVER FUNCTION

```
function dy = f(t,y)
% No Gyroscopic and Mass coupling. Only Spring Coupling.
%function to be integrated
dy = zeros(4,1);
global M1 M2 Mc K1 K2 Kc C1 C2 F2
Mc=0;  % only spring coupling
F2=(heaviside(t)-heaviside(t-0.075))/0.075;  % Rectangular Step Force
dy(1)=(-C1*y(1)/M1)+0*y(2)-(K1*y(3)/M1)+(Kc*y(4)/M1);
dy(2)=0*y(1)-(C2*y(2)/M2)+(Kc*y(3)/M2)-(K2*y(4)/M2)+(F2/M2);
dy(3)=y(1);
dy(4)=y(2);
```

4 SIMULATED POWER INPUT METHOD PROGRAM FOR A 2 DOF-SYSTEM

```
% The SIMULATED POWER INPUT METHOD
clear all
close all
clc
load('hit_plate_1_1.mat','xspan','y');
yP1=y;
load('hit_plate_2_1.mat','xspan','y');
yP2=y;
N=length(xspan);
t2=0.001;   % length of the transient hit in seconds
force=(heaviside(xspan-0)-heaviside(xspan-t2))/t2;
autospecd01=(conj(fft(yP1(:,3))).*fft(yP1(:,3)));
autospecd02=(conj(fft(yP1(:,4))).*fft(yP1(:,4)));
autospecd03=(conj(fft(yP2(:,3))).*fft(yP2(:,3)));
autospecd04=(conj(fft(yP2(:,4))).*fft(yP2(:,4)));
csspecd01=(conj(fft(force(:,1))).*fft(yP1(:,3)));
csspecd02=(conj(fft(force(:,1))).*fft(yP2(:,4)));

df=0.2; % frequency resolution
Cfreq=1:1:1000;
band=1000;
M1=1;        % Mass of the plate 1 Assumed
M2=1;        % Mass of the plate 2
Ek21=zeros(band,1);Ek11=zeros(band,1);Ek22=zeros(band,1);
```

```
Ek12=zeros(band,1);Pin1=zeros(band,1);Pin2=zeros(band,1);
k=0;
for m=1:1:band
    k=k+1;
        Ek21(m,1)=Ek21(m,1)+((M2/(2*pi))*real(autospecd02(k)));
        Ek11(m,1)=Ek11(m,1)+((M1/(2*pi))*real(autospecd01(k)));
        Ek22(m,1)=Ek22(m,1)+((M2/(2*pi))*real(autospecd04(k)));
        Ek12(m,1)=Ek12(m,1)+((M1/(2*pi))*real(autospecd03(k)));
        Pin1(m,1)=Pin1(m,1)+((1/pi)*real(csspecd01(k)));
        Pin2(m,1)=Pin2(m,1)+((1/pi)*real(csspecd02(k)));
    % Same Multiplication factor - can be removed.
%
Ek21(m,1)=Ek21(m,1)*2*pi;Ek11(m,1)=Ek11(m,1)*2*pi;Ek22(m,1)=Ek22(m,1)*2*pi;
%
Ek12(m,1)=Ek12(m,1)*2*pi;Pin1(m,1)=Pin1(m,1)*2*pi;Pin2(m,1)=Pin2(m,1)*2*pi;
    DE(m,1)=(Ek11(m,1)*Ek22(m,1))-(Ek12(m,1)*Ek21(m,1));
    A1(:,:,m)=[((Pin1(m,1)*Ek22(m,1))-(Pin2(m,1)*Ek21(m,1)))
(Pin1(m,1)*Ek12(m,1));(Pin2(m,1)*Ek21(m,1)) ((Pin2(m,1)*Ek11(m,1))-
(Pin1(m,1)*Ek12(m,1)))];
    B1(:,:,m)=A1(:,:,m)/(2*DE(m,1)*Cfreq(m)*2*pi*df);
end
for m=1:1:band
    LF1(m)=B1(1,1,m);
    LF2(m)=B1(2,2,m);
    CLF21(m)=B1(1,2,m);
    CLF12(m)=B1(2,1,m);
end
band1=1:1:band;
figure(1)
plot(band1,LF1,'-r*', 'DisplayName', 'n1', 'YDataSource', 'n1');
figure(2)
plot(band1,LF2,'-*r', 'DisplayName', 'n2', 'YDataSource', 'n2');
figure(3)
plot(band1,CLF12,'-*r', 'DisplayName', 'n12', 'YDataSource', 'n12');
figure(4)
plot(band1,CLF21,'-*r', 'DisplayName', 'n21', 'YDataSource', 'n21');
```

5 THEORETICAL MODES IN BAND AND MODAL DENSITY PROGRAM.

```
% USING THEORETICAL FORMULA
clear all
close all
clc
% Youngs' modulus of Aluminum
E=7e11; % units g/cm*s2.
Density=2.70;  % units gms/cm3.
h=0.64; % thickness of the Plates.
K=h/(2*sqrt(3)); % Radius of Gyration.  Try another formula also
C_l=sqrt(E/Density); % Longitudinal Wavespeed.
Ap(1)=2852.840; % Surface Area of Plate 1 Lai and Soom.
Ap(2)=2042.370; % Surface Area of Plate 2 Lai and Soom.
for i=1:2
    nw(i)=Ap(i)/(4*pi*K*C_l);
end
```

6 EXPERIMENTAL MODES IN BAND AND MODAL DENSITY PROGRAM.

```
%% Using the Experimental Accelerometer Data
close all
clear all
clc
Mass=[4.608 3.628];
A=importdata('Plate 1_ND.mat');
B=importdata('Plate 2_ND.mat');
C=importdata('Plate 1_1S.mat');
D=importdata('Plate 2_1S.mat');
E=importdata('Plate 1_3S.mat');
F=importdata('Plate 2_3S.mat');
DFRF(:,1,1)=A.H1_2(:,2); % Inertiance FRF's
DFRF(:,2,1)=B.H1_2(:,2);
DFRF(:,1,2)=C.H1_2(:,2);
DFRF(:,2,2)=D.H1_2(:,2);
DFRF(:,1,3)=E.H1_2(:,2);
DFRF(:,2,3)=F.H1_2(:,2);
% Calculating Average conductance ( real Part of Mobility) in the bands
df=1; % in Hz
% Constant Bands
% Cfreq=256:512:3840;
% band=8;
% lowbound=round((2:512:3685)/df);
% upbound=round((512:512:4196)/df);
% 1/3rd octave bands with full octave bandwidths
Cfreq=[100 125 160 200 250 315 400 500 630 800 1000 1250 1600 2000 2500 3150
4000];
band=length(Cfreq);
lowbound=round(Cfreq/sqrt(2)/df);
upbound=round(Cfreq*sqrt(2)/df);
COND_AVG=zeros(band,length(DFRF(1,1,:))*2);
for i=1:1:band
    for k=lowbound(i):1:upbound(i)
        for m=1:1:length(DFRF(1,1,:))
            COND_AVG(i,2*m-1)=COND_AVG(i,2*m-
1)+(imag(DFRF(k,1,m))/(2*pi*k*df)); % Plate 1 , Plate 2
            COND_AVG(i,2*m)=COND_AVG(i,2*m)+(imag(DFRF(k,2,m))/(2*pi*k*df));
        end
    end
    bandwidth(i)=upbound(i)-lowbound(i);
    for m=1:1:length(DFRF(1,1,:))
        COND_AVG(i,2*m-1)=COND_AVG(i,2*m-1)/bandwidth(i);
        COND_AVG(i,2*m)=COND_AVG(i,2*m)/bandwidth(i);
    end
end
for i=1:1:band
    for m=1:1:length(DFRF(1,1,:))
        modal_density(i,2*m-1)=COND_AVG(i,2*m-1)*2*Mass(1)/pi;
        modal_density(i,2*m)=COND_AVG(i,2*m)*2*Mass(2)/pi;
    end
end
for i=1:1:band
```

```
    for m=1:1:length(DFRF(1,1,:))
        MPB(i,2*m-1)=modal_density(i,2*m-1)*2*pi*bandwidth(i)*df;
        MPB(i,2*m)=modal_density(i,2*m)*2*pi*bandwidth(i)*df;
    end
end
df=[0 1 3];
for m=1:1:length(DFRF(1,1,:))
figure(4*m-3)
loglog(Cfreq,modal_density(:,2*m-1),'-*r');
% xlim([0 5000]);ylim([10e-5 10e-3]);
title(['Modal density of Plate 1- ',num2str(df(m)),' Sheets of Damping
added']);
grid on
figure(4*m-2)
loglog(Cfreq,modal_density(:,2*m),'-*r');
% xlim([0 5000]);ylim([10e-5 10e-3]);
title(['Modal density of Plate 2- ',num2str(df(m)),' Sheets of Damping
added']);
grid on
figure(4*m-1)
loglog(Cfreq,MPB(:,2*m-1),'-*r');
% xlim([0 5000]);ylim([10e-1 10]);
title(['Modes per band of Plate 1- ',num2str(df(m)),' Sheets of Damping
added']);
grid on
figure(4*m)
loglog(Cfreq,MPB(:,2*m),'-*r');
% xlim([0 5000]);ylim([10e-1 10]);
title(['Modes per band of Plate 2- ',num2str(df(m)),' Sheets of Damping
added']);
grid on
end
```

7 EXPERIMENTAL POWER INPUT METHOD PROGRAM

```
%% Using the time domain data Power Injection Method MESCOPE
close all
clear all
clc
t=clock;
A=importdata('Test 1_point 1.mat');
B=importdata('Test 2_point 1.mat');
C=importdata('Test 3_point 1.mat');
D=importdata('Test 1_point 20.mat');
E=importdata('Test 2_point 20.mat');
F=importdata('Test 3_point 20.mat');
dt=A.X1(2,1)-A.X1(1,1);
N=131072;
decimate=1;
%%  Using Eval Funciton
for d=1:4
```

```
    s = ['autospecd0' int2str(d) '=zeros(N,1);'];
    eval(s);
end
csspecd01=((conj(fft(A.X1(:,2))).*fft(A.X2(:,2)))+(conj(fft(B.X1(:,2))).*fft(
B.X2(:,2)))+(conj(fft(C.X1(:,2))).*fft(C.X2(:,2))))/3; % Average
csspecd02=((conj(fft(D.X1(:,2))).*fft(D.X2(:,2)))+(conj(fft(E.X1(:,2))).*fft(
E.X2(:,2)))+(conj(fft(F.X1(:,2))).*fft(F.X2(:,2))))/3;
for d=3:1:8
    s = ['autospecd01(:,1)=autospecd01(:,1)+(conj(fft(A.X' int2str(d)
'(:,2))).*fft(A.X' int2str(d) '(:,2)));'];
    eval(s);
    s = ['autospecd02(:,1)=autospecd02(:,1)+(conj(fft(C.X' int2str(d)
'(:,2))).*fft(C.X' int2str(d) '(:,2)));'];
    eval(s);
    s = ['autospecd03(:,1)=autospecd03(:,1)+(conj(fft(D.X' int2str(d)
'(:,2))).*fft(D.X' int2str(d) '(:,2)));'];
    eval(s);
    s = ['autospecd04(:,1)=autospecd04(:,1)+(conj(fft(F.X' int2str(d)
'(:,2))).*fft(F.X' int2str(d) '(:,2)));'];
    eval(s);
end
for d=3:1:5
    s = ['autospecd01(:,1)=autospecd01(:,1)+(conj(fft(B.X' int2str(d)
'(:,2))).*fft(B.X' int2str(d) '(:,2)));'];
    eval(s);
    s = ['autospecd03(:,1)=autospecd03(:,1)+(conj(fft(E.X' int2str(d)
'(:,2))).*fft(E.X' int2str(d) '(:,2)));'];
    eval(s);
end
for d=6:1:8
    s = ['autospecd02(:,1)=autospecd02(:,1)+(conj(fft(B.X' int2str(d)
'(:,2))).*fft(B.X' int2str(d) '(:,2)));'];
    eval(s);
    s = ['autospecd04(:,1)=autospecd04(:,1)+(conj(fft(E.X' int2str(d)
'(:,2))).*fft(E.X' int2str(d) '(:,2)));'];
    eval(s);
end
for d=1:4
    s = ['autospecd0' int2str(d) '=autospecd0' int2str(d) '/9;'];
    eval(s);
end

%% decimating data
for d=1:1:4
    for j=1:1:N/decimate
        autospec01(j,1)=autospecd01(j*decimate,1);
        autospec02(j,1)=autospecd02(j*decimate,1);
        autospec03(j,1)=autospecd03(j*decimate,1);
        autospec04(j,1)=autospecd04(j*decimate,1);
        csspec01(j,1)=csspecd01(j*decimate,1);
        csspec02(j,1)=csspecd02(j*decimate,1);
    end
end
clear autospecd01 autospecd02 autospecd03 autospecd04 csspecd01 csspecd02
autospecd01=autospec01;
autospecd02=autospec02;
autospecd03=autospec03;
```

```
autospecd04=autospec04;
csspecd01=csspec01;
csspecd02=csspec02;

%% Integration. USING TRAPEZOIDAL RULE
df=0.25*decimate; % frequency resolution
Cfreq=256:512:3840;
band=8;
lowbound=round((2:512:3685)/df);
upbound=round((512:512:4196)/df);
% 1/3rd octave bands with full octave bandwidths
% Cfreq=[100 125 160 200 250 315 400 500 630 800 1000 1250 1600 2000 2500
3150 4000];
% band=length(Cfreq);
% lowbound=round(Cfreq/sqrt(2)/df);
% upbound=round(Cfreq*sqrt(2)/df);
M1=4.80;        % Mass of the plate 1
M2=3.628;        % Mass of the plate 2
Ek21=zeros(band,1);Ek11=zeros(band,1);Ek22=zeros(band,1);
Ek12=zeros(band,1);Pin1=zeros(band,1);Pin2=zeros(band,1);
for m=1:1:band
    for k=lowbound(m):1:upbound(m)

Ek21(m,1)=Ek21(m,1)+((M2/(2*pi))*real(autospecd02(k))/((k*df*2*pi)^2));

Ek11(m,1)=Ek11(m,1)+((M1/(2*pi))*real(autospecd01(k))/((k*df*2*pi)^2));

Ek22(m,1)=Ek22(m,1)+((M2/(2*pi))*real(autospecd04(k))/((k*df*2*pi)^2));

Ek12(m,1)=Ek12(m,1)+((M1/(2*pi))*real(autospecd03(k))/((k*df*2*pi)^2));
        Pin1(m,1)=Pin1(m,1)+((1/pi)*imag(csspecd01(k))/(k*df*2*pi));
        Pin2(m,1)=Pin2(m,1)+((1/pi)*imag(csspecd02(k))/(k*df*2*pi));
    end
    DE(m,1)=(Ek11(m,1)*Ek22(m,1))-(Ek12(m,1)*Ek21(m,1));
    A1(:,:,m)=[((Pin1(m,1)*Ek22(m,1))-(Pin2(m,1)*Ek21(m,1)))
(Pin1(m,1)*Ek12(m,1));(Pin2(m,1)*Ek21(m,1)) ((Pin2(m,1)*Ek11(m,1))-
(Pin1(m,1)*Ek12(m,1)))];
    B1(:,:,m)=A1(:,:,m)/(2*DE(m,1)*Cfreq(m)*2*pi);
end
for m=1:1:band
    LF1(m)=B1(1,1,m);
    LF2(m)=B1(2,2,m);
    CLF21(m)=B1(1,2,m);
    CLF12(m)=B1(2,1,m);
end
band1=1:1:band;
figure(1)
plot(band1,LF1,'-r*', 'DisplayName', 'n1', 'YDataSource', 'n1');
figure(2)
plot(band1,LF2,'-*r', 'DisplayName', 'n2', 'YDataSource', 'n2');
figure(3)
plot(band1,CLF12,'-*r', 'DisplayName', 'n12', 'YDataSource', 'n12');
figure(4)
plot(band1,CLF21,'-*r', 'DisplayName', 'n21', 'YDataSource', 'n21');
etime(clock,t)
```

8 EXPERIMENTAL MODAL ANALYSIS PROGRAM

```
%% Modal Analysis Vibrometer Data
close all
clear all
clc
Nfft=6376; % number of lines in the FRF
nupon=176; % number of points in the grid
frequency=25:1:6400;
% The data is in a UFF file which is read through the function readuff.
% which stores data in a Matrix C.
% % % %1 sheet damping added
fin=fopen('Force_point_103_plate_1.asc');
C=readuff(Nfft,fin);
DFRF=C(:,103);
%% Picking the Natural Frequencies from the FRF.
figure(2)
plot(frequency,angle(DFRF(:,1)));xlim([0 4000]);
figure(1)
plot(frequency,abs(DFRF(:,1)));xlim([0 4000]);
peaks=0;
sel=input('Do you want to select peaks?yes or no   ','s');
while(strcmp(sel,'yes')==1)
    disp('press delete after zooming');
    h=zoom;
    set(h,'Motion','horizontal','Enable','on');
    waitfor(gcf,'CurrentCharacter',127)
    % 127 is ascii code for delete
    zoom off;
    disp('press enter after selecting peaks:Max of 10 Peaks Per iteration');
    [x,y]=ginput(10);   % Max 10 peaks
    peaks=[peaks;x];
    set(gcf,'currentcharacter',char(4));
    sel=input('Do you want to select more peaks?   ','s');
end
peaks=peaks(2:end);
for i=1:1:length(peaks)
    for j=1:1:length(frequency);
        if abs(frequency(j)-peaks(i))<0.5
            k(i)=j-1;
            break
        end
    end
end
%% Calculating Mode Shapes
for i=1:1:length(C(1,:))
    for j=1:1:length(k)
        MS(j,i)=C(k(j),i);
    end
end
f=sqrt(DFRF(:,1));
for i=1:1:length(MS(:,1))
    ms(i,:)=MS(i,:)./f(i);
end
```

```
%% Getting Lai and Soom plates Grid from position array generated from PSV
%dividing the location arrays into 2 arrays for the 2 plates. 1-P1 2-P2.
% Plate 2 has 77 points and Plate 1 has 99
[X,Y]=readpos(nupon);
figure(2)
plot(X,Y);
X2=X(1,1:77);Y2=Y(1,1:77);
for i=1:1:length(ms(:,1))
    ms1(:,:,i)=ms(i,1:77);
end
tolerance=0.1;
slope=1.1288;
for n=1:1:11 % number of lines along which the slope is 1.1288 on plate 2
    m=1; % index for number of points on each of those 11 lines.(total=7)
    X22(m,n)=X2(1,1);Y22(m,n)=Y2(1,1);ms2(m,n,:)=ms1(1,1,:);
    X2=X2(1,2:end);Y2=Y2(1,2:end);
    for i=1:1:length(X2(1,:))
        a=(Y2(1,i)-Y22(1,n))/(X2(1,i)-X22(1,n));
        if (a-slope<tolerance) && (a-slope>0)
            m=m+1;
            X22(m,n)=X2(1,i);
            Y22(m,n)=Y2(1,i);
            ms2(m,n,:)=ms1(1,i,:);
        end
    end
    for m=1:1:length(X22(:,1))
        for i=1:1:length(X2(1,:))-m+1
            if X22(m,n)==X2(1,i)
                X2=[X2(1,1:i-1) X2(1,i+1:end)];
                Y2=[Y2(1,1:i-1) Y2(1,i+1:end)];
                ms1=[ms1(1,1:i-1,:) ms1(1,i+1:end,:)];
            end
        end
    end
end
clear ms1;
% X21=X22(1:end,end:-1:1);Y21=Y22(1:end,end:-1:1);
X1=X(1,78:176);Y1=Y(1,78:176);
for i=1:1:length(ms(:,1))
    ms1(:,:,i)=ms(i,78:176);
end
tolerance=5;
slope=36.2308;
for n=1:1:11 % number of lines along which the slope is 36.2308 on plate 1
    m=1; % index for number of points on each of those 11 lines.(total=9)
    X12(m,n)=X1(1,1);Y12(m,n)=Y1(1,1);ms3(m,n,:)=ms1(1,1,:);
    X1=X1(1,2:end);Y1=Y1(1,2:end);
    for i=1:1:length(X1(1,:))
        a=(Y1(1,i)-Y12(1,n))/(X1(1,i)-X12(1,n));
        if (a-slope<tolerance) && (a-slope>0)
            m=m+1;
            X12(m,n)=X1(1,i);
            Y12(m,n)=Y1(1,i);
            ms3(m,n,:)=ms1(1,i,:);
        end
    end
    for m=1:1:length(X12(:,1))
```

```
        for i=1:1:length(X1(1,:))-m+1
            if X12(m,n)==X1(1,i)
                X1=[X1(1,1:i-1) X1(1,i+1:end)];
                Y1=[Y1(1,1:i-1) Y1(1,i+1:end)];
                ms1=[ms1(1,1:i-1,:) ms1(1,i+1:end,:)];
            end
        end
    end
end
figure(3)
hold on
plot(X12,Y12)
plot(X22,Y22)
hold off
%Plotting the Mode Shapes
for i=1:1:length(peaks)
    figure(i+4)
    hold on
    surf(X22,Y22,real(ms2(:,:,i)));
    surf(X12,Y12,real(ms3(:,:,i)));
    hold off
    view(45,60)
    grid on
end

function [X,Y]=readpos(nupon)
fin=fopen('Positions.txt'); %input from asc file
for p=1:15   %14 to skip- 15 to be read number of initial lines to skip
    line=fgetl(fin);
end
%%%%% Position
if line(5:6)~='-1'
    for p=1:nupon
        % reading character stings and converting into numbers and
        % storing them
        X(p)=str2num(line(42:53));
        Y(p)=str2num(line(55:66));
        line=fgetl(fin);
    end
end
fclose(fin);

% Given by Dr. Ewing edited accordingly.
function [transfer_function]=readuff(Nfft,fin)
% fin=fopen('Circular Plate 6th May top_2.asc');    %input from asc file

for p=1:5   %number of initial lines to skip
    line=fgetl(fin);
end
n=0;    %index of point number
while feof(fin)==0
    %%%%% Transfer Function
    if line(1)=='T'
%         if line(1:10)=='Transfer F'
            n=n+1;
            q=0;    %index of current fft line
            for p=1:10   %continue to read and write 10 more lines
```

```
               line=fgetl(fin);
            end
            for p=1:(Nfft-1)/3  %Nfft-1: 2 reading at the end of each frf, 3
fft lines per row
                line=fgetl(fin);
                q=q+1;
                % reading character stings and converting into numbers and
                % storing them

transfer_function(q,n)=str2num(line(1:13))+1i*str2num(line(14:26));
                q=q+1;

transfer_function(q,n)=str2num(line(27:39))+1i*str2num(line(40:52));
                q=q+1;

transfer_function(q,n)=str2num(line(53:65))+1i*str2num(line(66:78));
            end
            line=fgetl(fin);
            q=q+1;

transfer_function(q,n)=str2num(line(1:13))+1i*str2num(line(14:26));
    end
    line=fgetl(fin);
end
fclose(fin);
```

9 EXPERIMENTAL T.S.E.A METHOD PROGRAM

```
%% Transient Statistical Energy Analysis
clear all
close all
clc
N=30000;
load('exp1.mat','AFFT1');
AFFTE1=AFFT1(1:N,:,:);
clear AFFT1
load('exp2.mat','AFFT2');
AFFTE2=AFFT2(1:N,:,:);
clear AFFT2
%%% using local accelerations for transmitted energy.
% spatial average 2,3,4 columns are the accelerometers 1,2,3 on plate 1 and
% 5,6,7 columns are the accelerometers 4,5,6 on plate 2.
for k=1:1:length(AFFTE1(1,1,:))
    AFFT1(:,1,k)=AFFTE1(:,1,k);
    AFFT1(:,2,k)=(AFFTE1(:,2,k)+AFFTE1(:,3,k)+AFFTE1(:,4,k))/3;
    AFFT1(:,3,k)=(AFFTE1(:,5,k)+AFFTE1(:,6,k)+AFFTE1(:,7,k))/3;
    AFFT1(:,4,k)=AFFTE1(:,8,k);
    AFFT2(:,1,k)=AFFTE2(:,1,k);
    AFFT2(:,2,k)=(AFFTE2(:,2,k)+AFFTE2(:,3,k)+AFFTE2(:,4,k))/3;
    AFFT2(:,3,k)=(AFFTE2(:,5,k)+AFFTE2(:,6,k)+AFFTE2(:,7,k))/3;
    AFFT2(:,4,k)=AFFTE2(:,8,k);
end
```

```
decimate=4;
asd=length(AFFTE1(1,1,:));
%% decimating data
for d=1:1:asd
    for i=1:1:4
        for j=1:1:N/decimate
            AFFT1t(j,i,d)=AFFT1(j*decimate,i,d);
            AFFT2t(j,i,d)=AFFT2(j*decimate,i,d);
        end
    end
end
clear AFFT1 AFFT2
for d=1:1:asd
    for i=1:1:8
        for j=1:1:N/decimate
            AFFTE1t(j,i,d)=AFFTE1(j*decimate,i,d);
            AFFTE2t(j,i,d)=AFFTE2(j*decimate,i,d);
        end
    end
end
clear AFFT1 AFFT2 AFFTE1 AFFTE2
AFFT1=AFFT1t;
AFFT2=AFFT2t;
AFFTE1=AFFTE1t;
AFFTE2=AFFTE2t;
clear AFFT1t AFFT2t AFFTE1t AFFTE2t
%%
df=0.25*decimate; % frequency resolution
Cfreq=256:512:3840;
band=8;
lowbound=round((2:512:3685)/df);
upbound=round((512:512:4196)/df);
% 1/3 rd octave with full octave bins
% Cfreq=[100 125 160 200 250 315 400 500 630 800 1000 1250 1600 2000 2500
3150 4000];
% band=length(Cfreq);
% lowbound=round(Cfreq/sqrt(2)/df);
% upbound=round(Cfreq*sqrt(2)/df);
M1=4.608;        % Mass of the plate 1 Assumed
M2=3.628;        % Mass of the plate 2
x1=1:1:33;  % x is the number of times time data is taken
x=1:1:34;   % x is the number of times time data is taken
%INTEGRATING
Ek21=zeros(band,length(x));Ek11=zeros(band,length(x));Ek22=zeros(band,length(
x));Ek12=zeros(band,length(x));
Etr211=zeros(band,length(x));Etr212=zeros(band,length(x));
for m=1:1:band
%     for n=1:1:length(AFFT1(1,1,:))-1
    for n=1:1:length(AFFT1(1,1,:))
        for k=lowbound(m):1:upbound(m)

Ek21(m,n)=Ek21(m,n)+((M2/(2*pi))*real(AFFT1(k,3,34)*conj(AFFT1(k,3,n)))/((k*d
f*2*pi)^2));

Ek11(m,n)=Ek11(m,n)+((M1/(2*pi))*real(AFFT1(k,2,34)*conj(AFFT1(k,2,n)))/((k*d
f*2*pi)^2));
```

```
Ek22(m,n)=Ek22(m,n)+((M2/(2*pi))*real(AFFT2(k,3,34)*conj(AFFT2(k,3,n)))/((k*d
f*2*pi)^2));

Ek12(m,n)=Ek12(m,n)+((M1/(2*pi))*real(AFFT2(k,2,34)*conj(AFFT2(k,2,n)))/((k*d
f*2*pi)^2));

Etr211(m,n)=Etr211(m,n)+((1/pi)*imag(AFFT1(k,4,n)*conj(AFFTE1(k,4,34)))/(k*df
*2*pi));     % why not? - for directional change

Etr212(m,n)=Etr212(m,n)+((1/pi)*imag(AFFT2(k,4,n)*conj(AFFTE2(k,4,34)))/(k*df
*2*pi));     %-
        end
        A(:,:,n,m)=2*2*pi*Cfreq(m)*[Ek21(m,n) -Ek11(m,n);Ek22(m,n) -
Ek12(m,n)];
        C(:,:,n,m)=[Etr211(m,n);Etr212(m,n)];
        B(:,n,m)=A(:,:,n,m)\C(:,:,n,m);
    end
end
for i=1:1:band
    ans(:,i)=B(:,34,i);   %% row1 n21 row2 n12
end
B=B(:,1:33,:);
AE1=ones(x(end),band);
AE2=ones(x(end),band);
for i=1:1:band
    AE1(:,i)=AE1(:,i)*ans(1,i); % asymptotic values
    AE2(:,i)=AE2(:,i)*ans(2,i); % asymptotic values
end
for m=1:1:4
    figure(1)
    subplot(2,2,m)
    semilogy(x,AE1(:,m),x1,B(1,:,m),'-*r', 'DisplayName', 'n21',
'YDataSource', 'n21');ylim([1e-5 1e-1]);xlim([0 35]);
    title(['Coupling Loss Factor \eta21(t) in band
',num2str(m)],'FontWeight','bold','FontSize',10);
    ylabel('Loss Factor (unitless)');
    xlabel('time (sec)');
    AX=legend('\eta21','\eta21(t)','location','south');
    LEG = findobj(AX,'type','text');
    set(LEG,'FontSize',8)
end
hgsave('TSEA_NO_DAMPING_eta21(t)_fig_1.fig');
for m=5:1:band
    figure(2)
    subplot(2,2,m-4)
    semilogy(x,AE1(:,m),x1,B(1,:,m),'-*r', 'DisplayName', 'n21',
'YDataSource', 'n21');ylim([1e-5 1e-1]);xlim([0 35]);
    title(['Coupling Loss Factor \eta21(t) in band
',num2str(m)],'FontWeight','bold','FontSize',10);
    ylabel('Loss Factor (unitless)');
    xlabel('time (sec)');
    AX=legend('\eta21','\eta21(t)','location','south');
    LEG = findobj(AX,'type','text');
    set(LEG,'FontSize',8)
end
hgsave('TSEA_NO_DAMPING_eta21(t)_fig_2.fig');
```

```
for m=1:1:4
    figure(3)
    subplot(2,2,m)
    semilogy(x,AE2(:,m),x1,B(2,:,m),'-*r', 'DisplayName', 'n12',
'YDataSource', 'n12');ylim([1e-5 1e-1]);xlim([0 35]);
    title(['Coupling Loss Factor \eta12(t)in band
',num2str(m)],'FontWeight','bold','FontSize',10);
    ylabel('Loss Factor (unitless)');
    xlabel('time (sec)');
    AX=legend('\eta12','\eta12(t)','location','south');
    LEG = findobj(AX,'type','text');
    set(LEG,'FontSize',8)
end
hgsave('TSEA_NO_DAMPING_eta12(t)_fig_1.fig');
for m=5:1:band
    figure(4)
    subplot(2,2,m-4)
    semilogy(x,AE2(:,m),x1,B(2,:,m),'-*r', 'DisplayName', 'n12',
'YDataSource', 'n12');ylim([1e-5 1e-1]);xlim([0 35]);
    title(['Coupling Loss Factor \eta12(t)in band
',num2str(m)],'FontWeight','bold','FontSize',10);
    ylabel('Loss Factor (unitless)');
    xlabel('time (sec)');
    AX=legend('\eta12','\eta12(t)','location','south');
    LEG = findobj(AX,'type','text');
    set(LEG,'FontSize',8)
end
hgsave('TSEA_NO_DAMPING_eta12(t)_fig_2.fig');

% Calculating Averaged FFT's And FRF's
% loading Time Domain data
close all
clear all
clc
B=importdata('Pt1.mat');
A(:,1)=B.X1(:,1);
A(:,2)=B.X1(:,2);
A(:,3)=B.X2(:,2);
A(:,4)=B.X3(:,2);
A(:,5)=B.X4(:,2);
A(:,6)=B.X5(:,2);
A(:,7)=B.X6(:,2);
A(:,8)=B.X7(:,2);
A(:,9)=B.X8(:,2);
SF=131072;                  % number of samples per hammer Hit.
% samples=132:131:4400;
samples=34:33:1090;    % number of samples in per 1 msec of data
samples(end+1)=SF;
n=1;           % number of Hits to be considered
na=6;          % number of accelerometers
nd=8;          % number of accelerometers + force input + transduced
for i=1:1:nd   % plot time domain
    figure(i)
    plot(A(1:20000,i+1));
end
AFFT1=zeros(SF,nd,length(samples));
%AFRF1=zeros(SF,na,length(samples));
```

```
for k=1:1:length(samples)
    [AFFT,AFRF]=fourierfunction(A,SF,n,samples(k));
    AFFT1(:,:,k)=AFFT(:,:);
%     AFRF1(:,:,k)=AFRF(:,:);
    clear AFRF AFFT
end
% fourier transformation of truncated and total data.
save('exp1','AFFT1');
clear A AFFT1 B AFRF1

function[AFFT,AFRF]=fourierfunction(A,SF,n,Samples)
    X=0:SF:n*SF;   % X= number of hits+1.
    Y=X+Samples;   % truncating it at some time interval
    D=zeros(SF,length(A(1,:)),n);
for i=1:1:n
    temp=A(X(i)+1:Y(i),:);
    for j=1:1:Samples
        D(j,:,i)=D(j,:,i)+temp(j,:);
        % D is a 3D array whose every sheet has data from one hit.
    end
end
clear temp A
for i=1:1:n     % number of Hammer Hits.
    for j=2:5
        % column1 has the time, 2 has force input, 3-8 are the
        % accelerometers 1-6 and 9 is the force transducer.
        FFT(:,(j-1),i)=fft(D(:,j,i));
        if j~=2
            FRF(:,(j-2),i)=fft(D(:,j,i))./fft(D(:,2,i));
        end
    end
    for j=6:9
        FFT(:,(j-1),i)=fft(D(:,j,i));
        if j~=9
            FRF(:,(j-2),i)=fft(D(:,j,i))./fft(D(:,2,i));
        end
    end
end
% FFT is the matrix containing the FFT's of the force and acceleration
% FRF is the matrix containing the FRF's
AFRF=zeros(SF,length(FRF(1,:,1)));
AFFT=zeros(SF,length(FFT(1,:,1)));
for i=1:1:n
    AFRF(:,:)=AFRF(:,:)+FRF(:,:,i);
    AFFT(:,:)=AFFT(:,:)+FFT(:,:,i);
end
clear FRF FFT D
AFRF=AFRF/n;    % AFRF is the matrix containing the averaged FRF's
AFFT=AFFT/n;    % AFFT is the matrix containing the averaged FFT's
```

APPENDIX B. CONSTRAINED LAYER DAMPING PLACEMENT ON THE EXPERIMENTAL PLATES

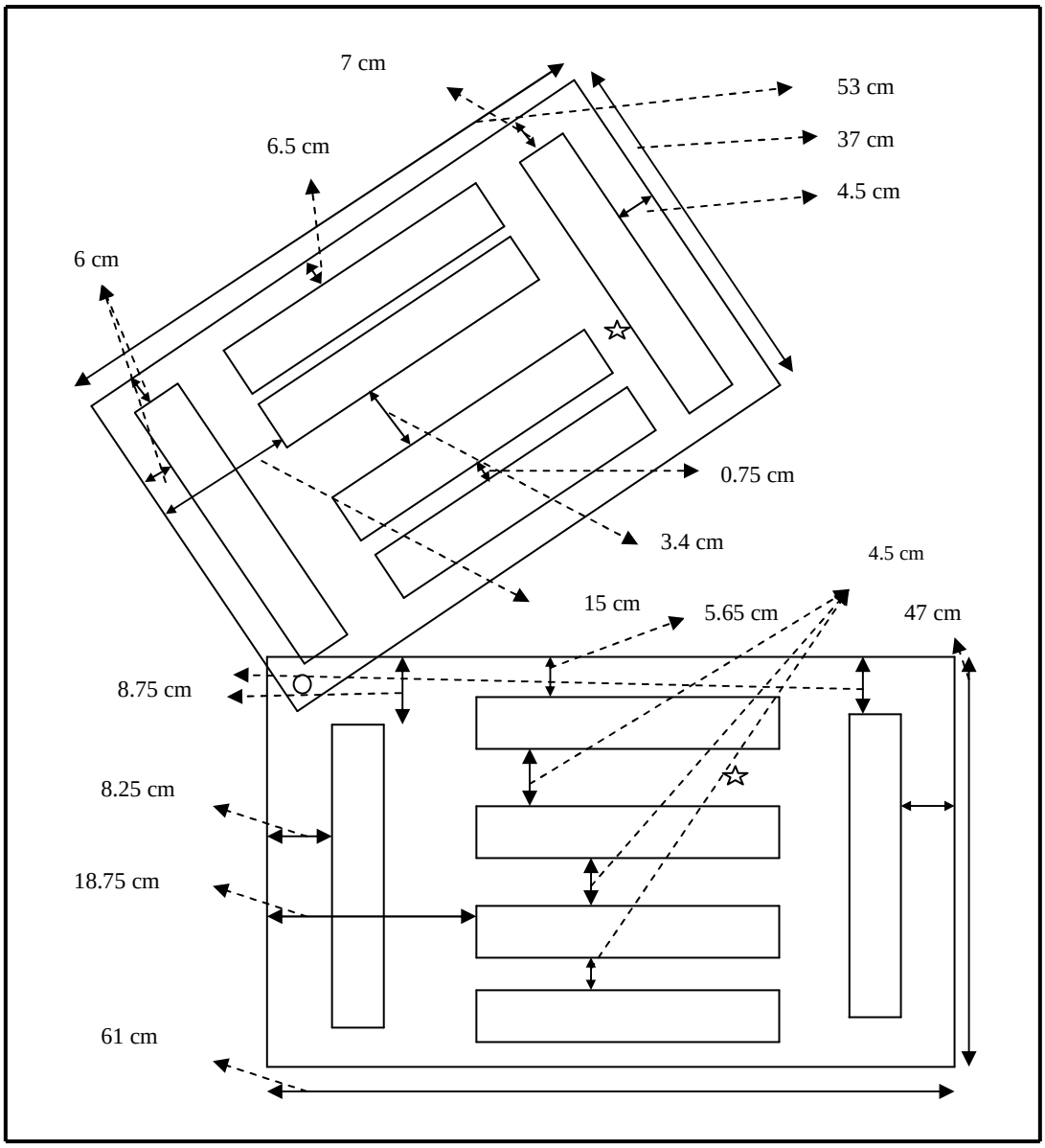

EXPERIMENTAL COUPLED PLATES – NOT DRAWN TO SCALE